

# **Combinatorial Testing of an ERK Inhibitor, SCH-772984 with PI3K/AKT/mTOR Inhibitors in Melanoma**

## **Master Thesis**

In order to obtain the academic degree

**Master of Science**

At Fachhochschule FH Campus Wien –  
University of Applied Sciences

**Submitted by:**

Geetha Avarappatt

**University ID:**

1210544043

**Supervisor:**

Antoni Ribas, M.D., Ph.D.

**Examiner:**

Ao. Univ. Prof. Dr. Martin Schreiber

**Date of submission:**

13. 01. 2015

## Abstrakt

**Hintergrund:** Ein bereits metastasierendes Melanom ist eine aggressive Krebsart im Menschen, wofür es keine effektiven Therapiemöglichkeiten gibt. Die somatischen Mutationen *BRAF*<sup>V600</sup> und *NRAS*<sup>Q61</sup> im Melanom aktiviert ständig den MAPK Signalweg, dies hat ein unkontrolliertes Zellwachstum zu Folge. Im Melanom kommt es auch zu Dysregulationen im PI3K/AKT/mTOR Signalweg. BRAF Inhibitoren (*BRAF*i) sind zunächst effektiv bei Melanomen mit *BRAF* Mutationen. Jedoch ist diese Art von Behandlung limitiert, aufgrund einer Resistenzentwicklung gegen diese Inhibitoren. Daher sind neue Strategien dringend notwendig, die diese Resistenzen vorbeugen und überwinden. Des Weiteren sind Behandlungsmöglichkeiten für Melanome, die keine *BRAF* Mutation haben (*NRAS Mutation und Wild-Typ Melanome*), sehr limitiert. Diese Studie handelt über das gemeinsame „*Targeting*“ der MAPK- und PI3K/AKT/mTOR Signalwege, da beide Signalwege bei der Progression von Melanomen eine wichtige Rolle spielen.

**Methoden:** Die Antitumor-Aktivität von ERK Inhibitor (*ERKi*; *SCH-772984*) kombiniert mit AKT- (*AKTi*; *MK-2206*) oder mTOR- (*mTORi*; *MK-8669*; *Ridaforolimus*) Inhibitor wurde in 31 humanen Melanom-Zelllinien mit definierten Dysregulationen ausgetestet. Es wurde die 50%ige Inhibitionskonzentration (*IC*<sub>50</sub>) der Inhibitoren alleine oder in Kombination ermittelt. Die Zellviabilität wurde mit einem ATP-basierenden Biolumineszenz Assay analysiert. Die synergistischen, additiven oder antagonistischen Wirkungen der Kombination der Inhibitoren wurden durch Kombination-Indizes (*CI*) ermittelt. Die Auswirkungen dieser Inhibitoren auf MAPK- und AKT Signalwege wurde mit Western Blots und auf Zellzyklus/Apoptose mit Durchflusszytometrie überprüft.

**Ergebnisse:** Der Großteil der Zelllinien war sensitiv gegenüber den kombinierten Therapien (*ERKi + AKTi*, *ERKi + mTORi*) mit einem *IC*<sub>50</sub> Wert von < 1 µM. Die meisten Zelllinien mit einer *BRAF* Mutation, die resistent gegen *ERKi* und *BRAF*i waren, wurden gegenüber den kombinierten Therapien sensitiv. Im Allgemeinen hatte die Kombination *ERKi* mit *mTORi* niedrigere *IC*<sub>50</sub> Werte verglichen mit *ERKi* in Kombination mit *AKTi*. Die kombinierten Inhibitoren bewirkten ein G1-Arrest und Apoptose in *NRAS* mutierte und Wild-Typ Zelllinien.

**Konklusion:** Die kombinierten Therapien erhöhten die Wachstumsinhibition der Melanom Zelllinien im Vergleich zu *ERKi* alleine. Außerdem war die Kombination der

Inhibitoren in den meisten Zelllinien synergistisch. Daher könnten diese kombinatorischen Therapien klinisch einsetzbar für Melanom-Therapien sein, ganz besonders für *NRAS* mutierte-, Wild-Typ Melanome und *BRAF* mutierte Melanome mit einer angeborenen oder erworbenen Resistenz.

**Schlagwörter:** Melanom, ERK Inhibitor, AKT Inhibitor, mTOR Inhibitor, kombinierte Therapien

## Abstract

**Background:** Metastatic human melanoma is an aggressive type of cancer for which there exist few effective therapies. *BRAF*<sup>V600</sup> and *NRAS*<sup>Q61</sup> somatic mutations in melanoma constitutively activate the MAPK pathway, resulting into uncontrolled cell growth. Also dysregulation in the PI3K/AKT/mTOR pathway occurs in melanoma. BRAF inhibitors (*BRAF*i) are initially effective in *BRAF* mutant melanoma, but this treatment is limited since the development of drug resistance. Therefore new strategies are urgently required to prevent and overcome this resistance. Furthermore treatment options for non-*BRAF* mutant melanoma (*NRAS* mutant and wild-type melanoma) are very limited. This study is about co-targeting the MAPK- and PI3K/AKT/mTOR pathways, since they play an important role in melanoma progression.

**Methods:** The antitumor activity of an ERK inhibitor (*ERKi*; *SCH-772984*) combined with AKT- (*AKTi*; *MK-2206*) or mTOR- (*mTORi*; *MK-8669*; *ridaforolimus*) inhibitor was tested in 31 human melanoma cell lines with defined pathway dysregulations. The 50% inhibitory concentration of the inhibitors alone and in combination (*IC*<sub>50</sub>) was determined. Cell viability was analyzed by ATP-based bioluminescence assay. Synergistic, additive or antagonistic effects of combining the drugs were analyzed by combination indices (*C*). The effects of these drugs were determined on MAPK- and AKT signaling by western blotting and on cell cycle/apoptosis by flow cytometry.

**Results:** The majority of cell lines was sensitive to the combinatorial treatments (*ERKi* + *AKTi*, *ERKi* + *mTORi*) with an *IC*<sub>50</sub> value < 1 μM. Most of the *BRAF* mutant cell lines that were resistant to *ERKi* and *BRAF*i became sensitive to the combinatorial treatments. In general the combination *ERKi* with *mTORi* had lower *IC*<sub>50</sub> values compared to *ERKi* combined with *AKTi*. The effects of the combined drugs induced G1 arrest and apoptosis in *NRAS* mutant and wild-type cell lines.

**Conclusion:** The combinatorial treatments enhanced the growth inhibition in melanoma cell lines compared to *ERKi* alone. Furthermore the combination of the drugs in most of the cells lines was synergistic. Therefore these combinatorial treatments may be clinically applicable for melanoma therapies, especially for *NRAS* mutant, wild-type and *BRAF* mutant melanomas with innate or acquired resistance.

**Keywords:** Melanoma, ERK inhibitor, AKT inhibitor, mTOR inhibitor, combinatorial treatments

## Contents

<b>Abstrakt .....</b>	<b>2</b>
<b>Abstract .....</b>	<b>4</b>
<b>List of abbreviations.....</b>	<b>7</b>
<b>1. Introduction.....</b>	<b>10</b>
1.1. Summary of targeted therapies in metastatic melanoma .....	12
1.2. Overview of master thesis.....	13
<b>2. Material and Methods .....</b>	<b>17</b>
2.1. Inhibitors and cell lines.....	17
2.2. Growth assays .....	19
2.3. Signaling pathway analyses.....	20
2.3.1. Protein isolation and quantification.....	20
2.3.2. Western blotting.....	21
2.3.3. Stripping of western blots.....	23
2.4. Cell cycle and apoptosis analyses by flow cytometry.....	23
2.5. Statistical analyses.....	25
<b>3. Results .....</b>	<b>26</b>
3.1. <i>BRAF</i> mutant melanoma cell lines .....	26
3.1.1. Growth inhibitory effects of the inhibitors.....	26
3.1.2. Effects of the inhibitors on signaling pathway.....	33
3.1.3. Effects of the inhibitors on cell cycle and apoptosis .....	36
3.2. <i>NRAS</i> mutant melanoma cell lines.....	40
3.2.1. Growth inhibitory effects of the inhibitors.....	40
3.2.2. Effects of the inhibitors on signaling pathway.....	46
3.2.3. Effects of the inhibitors on cell cycle and apoptosis .....	49

3.3. Wild-type <i>BRAF/NRAS</i> melanoma cell lines .....	53
3.3.1. Growth inhibitory effects of the inhibitors.....	53
3.3.2. Effects of the inhibitors on signaling pathway.....	57
3.3.3. Effects of the inhibitors on cell cycle and apoptosis .....	60
<b>4. Discussion.....</b>	<b>65</b>
<b>5. Conclusion .....</b>	<b>68</b>
<b>6. References .....</b>	<b>69</b>
<b>Acknowledgments .....</b>	<b>74</b>
<b>Statutory Declaration .....</b>	<b>74</b>
<b>Appendix .....</b>	<b>76</b>
List of figures.....	76
List of tables.....	78

## List of abbreviations

AB	antibody
AKT	protein kinase B
AKTi	AKT inhibitor ( <i>MK-2206</i> )
AR	acquired resistance
Asp 214	aspartic acid 214
ATP	adenosine triphosphate
<i>BRAF</i>	B-Raf proto-oncogene
BRAFi	BRAF inhibitor
BSA	bovine serum albumin
°C	Celsius
CEN	chicken erythrocyte nuclei
CI	combination index
COT	cancer Osaka thyroid kinase
CRAF	C-Raf proto-oncogene
CTLA4	cytotoxic T-lymphocyte-associated protein 4
DAPI	4',6-diamidino-2-phenylindole
DMSO	dimethyl sulfoxide
DNA	deoxyribonucleic acid
dH <sub>2</sub> O	distillated water
ECL	enhanced chemiluminescence
EDTA	ethylenediaminetetraacetic acid
EGFR	epidermal growth factor receptor
ERK	extracellular signal-regulated kinase
ERKi	ERK inhibitor ( <i>SCH722984</i> )
FBS	fetal bovine serum
FDA	Food and Drug Administration
GAPDH	glyceraldehyde 3-phosphate dehydrogenase
Gly 215	glycine 215
GSK2118436	BRAF inhibitor ( <i>dabrafenib</i> )
I	intermediate sensitive
IC <sub>50</sub>	50% inhibition concentration
IGFR-1	insulin-like growth factor receptor-1
IRBs	Institutional Review Boards

IT	incubation time
kDa	kilo dalton
MAPK	mitogen-activated protein kinase
MEK	mitogen-activated protein kinase kinase
MEKi	MEK inhibitor ( <i>trametinib</i> )
μM	micromolar
min	minutes
MK-2206	AKT inhibitor
MK-8669	mTOR inhibitor ( <i>ridaforolimus</i> )
MTA	materials transfer agreement
mTOR	mammalian target of rapamycin
mTORi	mTOR inhibitor ( <i>MK-8669</i> ; <i>ridaforolimus</i> )
n/a	not applicable
NAD	nicotinamide adenine dinucleotide
nM	nanomolar
<i>NRAS</i>	neuroblastoma RAS viral ( <i>v-ras</i> ) oncogene homolog
pAKT	phospho-AKT
pAKT Ser473	phospho-AKT serin 473
PARP	poly [ADP-ribose] polymerase
PBS	phosphate buffered saline
PBS-T	phosphate buffered saline-Tween 20
PD-1	programmed death 1
PDGFRβ	platelet derived growth factor beta
pERK	phospho-ERK
pERK1/2 Thr202/Tyr204	phospho-ERK1/2 threonine 202/tyrosine 204
PI3K	phosphatidylinositol 3-kinase
PLX4032	BRAF inhibitor ( <i>vemurafenib</i> )
pMEK	phospho-MEK
pMEK Ser217/221	phospho-MEK serin 217/221
pRSK	phospho-RSK
P-p90RSK Thr359/Ser363	phospho-p90RSK threonine 359/serin 363
<i>PTEN</i>	phosphatase and tensin homolog
PVDF	polyvinylidene difluoride
R	resistant
RAS	Rat sarcoma



RAF	rapidly accelerated fibrosarcoma; RAF kinase
rpm	revolutions per minute
RPMI	Roswell Park Memorial Institute
RSK	ribosomal S6 kinase
RT	room temperature
RTKs	receptor tyrosine kinases
S	sensitive
SCH-772984	ERK inhibitor
sec	seconds
STDV	standard deviation
tAKT	total AKT
tERK1/2	total ERK1/2
tMEK1/2	total MEK1/2
tRSK	total RSK
UCLA	University of California, Los Angeles
V	volt
vs.	versus
WB	western blot
WT	wild-type

## 1. Introduction

All the experiments of this master thesis were conducted at the Department of Medicine, Division of Hematology-Oncology, University of California in Los Angeles (UCLA) under the supervision of Antoni Ribas, M.D., Ph.D. and Lidia Robert, M.D. This master thesis was funded with a scholarship from Austrian Marshall Plan Foundation.

Metastatic human melanoma is an aggressive type of cancer for which there exist few effective therapies<sup>1</sup>. Approximately 50% of all human melanomas harbor activating mutations in the serine-threonine protein kinase BRAF (*B-Raf proto-oncogene*), most commonly at position V600E (*BRAF<sup>V600E</sup>*)<sup>2, 3</sup>. This mutation constitutively activates BRAF and downstream signal transduction in the mitogen-activated protein kinase (MAPK) pathway, resulting in uncontrolled cell growth<sup>1, 4</sup>. The second most melanoma driver event that has been identified is *NRAS (neuroblastoma RAS viral (v-ras) oncogene homolog)* mutation, primarily at the Q61 codon, which occurs with a frequency of 10-25%<sup>5-9</sup>. RAS activation triggers the MAPK pathway via interactions with the RAF oncoproteins, such as BRAF and CRAF (*C-Raf proto-oncogene*)<sup>5, 10</sup>. About 40% of the remaining melanomas appear as *BRAF* and *NRAS* wild-types (*WT*)<sup>11</sup>. In addition, melanomas also have frequent alterations in the phosphatidylinositol 3-kinase (*PI3K*) and v-akt murine thymoma viral oncogene homolog 1 (*AKT*) pathway, another important key signal transduction pathway for cell growth and survival<sup>4</sup>. These alterations cause the activation of multiple pathways downstream of AKT; the major one is going through the mechanistic target of rapamycin (*mTOR*)<sup>4</sup>. Therefore, approaches have been proposed in melanomas to inhibit the MAPK- and PI3K/AKT pathways at the same time<sup>4, 12</sup>. The following figure illustrates the RAS/RAF/MEK/ERK- (*MAPK*) and PI3K/AKT/mTOR pathways. It also shows the three inhibitors, MK-2206 (*AKTi*), MK-8669 (*mTORi*) and SCH-772984 (*ERKi*), which were used in this study.

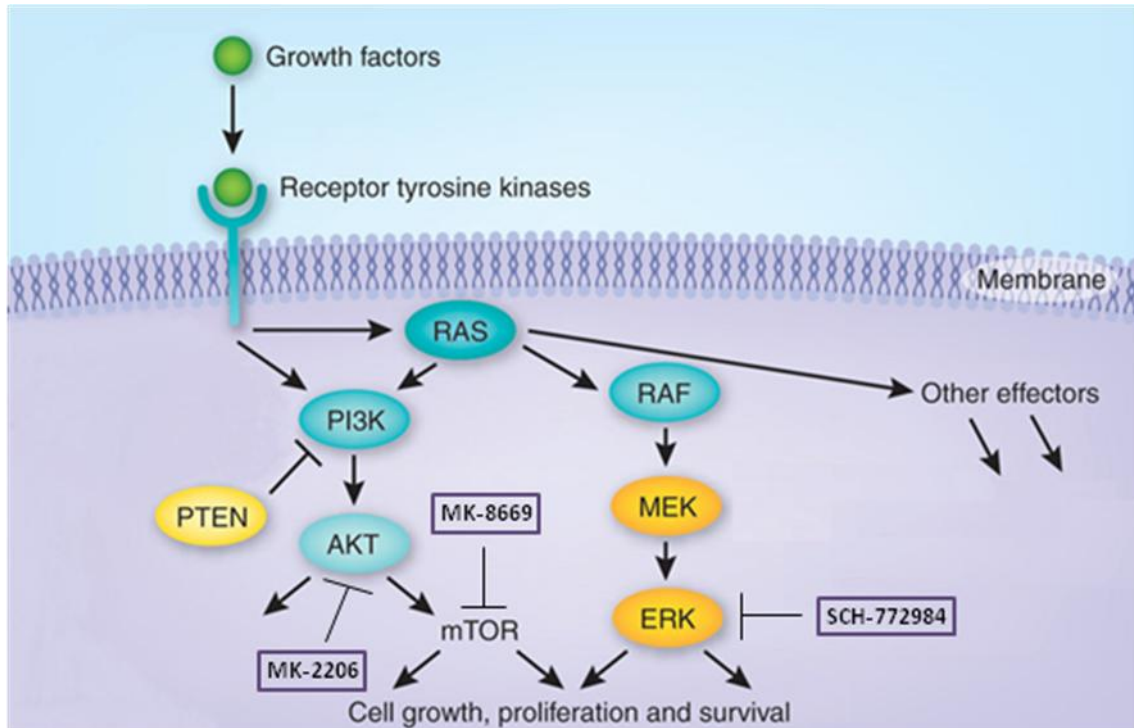


**Figure 1: MAPK- and PI3K/AKT/mTOR signaling pathway (modified according to <sup>13</sup>).** This figure shows the two main signaling pathways (*MAPK* and *PI3K/AKT/mTOR*) involved in melanoma progression <sup>12</sup>. The components shown in blue are commonly mutated in human tumors, leading to activation of the signaling network <sup>13</sup>. In addition in various tumors the loss or mutation of *PTEN* (yellow) leads to hyperactive PI3K signaling <sup>13, 14</sup>. The drugs MK-2206, MK-8669, SCH-772984 (all three in purple), which are shown in this figure, were used in this study to target AKT, mTOR and ERK.

Growth factors activate via receptor tyrosine kinases RAS proteins, resulting to stimulation of the PI3K/AKT/mTOR pathway and RAF/MEK/ERK kinase cascade and other pathways <sup>13, 15</sup>. These lead to cell growth, proliferation and survival <sup>13, 15</sup>. The MAPK- and PI3K/AKT/mTOR pathways play an important role in melanoma progression <sup>4, 12, 16</sup>, especially in the development of resistance to BRAF inhibitors (*BRAF*) <sup>4, 11, 17</sup>. For example BRAFi induce a high rate of tumor regressions in patients with *BRAF*<sup>V600E</sup> mutant metastatic melanoma by interrupting oncogenic *BRAF*<sup>V600E</sup> signaling through the MAPK pathway, which commonly supports cell survival and proliferation <sup>2, 3</sup>. However, the BRAF inhibitor-based therapy is limited primarily by the development of acquired resistance against this inhibitor leading to tumor progression around six months after treatment <sup>3, 4, 18</sup>. Furthermore this therapy is not effective in non-*BRAF* mutant melanoma, like *NRAS* mutant or wild-type melanoma <sup>11</sup>. In fact treating non-*BRAF* mutant melanoma with BRAFi would result in MAPK activation,

mediated by CRAF<sup>11, 19, 20</sup>. Resistance to BRAFi occurs via reactivation of MAPK pathway by secondary mutations in *NRAS*<sup>21</sup> or *MEK*<sup>22, 23</sup>, up-regulation of a bypass COT- (*cancer Osaka thyroid kinase*) pathway<sup>24</sup>, *BRAF* gene amplification<sup>25</sup> or truncations in the BRAF protein through alternative splicing, which leads to lack of inhibition of the drug<sup>17, 25, 26</sup>. Acquired resistance to BRAFi can also occur by enhanced signaling via PI3K/AKT pathway through deletion of *PTEN* (*phosphatase and tensin homolog*)<sup>27</sup> or the over-expression/activation of RTKs (*receptor tyrosine kinases*), such as PDGFR $\beta$  (*platelet derived growth factor beta*)<sup>21, 28</sup>, EGFR (*epidermal growth factor receptor*)<sup>29</sup> or IGF-1 (*insulin-like growth factor receptor-1*)<sup>30</sup>. Therefore new approaches in melanoma treatments are needed to address these resistance mechanisms<sup>31</sup>.

This study tests the combinatorial effects of an ERK (*extracellular signal-regulated kinase*) inhibitor (*ERKi*; SCH-772984) with an AKT (*protein kinase B*) inhibitor (*AKTi*; MK-2206) or a mTOR (*mammalian target of rapamycin*) inhibitor (*mTORi*; MK-8669) in human melanoma cell lines to analyze their antitumor activity. SCH-772984 (*ERKi*) is an ATP (*adenosine triphosphate*) competitive and non-competitive inhibitor, with allosteric properties<sup>11, 32</sup>. ERK1 and ERK2 activation by phosphorylation of MEK (*mitogen-activated protein kinase kinase*) is inhibited with SCH-772984<sup>11, 32</sup>. MK-2206 (*AKTi*) is an allosteric, highly potent, non-ATP competitive, selective inhibitor of serine/threonine protein kinase AKT. It binds to AKT and inhibits the activity of it, which may result into the inhibition of the PI3K/AKT signaling<sup>33 – 37</sup>. Currently MK-2206 is in phase I/II trial for treatments of solid tumors and other cancer types<sup>33, 38</sup>. MK-8669 (*mTORi*, also known as *ridaforolimus*) is a non-prodrug analog of rapamycin<sup>39, 40</sup>. It is a selective and potent inhibitor of serine/threonine kinase mTOR<sup>39, 40</sup>. This mTOR inhibitor is also in phase I/II trial for different cancer types<sup>39, 41</sup>.

## 1.1. Summary of targeted therapies in metastatic melanoma

The most commonly mutation *BRAF*<sup>V600</sup> in melanoma is treated selectively with the FDA (*Food and Drug Administration*) approved type I BRAF inhibitors vemurafenib (*PLX4032*) or dabrafenib (*GSK2118436*)<sup>31, 42 – 44</sup>. MEK inhibitors (*MEKi*), like trametinib are also used to treat BRAF mutant melanomas. Trametinib blocks MEK1 and MEK2 in the MAPK pathway, downstream of BRAF. It inhibits effectively cell proliferation and tumor growth of *BRAF* mutant melanoma<sup>45</sup> and it may have clinical activity in *NRAS*

mutant melanoma as well <sup>46</sup>. Nevertheless resistance to MEKi also occurs through MAPK dependent mechanism <sup>47 - 49</sup>. The combining of dabrafenib and trametinib was evaluated in a phase I/II clinical trial. This combinatorial treatment resulted into progression-free survival of 9,4 months compared to 5,8 months in patients treated with dabrafenib alone <sup>31</sup>.

Targeted immunotherapies are an alternative treatment for metastatic melanoma. For example ipilimumab is a FDA approved human monoclonal antibody (*IgG1*) against CTLA4 (*cytotoxic T-lymphocyte-associated protein 4*). CTLA4 is an inhibitory receptor on T cells and induced after T cell activation to down-regulate the immune system, this kind of immune regulatory mechanism is used by cancers to hide from the immune system. Blocking CTLA4 with ipilimumab improved overall survival in patients with metastatic melanoma <sup>50, 51</sup>. Another inhibitory T cell receptor is PD-1 (*programmed death 1*), it also down-regulates the T cell function through the signals of binding to its ligands PD-L1 or PD-L2 <sup>52 - 54</sup>. Multiple normal and cancerous tissues express PD-L1 <sup>52 - 54</sup>, whereas antigen-presenting cells primarily express PD-L2 <sup>55</sup>. Recently pembrolizumab (*Keytruda*), an anti-PD-1 antibody was approved by FDA, since this antibody has shown promising antitumor responses in clinical trials for melanoma with less toxicity than for example with ipilimumab <sup>56, 57</sup>.

## 1.2. Overview of master thesis

In this study the MAPK pathway was inhibited by ERKi and PI3K/AKT/mTOR pathway was inhibited with AKTi and mTORi.

The Dr. Ribas lab has studied the in vitro antitumor effects of the class I BRAF inhibitor PLX4032/vemurafenib against a panel of over 50 human melanoma tumor cell lines established from patient's biopsies over the past 10 years at the UCLA's Jonsson Comprehensive Cancer Center. These cell lines have been genetically characterized for *NRAS/BRAF* mutations and other oncogenic events, as *AKT* mutations or *PTEN* loss <sup>58</sup>. In addition, the Dr. Ribas lab has derived cell lines with acquired resistance to class I BRAF inhibitors and from patients enrolled in clinical trials with vemurafenib <sup>4</sup>.

Recently the Dr. Ribas lab tested the antitumor activity of ERK inhibitor (*SCH-772984*) alone and in combination with BRAF inhibitor (*vemurafenib*) in a panel of human

melanoma cell lines. The combination was synergistic in a majority of cell lines, including *NRAS* mutant and wild-type melanoma cell lines. The combined treatment also delayed the acquired resistance in long term *in vitro* assays <sup>11</sup>. Furthermore investigator noted in prior studies of the effects of BRAF inhibitors on melanoma cell lines that in some of the naturally resistant and acquired resistant cell lines there is a differential signaling through the AKT/mTOR pathway compared to sensitive cell lines <sup>4</sup>. This resistance can be overcome by combining a MEK inhibitor with an AKT or an mTOR inhibitor <sup>4</sup>.

Therefore the hypothesis of this study is that the addition of an inhibitor of the AKT/mTOR pathway to an ERK inhibitor could possibly treat the natural or acquired resistance to BRAF inhibitors, and treat *NRAS* mutant and wild-type melanomas since non-*BRAF* mutant melanomas have limited treatment options <sup>11</sup>.

The antitumor activity of the ERK inhibitor combined with AKT or mTOR inhibitor was tested by performing growth assays in 31 human melanoma cell lines with defined pathway dysregulations and melanoma cell lines with or without acquired resistance to BRAF inhibitors. Of these 31 cell lines were 15 *BRAF* mutant-, 11 *NRAS* mutant- and 5 wild-type *BRAF* and *NRAS* melanoma cell lines. The concentration of the inhibitors alone and in combination that inhibited 50% of cell growth ( $IC_{50}$ ) was defined. Cell viability was determined by ATP-based bioluminescence assay. Synergistic, additive or antagonistic effects of combining the drugs were analyzed by combination indices (*C*). Six cell lines (*M370*, *M410*, *M243*, *M318*, *M230* and *M285*) were selected for the western blot-, apoptosis- and cell cycle analyses. Two of each mutations (*BRAF* and *NRAS*) and wild-type melanoma cell lines were chosen. The cells were selected by comparing the  $IC_{50}$  values of ERKi alone to the  $IC_{50}$  values of the combinatorial testing. For example a cell line of each type with substantial lower  $IC_{50}$  values of the combinatorial treatments than the  $IC_{50}$  value of ERKi in monotherapy was chosen. The second cell line of each type was selected by seeing not much difference in the  $IC_{50}$  values between the treatments. A microscopic image of these six cell lines are shown in figure 2. All these six cell lines had a good growth rate; especially M410 and M230.

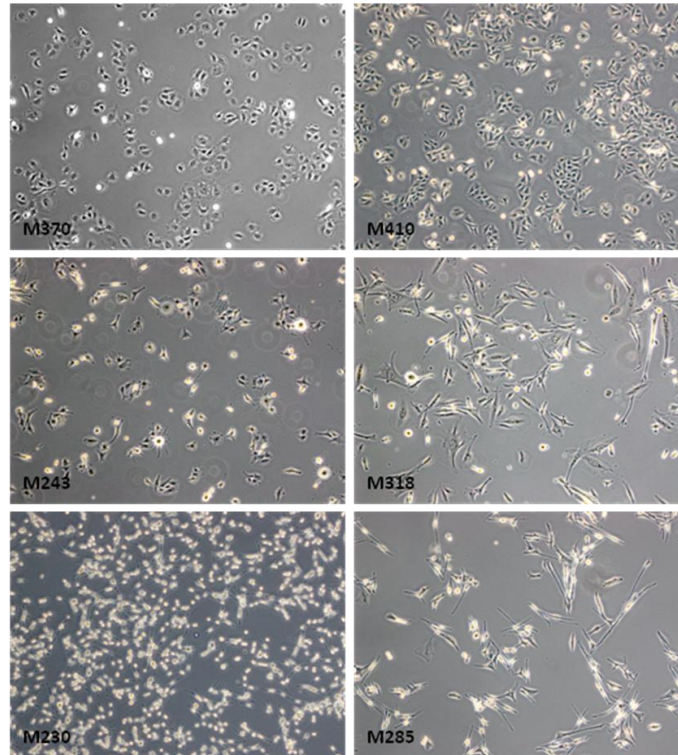


**Figure 2: Microscopic imaging of melanoma cell lines before any treatment.** This figure shows six different melanoma cell lines with various sizes and shapes. M370, M410: *BRAF* mutant melanoma cell lines. M243, M318: *NRAS* mutant melanoma cell lines. M230, M285: wild-type melanoma cell lines. These pictures were taken with a 50x magnification.

The major signaling pathway modulation was studied by western blot (*WB*) analyses by determining the effects of single agent (*ERKi*) and combinatorial treatments (*ERKi + AKTi*; *ERKi + mTORi*) on phosphorylated signaling molecules in the MAPK- and AKT pathways. The effects on cell cycle analyses and apoptosis was studied by flow cytometry. Cells were stained with the fluorescent dye DAPI (*4',6-diamidino-2-phenylindole*), that binds DNA (*deoxyribonucleic acid*). The fluorescence signal of individual cells was measured by the flow cytometer. The data were plotted as cell number versus fluorescence intensity (*proportional to DNA content*). The distribution of cells was shown in two peaks (*G1 and G2/M*; see *Figure 11B*, *Figure 19B* and *Figure 26B*), corresponding to their DNA contents (*2n or 4n*); therefore cells in G1 or G2/M phases of the cell cycle could be determined. Also the cells in between these two phases (*S phase*) were determined<sup>59</sup>. Apoptosis was analyzed by staining the treated cells with an apoptosis specific marker, which was Alexa Flour® 700 linked with anti-

cleaved PARP (*poly [ADP-ribose] polymerase*) antibody. Cleaved PARP plays an important role in induced apoptosis<sup>60</sup>. PARP is a nuclear chromatin-associated enzyme that catalyzes the poly(ADP-ribosyl)ation of a variety of nuclear proteins, e.g. histones, with NAD (*nicotinamide adenine dinucleotide*) as substrate. DNA damages increase the catalytic activity of PARP. Furthermore caspase-3, a member of the caspase family that plays a central role in apoptosis, cleaves PARP between aspartic acid 214 (*Asp 214*) and glycine 215 (*Gly 215*) to form 24- and 89 kDa fragments which results in loss of normal PARP function. Inactivation of PARP leads DNA-damaged cells to undergo apoptosis rather than necrosis and the 89 kDa fragment of PARP is considered to be a marker for apoptosis<sup>60,61</sup>.

Resistance to BRAF inhibitors in the melanoma field is a major clinical problem. Therefore new strategies are urgently required to prevent and overcome this resistance<sup>31</sup>. For *non-BRAF* mutant melanoma (*NRAS mutant and wild-type melanoma*) treatment options are very limited<sup>11</sup>. So with this study it was possible to analyze the patterns of sensitivity or resistance to the treatment with ERK inhibitor combined with AKT- or mTOR inhibitor in human melanoma cell lines. Also the suitability of combinatorial therapy with ERK inhibitor with AKT and mTOR inhibitors in future clinical trials in patients with metastatic malignant melanoma can be assessed.

The goal of this study was to test the antitumor activity of the ERKi combined with AKTi and ERKi combined with mTORi against human malignant melanoma cell lines with defined oncogenic alterations. Moreover to overcome the resistance of *BRAF* mutant melanoma to BRAFi with ERK inhibitor combined with inhibitors of the PI3K/AKT/mTOR pathway. To sum up, the testing of novel targeted therapies in fully genotyped cell lines may allow the definition of patterns of future response or resistance in the clinic.



## 2. Material and Methods

### 2.1. Inhibitors and cell lines

The inhibitors SCH722984 (*ERK*), MK-2206 (*AKT*) and MK-8669 (*mTOR*) were provided by Merck Sharp & Dohme Corp. (*Whitehouse Station, NJ*) through a materials transfer agreement (*MTA*). Vemurafenib (*PLX4032*), which is a BRAF inhibitor, was commercially purchased from Selleck Chemicals (*Houston, TX*). All these drugs came as a powder and were reconstituted in 100% dimethyl sulfoxide (*DMSO*; *Fisher Scientific, Fair Lawn, NJ*) to a final stock concentration of 10 mM, according to their molecular weight.

All human melanoma cell lines (*M series*), besides the cell lines SKMEL-173 and WM1366, were established from patient biopsies at the UCLA's Jonsson Comprehensive Cancer Center under UCLA Institutional Review Boards (*IRBs*) approval #02-08-067<sup>58</sup>. The cell lines SKMEL-173 and WM1366 were obtained from American Type Culture Collection (*Rockville, MD*)<sup>62</sup>. In addition, the Dr. Ribas lab has derived cell lines with *in vitro* acquired resistance (*cell lines were labeled with "AR"*) to BRAF inhibitors (*vemurafenib*)<sup>4</sup>. All these cell lines were cultured in tissue culture flask (*TPP Techno Plastic Products AG, Switzerland*) with RPMI (*Roswell Park Memorial Institute*) 1640, 1X with L-glutamine (*Mediatech, Inc., Manassas, VA*) media containing 10% fetal bovine serum (*FBS*; *Omega Scientific, Inc., Tarzana, CA*) and 1% penicillin, streptomycin and amphotericin B (*Antibiotic Antimycotic Solution 100X*; *Omega Scientific, Inc., Tarzana, CA*). Furthermore the acquired resistant cell lines were cultured with 1  $\mu$ M vemurafenib to keep these cells resistant to BRAFi. The cell cultures were kept in an incubator (*SANYO CO<sub>2</sub> Incubator, SANYO Electric Biomedical Co., Ltd.*) with a humidified atmosphere of 5% CO<sub>2</sub> at 37°C. When the cells reached a confluency of 75 – 90%, they were subcultured into new flasks by trypsinization (*Trypsin EDTA (ethylenediaminetetraacetic acid) 1x*; *Omega Scientific, Inc., Tarzana, CA*). It was important to keep the cells in a sterile environment, which was ensured by working in a Biological Safety Cabinet (*SterilGARD®III Advance<sup>o</sup>, The Baker Company, Sanford, ME*).

The following table shows the 31 cell lines which were used in this study. This table also includes the mutational status of these cell lines and their sensitivity to vemurafenib (*BRAF*) which were previously tested by Dr. Ribas lab (*UCLA*)<sup>11, 58, 63</sup>.

Effect to BRAFi	Cell lines
S	M395
S	M397
S	M792
S	M411
S	M249
S	M229
I	M409
I	M255
R	M308
R	M410
R	M233
R	M370
R	M381
R	M397AR
R	M409AR1
R	M243
R	M245
R	M296
R	M311
R	M408
R	M412-A
R	M412-B
R	SKMEL-173
R	WM1366
R	M244
R	M318
R	M230
R	M285
R	M375
R	M418
R	PB (M228)

**Table 1: 31 melanoma cell lines with their mutational status and sensitivity to vemurafenib (*BRAF*, *PLX4032*).** 15 *BRAF* mutant-, 11 *NRAS* mutant- and 5 wild-type *BRAF* and *NRAS* melanoma cell lines were used for the combinatorial testing of the drugs ERKi, AKTi and mTORi in this study. S: sensitive, I: intermediate sensitive, R: resistant, AR: acquire resistant, WT: wild-type, BRAFi = vemurafenib, PLX4032.

## 2.2. Growth assays

On day 0, melanoma cell lines were seeded in 96-well plates (3.000 cells per well). On day 1, cells were treated at a dilution range in duplicates with ERKi, AKTi, mTORi alone (*monotherapy*) or in combination (*combinatorial testing; ERKi with AKTi or ERKi with mTORi at a ratio of 1:1*) in a constant amount of DMSO for 120 hours. This incubation time (*IT*) of 120 hours was chosen by the experience of previous experiments with different drugs from the lab <sup>11, 17</sup>.

All cell lines (*total of 31 cell lines*) were treated with the drugs in combination. The cell lines which showed after the combinatorial testing promising data were selected to test the drugs individually (*total of 18 cell lines*) to analyze the combination indices (*CI*; see *chapter 2.5. Statistical analyses*). The starting concentration of each drug was 10  $\mu$ M which was diluted in a two-fold serial dilution over a range from 1:2 to 1:256 (10  $\mu$ M to 39 nM). As a control parameter cells were also incubated with DMSO only (*no drug treatment*).

The cell viability was analyzed by the CellTiter-Glo<sup>®</sup> Luminescent Cell Viability Assay (*Promega, Madison, WI*). This bioluminescent assay system uses thermostable luciferase to generate a luminescent signal. This signal was proportional to the amount of ATP present in the cells. Based on the quantification of ATP, which indicates the presence of metabolically active cells, it was possible to determine the number of viable cells in culture <sup>64, 65</sup>. Furthermore the reagents of this assay also inhibit endogenous enzymes, e.g. ATPases, which would interfere with the accurate detection of ATP. The reagents of this bioluminescent assay were prepared by following the manufacturer's instructions. First the buffer was thawed at room temperature (*RT*) and mixed with the substrate by vortexing to obtain a homogenous solution, which forms the CellTiter-Glo<sup>®</sup> reagent. This reagent was directly added to the cells after the *IT* (120 h) of the inhibitors and another *IT* of 30 minutes at *RT* to equilibrate the plate with the cells and contents. These contents were mixed for few seconds on an orbital shaker to induce cell lysis. For the stabilization of the luminescent signal the plate was incubated at *RT* for 10 minutes <sup>64</sup>. The luminescence was recorded by using a luminometer (*DTX 880 Multimode Detector; Beckman Coulter, Inc., Brea, CA*) and analyzed by the software programs Multimode Analysis Software (*Beckman Coulter, Inc., Brea, CA*), Microsoft Excel (*Microsoft Corporation, Redmond, WA*) and GraphPad Prism

(GraphPad Software, Inc., La Jolla, CA). Each experiment was repeated at least three times and the average of minimum two was used to calculate the IC<sub>50</sub> values of each condition for each cell line.

## **2.3. Signaling pathway analyses**

Six melanoma cell lines (*M410, M370, M243, M318, M230 and M285*) were selected to look at the signaling pathways. They were seeded in 12-well plates (*300.000 cells per well*). On the following day the media was replaced with new media containing DMSO as a control, 1  $\mu$ M ERKi, 1  $\mu$ M ERKi in combination with 1  $\mu$ M AKTi or 1  $\mu$ M ERKi in combination with 1  $\mu$ M mTORi (*four conditions*). The IT of these four conditions was 24 hours.

### **2.3.1. Protein isolation and quantification**

After the 24 hours the cells were prepared for the cell lysis to isolate their proteins. First the media was removed and then the cells were washed twice with cold PBS (*phosphate buffered saline; Lonza, BioWhittaker<sup>®</sup>, Walkersville, MD*). The cells were lysed with a lysis buffer for 30 min at 4°C. Lysis buffer contained Ripa buffer (*Sigma-Aldrich, Co., St. Louis, MO*), phosphatase inhibitor (*Sigma-Aldrich, Co., St. Louis, MO*) as cocktail 1 and cocktail 2 at 1:100 and protease inhibitor (*Protease Inhibitor Cocktail Tablets; Roche Diagnostics, Indianapolis, IN*). Proteins were extracted from the cell lysates by centrifugation (*14000 rpm for 10 min at 4°C*) and stabilized with a loading buffer and a heating step at 76°C for 11 min. The loading buffer includes NuPage<sup>®</sup> LDS Sample Buffer (*Novex<sup>®</sup>, Carlsbad, CA*) and NuPage<sup>®</sup> Sample Reducing Agent (*Invitrogen<sup>™</sup>, Carlsbad, CA*). The protein extracts with loading buffer were used for western blot analyses and the remaining protein extracts without loading buffer were used for the total protein quantification. The quantification was done by the Pierce<sup>®</sup> BCA Protein Assay Kit (*Thermo Fisher Scientific Inc., Rockford, IL*). The BCA assay kit comes with a reagent A, a reagent B and ten albumin standards which were used to create a standard curve for the calculation of the protein concentration in the samples. The reagents were mixed together in a ratio of 1:50 and added to the blank sample (*only lysis buffer*), protein samples and to the standard samples. The standard samples also included the lysis buffer. All samples were analyzed in duplicates. The IT was 30 – 60 min at 37°C. Since the samples were pipetted in a 96-well plate the absorbance of

each sample was measured by the plate reader DTX 880 Multimode Detector (*Beckman Coulter, Inc., Brea, CA*), which also can function as a spectrophotometer. The average absorbance measurement of the blank sample was subtracted from all the other samples. The standard curve and the protein concentrations were determined by Microsoft Excel to calculate the volume for 10 µg lysate protein.

### **2.3.2. Western blotting**

Protein extracts were separated with the polyacrylamide gel “NuPage<sup>®</sup> 4 – 12% Bis-Tris Gel” (*Novex<sup>®</sup>, Carlsbad, CA*) in running buffer (*NuPage<sup>®</sup> MES SDS Running buffer 20X; Novex<sup>®</sup>, Carlsbad, CA*) at 100 volt (V) for around 1,5 hours. Each sample contained 10 µg of protein lysate. The gel was transferred to a PVDF (*polyvinylidene difluoride*) membrane (*Amersham Hybond<sup>TM</sup>-P; GE Healthcare, Buckinghamshire, UK*) in ice cold transfer buffer (*Tris-Glycine Transfer Buffer 25X; Novex<sup>®</sup>, Carlsbad, CA*) with methanol (*Fisher Scientific, Fair Lawn, NJ*) at 100 V for around 1,5 hours. Depending on the primary antibody (AB) the membrane was blocked for 1 hour in PBS containing 0,1% Tween 20 (*PBS-T*) with 5% nonfat milk (*Blotting-Grade Blocker; Bio-Rad Laboratories, Inc., Hercules, CA*) or 5% bovine serum albumin (*BSA; Sigma-Aldrich, Co., St. Louis, MO*). After the blocking step the membrane was exposed to various primary antibodies overnight at 4°C, beside the primary antibody against GAPDH (*glyceraldehyde 3-phosphate dehydrogenase*), which had an IT of 1 hour at RT. Primary antibodies included pAKT Ser473 (*phospho-AKT serin 473*), tAKT (*total AKT*), pERK1/2 Thr202/Tyr204 (*phospho-ERK1/2 threonine 202/tyrosine 204*), tERK1/2 (*total ERK1/2*), pMEK Ser217/221 (*phospho-MEK serin 217/221*), tMEK1/2 (*total MEK1/2*), P-p90RSK Thr359/Ser363 (*phospho-p90RSK (ribosomal S6 kinase) threonine 359/serin 363*), tRSK (*total RSK*) and GAPDH. Next, the membrane was washed three times with PBS-T and incubated with the secondary antibody conjugated to horseradish peroxidase for 1 hour at RT. Secondary antibodies included anti-mouse and anti-rabbit and were used depending on what the origin of the primary antibody was. All primary and secondary antibodies were purchased from Cell Signaling Technology<sup>®</sup> (*Danvers, MA*). The following table (see *Table 2*) shows the dilution of each antibody that was used, as well as the molecular weight (*kDa*) of the protein to detect and the origin of the antibody.

AB	Dilution	MW (kDa)	Origin
pAKT	1:1000	60	mouse
tAKT	1:1000	60	rabbit
pERK1/2	1:1500 or 1:2500*	42,44	rabbit
tERK1/2	1:1500	42,44	rabbit
pMEK	1:1500	45	rabbit
tMEK	1:1500	45	rabbit
pRSK	1:1000	90	rabbit
tRSK	1:1000	90	rabbit
GAPDH	1:5000	37	rabbit
Anti-rabbit	1:3500		
Anti-mouse	1:3500		

**Table 2: Primary and secondary antibodies of western blot analyses.** This table shows the dilution of the antibodies (AB) which were used for the western blot analyses. It also includes the molecular weight (MW) and origin of each primary antibody. \* The dilution 1:1500 was used for the samples: M370, M230 and M285. The dilution 1:2500 was used for the western blot samples: M410, M243 and M318.

The immunoreactivity was detected by using the enhanced chemiluminescence (ECL) kit Pierce<sup>®</sup> ECL 2 Western Blotting Substrate (*Thermo Fisher Scientific Inc., Rockford, IL*) and visualized by scanning the membrane with a Typhoon 9410 scanner (*Amersham Biosciences Co, Piscataway, NJ*). Another way to visualize the reactivity was to place an autoradiography film (*Kodak X-Omat LS film, Sigma-Aldrich, Co., St. Louis, MO*) on the western blot and developing the film in a dark room with the film processor SRX-101A (*Konica Minolta Medical Imaging USA, Inc., Wayne, NJ*). This method was only done if the visualization of the immunoreactivity with the Typhoon scanner wasn't detectable, given that the film processor method is more sensitive than the Typhoon scanner. The scanned protein bands were put together with Adobe<sup>®</sup> Photoshop<sup>®</sup> Elements 7.0 (*Adobe Systems Incorporated, San José, CA*) and quantified by using the software ImageQuant<sup>®</sup> 5.2 (*Molecular Dynamics, Inc., Sunnyvale, CA*) and Microsoft Excel.

### 2.3.3. Stripping of western blots

To reanalyze the same membrane against a different protein, the blot was first embedded in a solution with acetone (*Fisher Scientific, Fair Lawn, NJ*) and methanol for at least 48 hours to remove the chemiluminescence signal of the ECL kit. Then the membrane was put for few seconds (sec) in methanol and washed in distilled water ( $dH_2O$ ) once and three times in PBS-T. This was followed by incubating the membrane for 15 min at RT in stripping buffer (*Restore™ Western Blot Stripping Buffer, Thermo Fisher Scientific Inc., Rockford, IL*), which would remove the primary and secondary AB. The membrane was washed again three times with PBS-T and blocked for 30 min at RT with 5% nonfat milk or 5% BSA in PBS-T depending on the primary antibody. The membrane was probed again with a different primary antibody. The further steps to analyze the WB were the same as described in chapter 2.3.2.

## 2.4. Cell cycle and apoptosis analyses by flow cytometry

Six melanoma cells lines M410, M370, M318, M243, M230 and M285 were seeded in 6-well plates (*200.000 cells per well*). On the following day the media was replaced with new media containing DMSO as a vehicle control, 1  $\mu$ M staurosporine (*induces cell apoptosis*<sup>66</sup>, *therefore it was a positive control for apoptosis*), 1  $\mu$ M ERKi, 1  $\mu$ M AKTi, 1  $\mu$ M mTORi, 1  $\mu$ M ERKi in combination with 1  $\mu$ M AKTi or 1  $\mu$ M ERKi in combination with 1  $\mu$ M mTORi. In total there were seven conditions. The IT of these seven conditions was 48 hours. After the IT the floating as well as the adherent cells were collected by trypsinization and fixed for 20 min at 4°C with BD Cytifix/Cytoperm™ solution (*BD Biosciences, San Diego, CA*) and washed once with BD Perm/Wash™ Buffer 1X (*BD Biosciences, San Diego, CA*). For apoptosis analyses, cells were stained with the antibody Alexa Flour® 700 Mouse Anti-Cleaved PARP (*BD Pharmingen™, BD Biosciences, San Diego, CA*) for 30 min on ice, followed by washing the cells with BD Perm/Wash™ Buffer 1X. One extra sample, which was incubated with DMSO, was not stained with anti-cleaved PARP. This unstained sample was necessary for the gating procedure which will be explained in more detail later in this chapter. For cell cycle studies, all samples were stained at least for 3 hours at 4°C in the dark with 3  $\mu$ M 4',6-diamidino-2-phenylindole (*DAPI; Sigma-Aldrich, Co., St. Louis, MO*) solution diluted in PBS containing 1% BSA and 0,1% Nonident P-40. DAPI intercalates to the A-T base pairs. Each DAPI solution had previously been tested with CEN (*chicken*

*erythrocyte nuclei*) for assurance of coefficient of variance. CEN was also used to assess resolution and linearity. All flow cytometry experiments were performed by using the BD LSR II flow cytometer (*BD Biosciences*) and its software BD FACSDiva (*BD Biosciences*). The data were analyzed with FlowJo version 7.6.5 (*Tree Star Inc, Ashland, OR*). Figure 3 demonstrates schematically the gating strategy that was used for this flow experiment. It shows the apoptosis and the cell cycle data of M230 as an unstained DMSO sample (*no anti-cleaved PARP staining*) and as a treated sample with ERKi and AKTi. First the unstained sample was gated (*Figure 3A*) by selecting only the singlet (*one cell as an event*) to discriminate the doublet (*two cells as an event*). The gate of the unstained sample (*Figure 3B*) was then overlaid over the other samples (*Figure 3F*), so that only the cleaved PARP positive cells were counted for the apoptosis analysis. Cell cycle analyses (*Figure 3C, G*) were done by FlowJo. By changing the parameters of the x- or y-axis it was possible to show DAPI and cleaved PARP positive cells (*Figure 3D, H*).

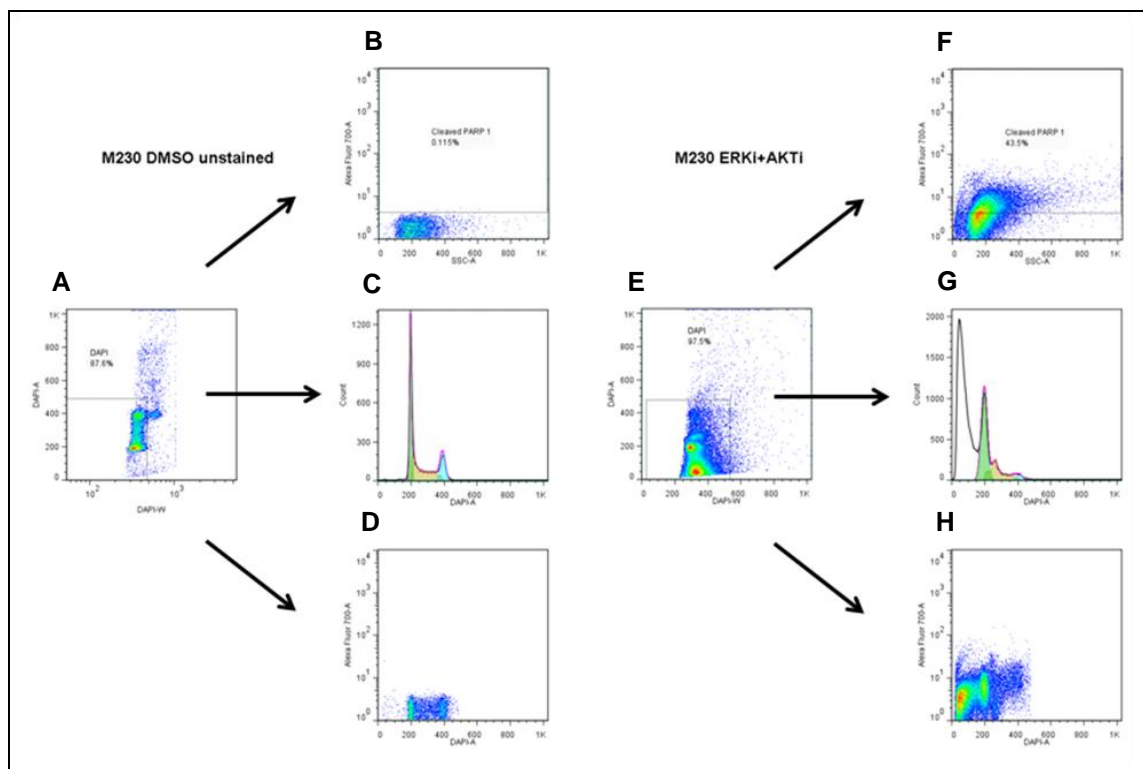


**Figure 3: Gating strategy of cell cycle and apoptosis analyses.** Left column (A-D) shows M230 DMSO unstained sample (*no anti-cleaved PARP staining*) and right column shows (E-H) M230 treated with ERKi and AKTi. A, E: gating of singlet. B, F: gating of cleaved PARP. C, G: cell cycle progression, DAPI (x-axis), cell count (y-axis). D, H: DAPI (x-axis) and cleaved PARP (y-axis) positive cells.



It was planned to repeat each experiment at least three times, but it could be only repeated two times independently, since the flow cytometer had some technical issues which couldn't be fixed on time.

## **2.5. Statistical analyses**

The data of growth assays were analyzed by determining the  $IC_{50}$  values, which define the concentration of the drugs that inhibited 50% of cell growth. These values were calculated on the basis of the growth inhibition curves with Microsoft Excel. Furthermore the Chou-Talalay method for drug combination studies was used to analyze the combination index (*CI*) by the software CalcuSyn Version 2.0 (Biosoft<sup>®</sup>, Cambridge, United Kingdom). The *CI* indicates the quantitative definition for synergism  $CI < 1$ , additive effect  $CI = 1$  or antagonism  $CI > 1$  in drug combinations<sup>67, 68</sup>.

Error bars in the graphs (see *chapter 3. Results*) represent the standard deviation (*STDV*) of the mean value, which were done by Microsoft Excel or GraphPad Prism. An unpaired, one tailed t-test was performed by GraphPad Prism in the apoptosis analyses and p-values  $< 0,05$  were considered to be statistically significant.

### 3. Results

This chapter is summarizing all the important data of this study. First the *BRAF* mutant melanoma cell lines are presented followed by the *NRAS* mutant melanoma cell lines and WT melanoma cell lines. The results include the growth assay data showing the cell growth inhibition curves of the tested drugs, the calculation of the  $IC_{50}$  and CI values. The results of protein studies are presented by western blots and their quantifications. The last data shows the cell cycle and apoptosis studies.

#### 3.1. *BRAF* mutant melanoma cell lines

##### 3.1.1. Growth inhibitory effects of the inhibitors

All 15 *BRAF* mutant melanoma cell lines were tested in duplicates with ERKi in combination with AKTi and ERKi in combination with mTORi. As a comparison, the sensitivity to ERKi was also determined. The cell lines with good results according to their  $IC_{50}$  values, in total 9, were selected for testing the drugs individually, which means the cells were treated in duplicates for monotherapy with AKTi or mTORi. The cell lines with monotherapy and combinatorial data were candidates for determining synergy, intermediate sensitivity and antagonism using the CI. Every experiment was repeated three times ( $n = 6$ ).

The most frequent observed *BRAF* mutation was *BRAF*<sup>V600E</sup>. This mutation is present in 14 of 15 cell lines. Only M381 contains *BRAF*<sup>V600R</sup> substitution<sup>63</sup>. Among the 15 cell lines, sensitivity to ERKi or ERKi combined with AKTi or ERKi combined with mTORi fell into three groups: sensitive ( $IC_{50} < 1 \mu M$ ), intermediate sensitivity ( $IC_{50} 1 - 2 \mu M$ ) and resistant ( $IC_{50} > 2 \mu M$ ). The course of growth inhibition curves was also taken into consideration to determine the sensitivity of the cell lines to the different inhibitors.

The following figures (*Figure 4 – 7*) show the growth inhibition curves of the tested cell lines. Table 3 summarizes the  $IC_{50}$  values of single agent (*monotherapy*) as well as in combination (*combinatorial treatment*). In addition as a comparison the sensitivity to vemurafenib (*BRAF*i) is also shown, which was determined previously by the Dr. Ribas lab<sup>11, 58, 63</sup>. Furthermore the CI is also included in this table. Figure 8 is showing the  $IC_{50}$  values visually as a bar graph.

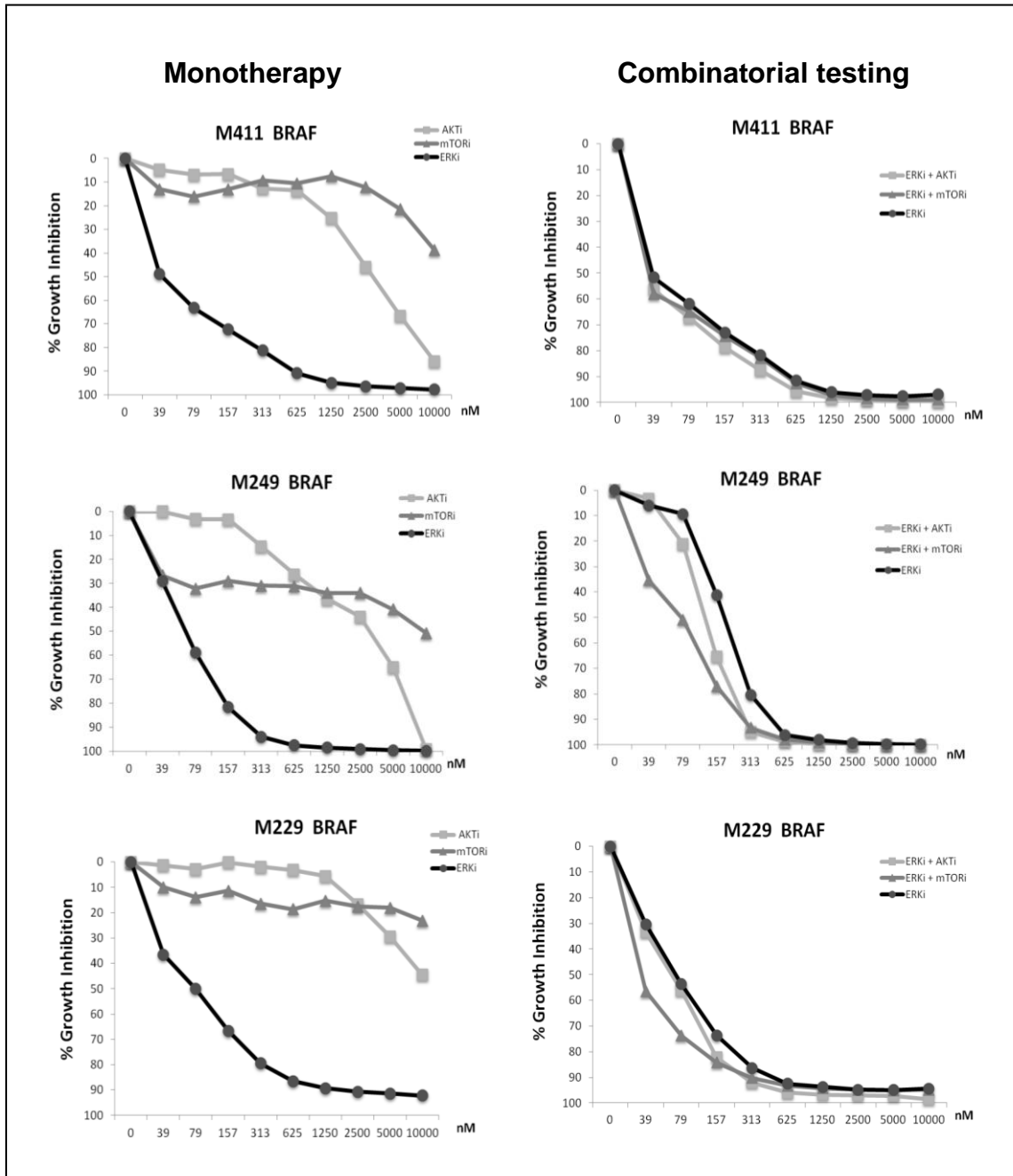


**Figure 4: Growth inhibition curves of treated *BRAF* mutant melanoma cell lines I.** Three *BRAF* mutant melanoma cell lines (*M411*, *M249* and *M229*) are shown in this figure. The left column shows the effect of testing the drugs in monotherapy and the right column shows as comparison the combinatorial testing of the drugs in the same cell lines. After 120 hours treatment with 0 – 10  $\mu$ M ERKi (circles; left and right column), AKTi (squares; left column), mTORi (triangles; left column), ERKi + AKTi (squares; right column) or ERKi + mTORi (triangles; right column) cell viability was determined by bioluminescence assay. Results are representative data in duplicates from three independent experiments ( $n = 6$ ).

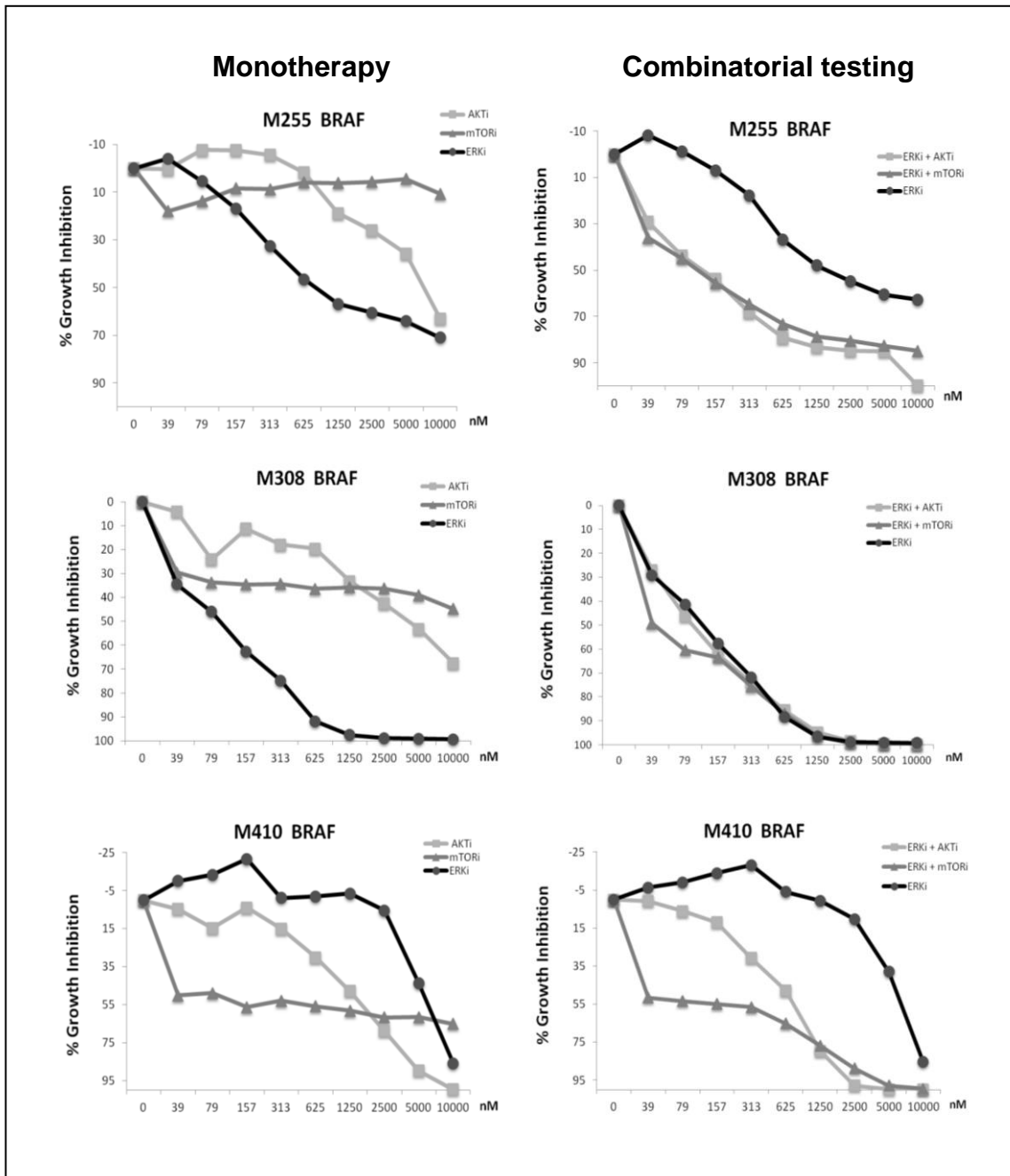


**Figure 5: Growth inhibition curves of treated *BRAF* mutant melanoma cell lines II.** Three *BRAF* mutant melanoma cell lines (*M255*, *M308* and *M410*) are shown in this figure. The left column shows the effect of testing the single drugs and the right column shows the effect of the drugs in combination. After 120 hours treatment with 0 – 10  $\mu$ M ERKi (circles; left and right column), AKTi (squares; left column), mTORi (triangles; left column), ERKi + AKTi (squares; right column) or ERKi + mTORi (triangles; right column) cell viability was determined by bioluminescence assay. Results are representative data in duplicates from three independent experiments ( $n = 6$ ).

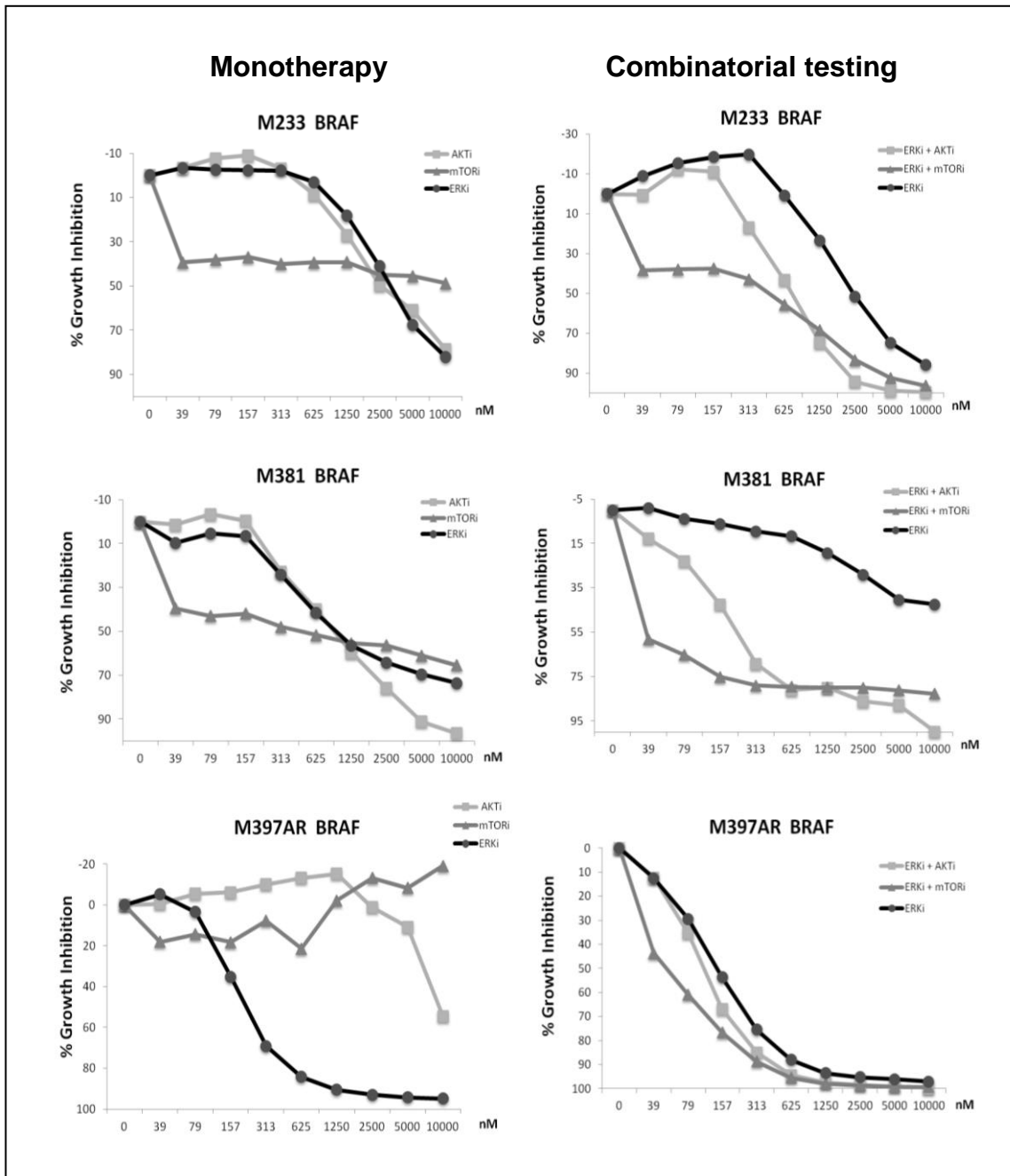


**Figure 6: Growth inhibition curves of treated *BRAF* mutant melanoma cell lines III.** Three *BRAF* mutant melanoma cell lines (*M233*, *M381* and *M397AR*) are shown in this figure. The left column shows the effect of testing the drugs in monotherapy and the right column shows the combinatorial testing of the drugs. After 120 hours treatment with 0 – 10  $\mu\text{M}$  ERKi (circles; left and right column), AKTi (squares; left column), mTORi (triangles; left column), ERKi + AKTi (squares; right column) or ERKi + mTORi (triangles; right column) cell viability was determined by bioluminescence assay. Results are representative data in duplicates from three independent experiments ( $n = 6$ ).

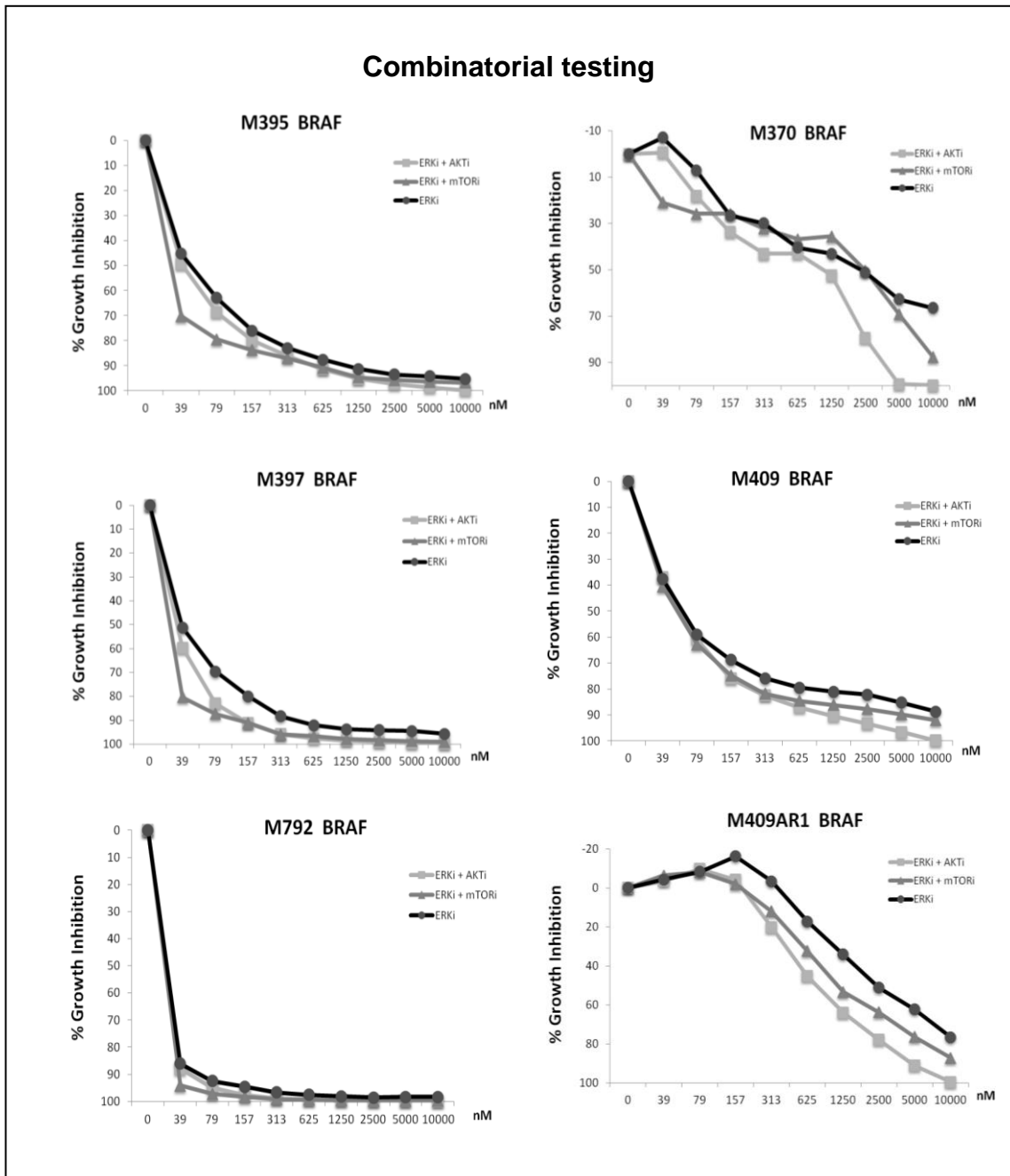


**Figure 7: Growth inhibition curves of treated *BRAF* mutant melanoma cell lines IV.** Six *BRAF* mutant melanoma cell lines (*M395*, *M370*, *M397*, *M409*, *M792* and *M409AR1*) are shown in this figure. Both columns show the combinatorial testing of the drugs. After 120 hours treatment with 0 – 10  $\mu$ M ERKi (*circles*), ERKi + AKTi (*squares*) or ERKi + mTORi (*triangles*) cell viability was determined by bioluminescence assay. Results are representative data in duplicates from three independent experiments ( $n = 6$ ).

<b>BRAF</b>		<b>Average of IC<sub>50</sub> (nM)</b>					<b>CI</b>	
<b>BRAFi</b>	<b>Cell lines</b>	<b>ERKi</b>	<b>AKTi</b>	<b>mTORi</b>	<b>ERKi + AKTi</b>	<b>ERKi + mTORi</b>	<b>E + A</b>	<b>E + m</b>
S	M395	9,3	n/a	n/a	9,3	0,1	n/a	n/a
S	M397	2,2	n/a	n/a	0,2	0,1	n/a	n/a
S	M792	0,1	n/a	n/a	0,1	0,1	n/a	n/a
S	M411	79,3	2909,2	47191182,0	18,1	13,1	0,8	0,4
S	M249	273,6	3541,7	4222088,9	192,6	69,9	0,8	0,4
S	M229	29,4	19924348,0	1,5 x 10 <sup>15</sup>	20,8	5,5	1,0	0,2
I	M409	54,0	n/a	n/a	45,6	35,4	n/a	n/a
I	M255	2201,6	12101,2	6,4 x 10 <sup>32</sup>	162,1	81,4	0,1	0,03
R	M308	414,1	3122,2	264491,4	235,5	155,1	0,7	0,4
R	M410	9944,6	914,0	89,7	494,4	64,8	0,3	0,9
R	M233	2273,2	12251,8	6,5 x 10 <sup>15</sup>	714,9	239,1	0,7	0,1
R	M370	2639,8	n/a	n/a	517,0*	2055,2	n/a	n/a
R	M381	17982,7	724,8	213,3	389,5	16,9	0,5	0,1
R	M397AR	176,5	434431,3	8,1 x 10 <sup>11</sup>	100,3	32,8	0,7	0,3
R	M409AR1	2120,7	n/a	n/a	863,5*	1253,5	n/a	n/a

■ Resistant (R)     
■ Intermediate (I)     
■ Sensitive (S)

**Table 3: IC<sub>50</sub> and CI values of BRAF mutant melanoma cell lines after treating with ERKi, AKTi, mTORi, ERKi combined with AKTi or ERKi combined with mTORi.** The cells were exposed to 0 – 10 µM of ERKi, AKTi, mTORi or the combination of drugs (*ERKi + AKTi*; *ERKi + mTORi*). After 120 hours treatment the cell viability was determined by bioluminescence assay. Results are the mean of the representative data in duplicates from two or three independent experiments. Cells are sensitive (S; *green*) if the IC<sub>50</sub> value is less than 1 µM, intermediate sensitive (I; *yellow*) if IC<sub>50</sub> is 1 – 2 µM and resistant (R; *red*) when IC<sub>50</sub> is more than 2 µM. Combination index values (CI) for ERKi combined with AKTi (*E + A*) and ERKi combined with mTORi (*E + m*) are also presented. Values less than 1 indicates synergism, CI = 1 indicates an additive effect and CI > 1 indicates antagonism. This table also includes as a comparison the sensitivity to vemurafenib (*BRAFi*), which was determined previously by the Dr. Ribas lab<sup>11, 58, 63</sup>. n/a: not applicable. \* M370 and M409AR1 show both in this table a sensitive value for IC<sub>50</sub>, but comparing with the growth inhibition curve in figure 7, it didn't show any improvement in the combinatorial treatment and therefore M370 and M409AR1 were considered as intermediate sensitive to ERKi combined with AKTi.

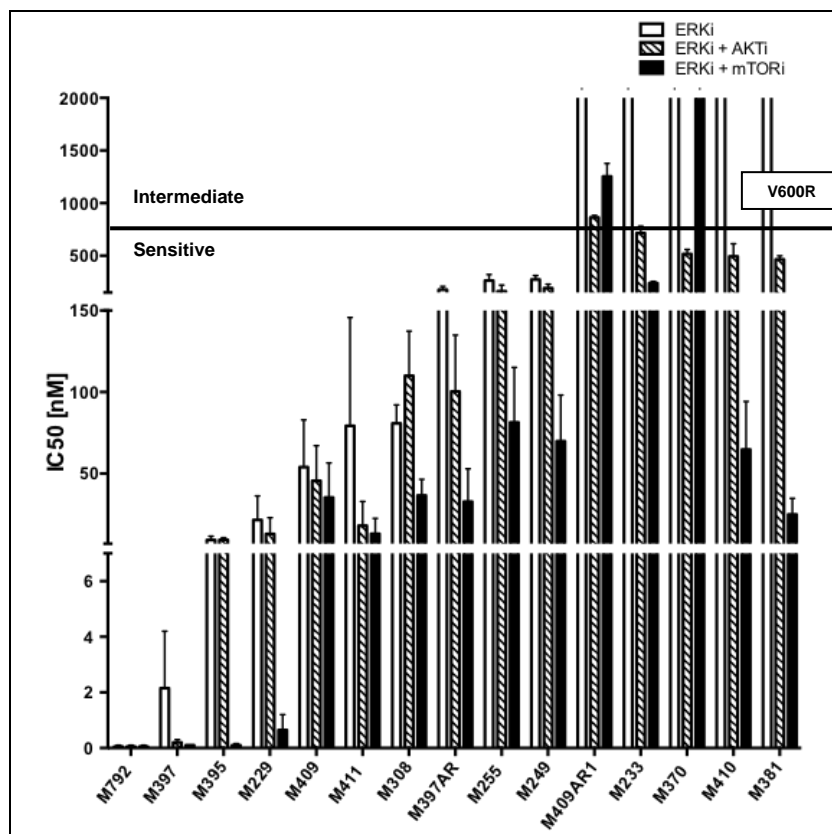


**Figure 8: Bar graph of  $IC_{50}$  values of *BRAF* mutant melanoma cells treated with ERKi, ERKi combined with AKTi or ERKi combined with AKTi.** *BRAF* mutant melanoma cell lines were exposed to 0 – 10  $\mu$ M ERKi (white bars) or ERKi combined with AKTi (striped bars) or ERKi combined with mTORi (black bars) for 120 hours. Cell viability was determined by ATP-based bioluminescence assay. The average of  $IC_{50}$  values of two or three independent experiments in duplicates are represented by the bars and the error bars indicate the standard deviation (STDV). M381 has a *BRAF*<sup>V600R</sup> mutation, which is denoted in the bar graph. The rest of the cell lines have a V600E mutation. The horizontal bar at 1  $\mu$ M represents the threshold between sensitive ( $IC_{50} < 1 \mu$ M) and intermediate sensitivity ( $IC_{50} 1 - 2 \mu$ M).  $IC_{50}$  values higher than 2  $\mu$ M indicate resistant cell lines. The cells are arranged to their  $IC_{50}$  values of ERKi (white bars are increasing).

The data of the growth assay studies show that the addition of either AKTi or mTORi to ERKi resulted in more potent cell growth inhibition compared to ERKi alone. Nine *BRAF* mutant melanoma cell lines were sensitive to ERKi with  $IC_{50}$  less than 1  $\mu$ M and six cell lines were resistant to ERKi. These six cell lines were M255, M410, M233, M370, M381 and M409AR1. The combination of the drugs showed that 13 cell lines



were sensitive to ERKi combined with AKTi. Despite M370 and M409AR1 had a sensitive IC<sub>50</sub> value, the growth inhibition graph of these cell lines didn't showed any improvement in the combinatorial treatment and therefore M370 and M409AR1 were considered as intermediate sensitive to ERKi combined with AKTi. 13 cell lines were sensitive to ERKi in combination with mTORi. Only M370 still remained to be resistant and M409AR1 showed intermediate sensitivity after treating with ERKi combined with mTORi. More importantly, the cell lines M255, M410, M233 and M381, which were sensitive to the combined treatment (*ERKi + AKTi*) but only resistant to ERKi, were intermediate sensitive (*M255*) or resistant (*M410, M233 and M381*) to vemurafenib (*BRAF<sub>i</sub>*). The non-V600E mutant melanoma cell line M381 was resistant to ERKi and as well as to BRAFi but was sensitive to ERKi combined with AKTi and ERKi combined with mTORi. Furthermore M233 has an AKT1 amplification and a *PTEN* homozygous deletion, whereas M255 has an *AKT2* amplification. Also M249 has an *AKT2* amplification as well as a *PTEN* deletion, in M229 occurs an *AKT1* amplification and M308 has an *AKT2* amplification too, but all these three cell lines were sensitive to ERKi in monotherapy and to the combinatorial treatments. These oncogenic events were previously tested<sup>58</sup>. In general, cell lines sensitive to ERKi were also sensitive to the combination of the drugs with lower IC<sub>50</sub> values. Furthermore the combination ERKi and mTORi also showed lower IC<sub>50</sub> values in the majority of cell lines (*12 out of 15*) compared to ERKi combined with AKTi. To understand whether the enhanced growth inhibition of the cells by the combined treatment were additive or synergistic, the CI values of the two combined drugs at IC<sub>50</sub> were calculated. All nine cell lines showed synergy (*CI < 1 μM*) combining ERKi with mTORi. Combining ERKi with AKTi showed also synergistic effect in all cell lines, except M299, which had only an additive effect (*CI = 1*).

### **3.1.2. Effects of the inhibitors on signaling pathway**

Western blot analyses were performed to determine the effects of ERKi combined with AKTi or mTORi on the MAPK- and PI3K/AKT pathway. The cell line M410, which was sensitive to both combined treatments, but resistant to ERKi alone and M370, which was resistant to the inhibitors alone and to the combination ERKi with mTORi, but intermediate sensitive to ERKi combined with AKTi, were selected to analyze the differences in the signaling pathways. Both cell lines were resistant to BRAFi. The aim of this selection was to have a cell line that had a good (*M410*) and not so good (*M370*) response to the combinatorial testing. This was specified by the differences between

the IC<sub>50</sub> value of ERKi alone compared to the IC<sub>50</sub> values of the combinatorial testing. The good responding cell line had a greater difference between the IC<sub>50</sub> values than the not so good responding cell line. In addition M410 demonstrated good synergy for the combinatorial treatments. Based on previous studies, 24 hours was selected as an optimal time point to compare the signaling in the cells<sup>11</sup>. After this 24 hours incubation of DMSO and the inhibitors with or without in combination, western blot analyses were performed, which is shown in figure 9, including the quantification of western blots. Figure 10 visualizes the quantification data as a bar graph.

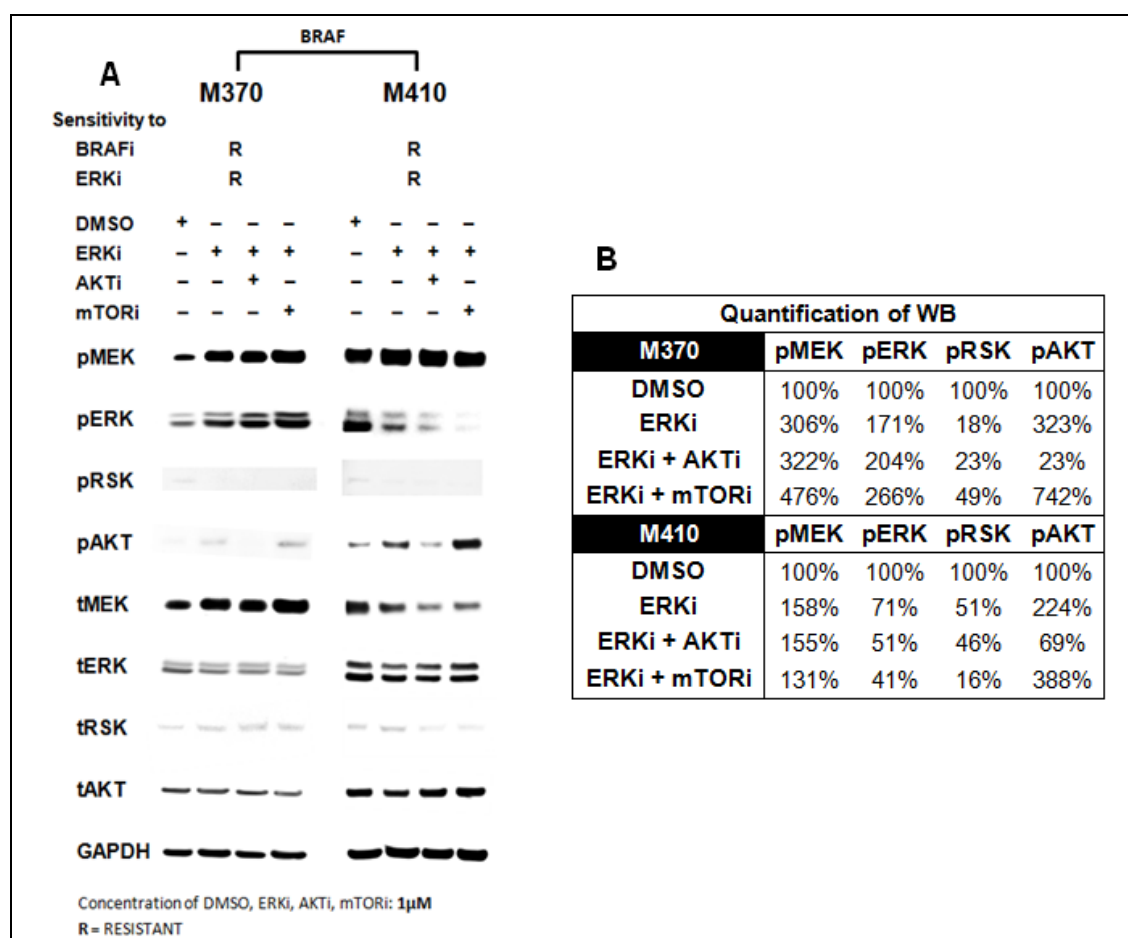


**Figure 9: Western blot analyses of BRAF mutant melanoma cells after exposure to DMSO, ERKi, ERKi combined with AKTi or ERKi combined with mTORi for 24h.** **A.** The cells M370 and M410 were treated with 1 µM DMSO (*solvent control*), ERKi, ERKi combined with AKTi or ERKi combined with mTORi for 24h. The effects of the various inhibitors are shown by determining phosphorylated (*p*) or total (*t*) MEK, ERK1/2, RSK and AKT. GAPDH served as loading control between the different conditions. M370 was resistant to ERKi + mTORi and intermediate sensitive to ERKi + AKTi. M410 was sensitive to the combinatorial treatments. Both cell lines were resistant to BRAFi and ERKi alone. R: resistant. **B.** This table presents the quantification of only the phosphorylated proteins.

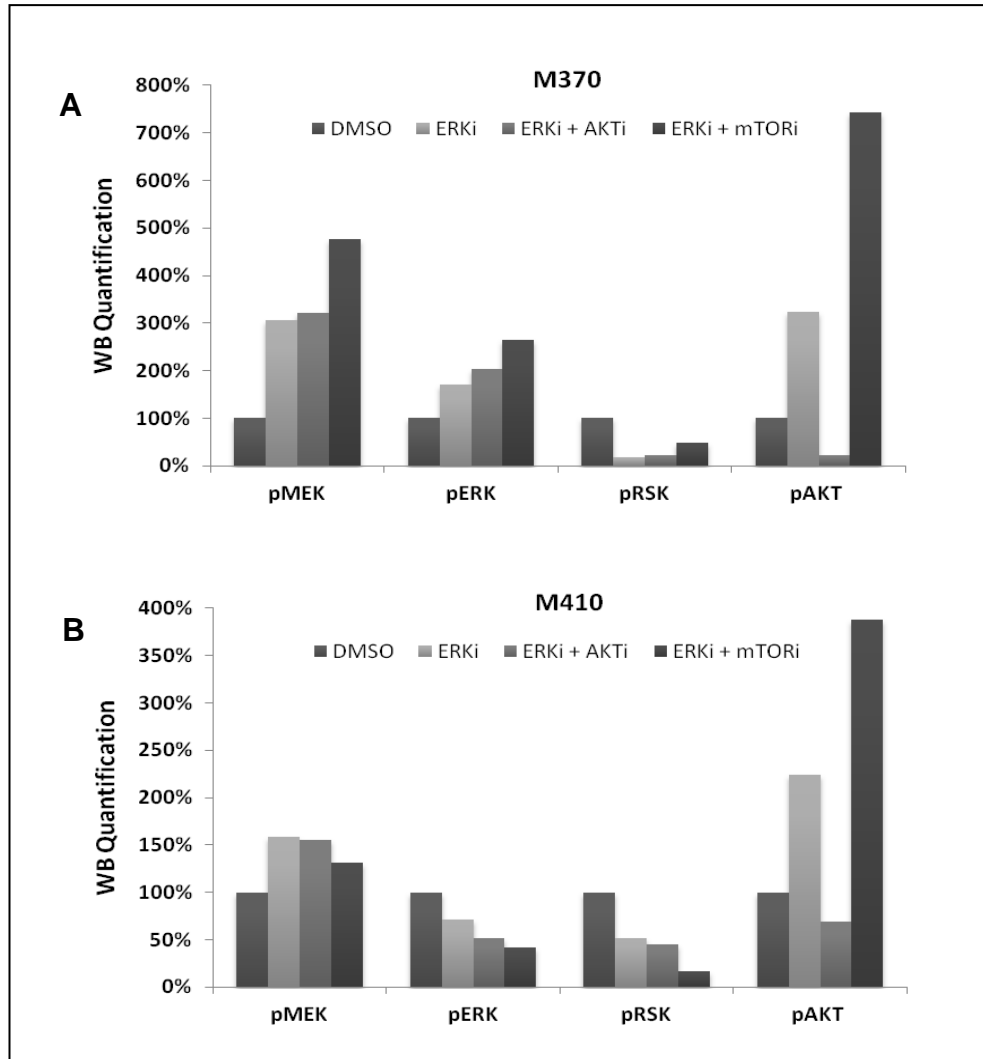


**Figure 10: Quantification of phosphorylated proteins of *BRAF* mutant melanoma cells after exposure to DMSO, ERKi, ERKi combined with AKTi or ERKi combined with mTORi for 24h.** In this figure the phosphorylated (*p*) proteins: MEK, ERK1/2, RSK and AKT are quantified. **A.** M370 was resistant to ERKi + mTORi and intermediate sensitive to ERKi + AKTi. **B.** M410 was sensitive to the combinatorial treatments.

The baseline for the phospho protein levels was the corresponding solvent control (*cells incubated for 24h DMSO*), which was quantified as 100%. For M370, treatment with ERKi and the two combinations resulted in an increase in pMEK and pERK but a decrease in pRSK. Protein pRSK was only decreased partially with the treatment ERKi combined with mTORi (49%) compared to ERKi alone (18%). The protein pAKT was only decreased with the treatment ERKi combined with AKTi (23%), which correlated with the results in the growth inhibition (*M370 was intermediate sensitive to ERKi +*

*AKTi*). Treatment with ERKi and ERKi combined with mTORi resulted in an increase in pAKT. M410 had an increase in pMEK level with all the treatments and pERK was decreased with the combinatorial treatment (*ERKi + AKTi: 51%; ERKi + mTORi: 41%*) more than the monotherapy with ERKi (*71%*). ERKi combined with mTORi decreased pRSK the most with 16% compared to ERKi (*51%*) or ERKi combined with AKTi (*46%*). Protein pAKT was decreased with ERKi combined with AKTi but increased in ERKi and ERKi combined with mTORi. Total proteins had no changes in both cell lines, besides tMEK, which was tested again but with the same results. GAPDH, as expected, had in both cell lines and in all conditions the same protein levels (*loading control*).

### **3.1.3. Effects of the inhibitors on cell cycle and apoptosis**

To test the effects of ERK and AKT or mTOR inhibition on cell cycle progression and apoptosis, cells were treated with ERKi, AKTi, mTORi, ERKi combined with AKTi or mTORi for 48 hours. The cells were also incubated with 1  $\mu$ M staurosporine, which was representing the positive control for apoptosis. The cells were stained with DAPI and intracellularly for cleaved PARP and analyzed by flow cytometry. The *BRAF* mutant cell lines M370 and M410 were chosen for cell cycle and apoptosis studies with the same selection criterions of western blot analyses. M370 was resistant to ERKi combined with mTORi and intermediate sensitive to ERKi combined with AKTi. M410 was sensitive to the combinatorial treatments. Both cell lines were resistant to BRAFi and ERKi alone.

The following figures 11 and 12 are presenting the cell cycle progression and apoptosis, whereby figure 12 is showing these data quantitative as bar graphs. Table 4 is also presenting the cell cycle progression and apoptosis data quantitative. Table 5 shows the p-values of the unpaired, one tailed t-test, which was performed to compare ERKi in monotherapy with the combinatorial treatments regarding to the apoptotic effects of the inhibitors. The percentages of cleaved PARP in the different conditions were compared for this statistical test. p-values < 0,05 were considered to be statistically significant.

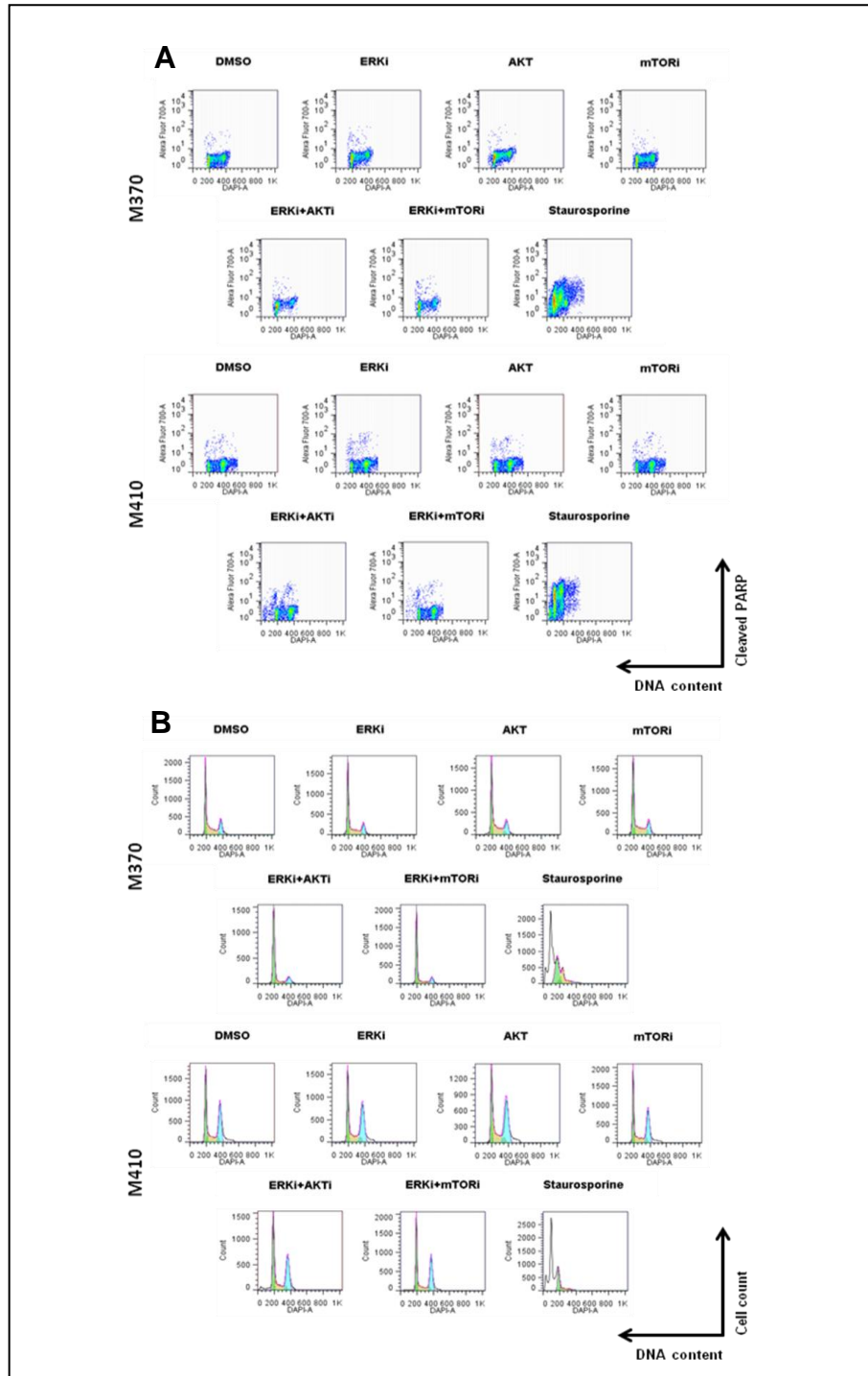


**Figure 11: Cell cycle progression and apoptosis in *BRAF* mutant melanoma cell lines after exposure to DMSO, ERKi, AKTi, mTORi, ERKi combined with AKTi or ERKi combined with mTORi and staurosporine for 48h. M370 and M410 are shown in this figure. Figures are representative of duplicate experiments. **A.** Induced apoptosis was tested by cleaved PARP (*y-axis*). DAPI (*x-axis*). **B.** Cell cycle progression was determined by DAPI staining solution (*x-axis*). Cell count (*y-axis*).**

Quantitative analysis of apoptosis and cell cycle (%)										
M370	Average					STDV				
	PARP	Sub-G1	G1	S	G2	PARP	Sub-G1	G1	S	G2
DMSO	5,225	0,945	48	36,6	25	1,69	1,336	9,051	1,697	2,121
ERKi	20,35	5,375	49,7	31,05	16,85	2,192	0,488	2,828	2,758	1,202
AKTi	21,445	2,875	48,65	35,1	21,7	18,463	1,478	6,576	0,99	0,141
mTORi	5,195	1,72	48,55	34,4	21,5	0,417	2,432	7,566	4,243	1,131
ERKi + AKTi	23,7	7,015	62,4	21,1	15,45	2,404	5,353	6,223	3,677	6,435
ERKi + mTORi	22,55	5,48	60,4	21,85	14,35	1,061	0,891	4,808	1,768	3,465
Staurosporine	62,7	87,4	8,61	4,37	0,12	n/a	n/a	n/a	n/a	n/a
M410	Average					STDV				
	PARP	Sub-G1	G1	S	G2	PARP	Sub-G1	G1	S	G2
DMSO	2,83	1,555	30	25,3	50,4	1,344	0,771	0,707	0,566	8,91
ERKi	4,59	2,205	31	26,45	45,8	2,249	0,841	0,141	2,192	1,838
AKTi	3,825	1,795	36,35	24,05	47,65	0,332	0,742	1,626	2,758	6,01
mTORi	3,63	2,515	33,95	22,4	49,3	0,283	1,266	2,192	1,273	0,849
ERKi + AKTi	13,25	1,385	45,5	19,95	40,3	4,455	0,191	8,344	1,768	8,768
ERKi + mTORi	5,815	3,4	36,3	20,95	44,25	0,389	2,022	0,566	1,485	1,909
Staurosporine	69	66,4	28,4	7,43	0,96	n/a	n/a	n/a	n/a	n/a

**Table 4: Quantitative analysis of cell cycle progression and apoptosis in *BRAF* mutant melanoma cell lines after exposure to DMSO, ERKi, AKTi, mTORi, ERKi combined with AKTi or ERKi combined with mTORi and staurosporine for 48h.** In this table are M370 and M410 presented. The average was calculated from the data of two independently experiments. Every condition besides the incubation of the cells with staurosporine (*positive control for apoptosis*) was done twice. Percentage of apoptotic cells positive for cleaved PARP is shown in the first column. Quantitative analysis of cell cycle progression by DAPI staining using flow cytometry shows the percentage of cells in sub-G1 (*equivalent to G0*), G1, S-phase and G2. n/a: not applicable. STDV: standard deviation.

p-values of t-test		
Cleaved PARP	M370	M410
ERKi vs. ERKi + AKTi	0,14	0,07
ERKi vs. ERKi + mTORi	0,16	0,26

**Table 5: Statistical analyzing with t-test of cleaved PARP in *BRAF* mutant melanoma cell lines.** M370 and M410 are shown in this table. ERKi in monotherapy was compared with the combinatorial treatments (*ERKi + AKTi*, *ERKi + mTORi*) for apoptosis. p-values < 0,05: statistically significant.

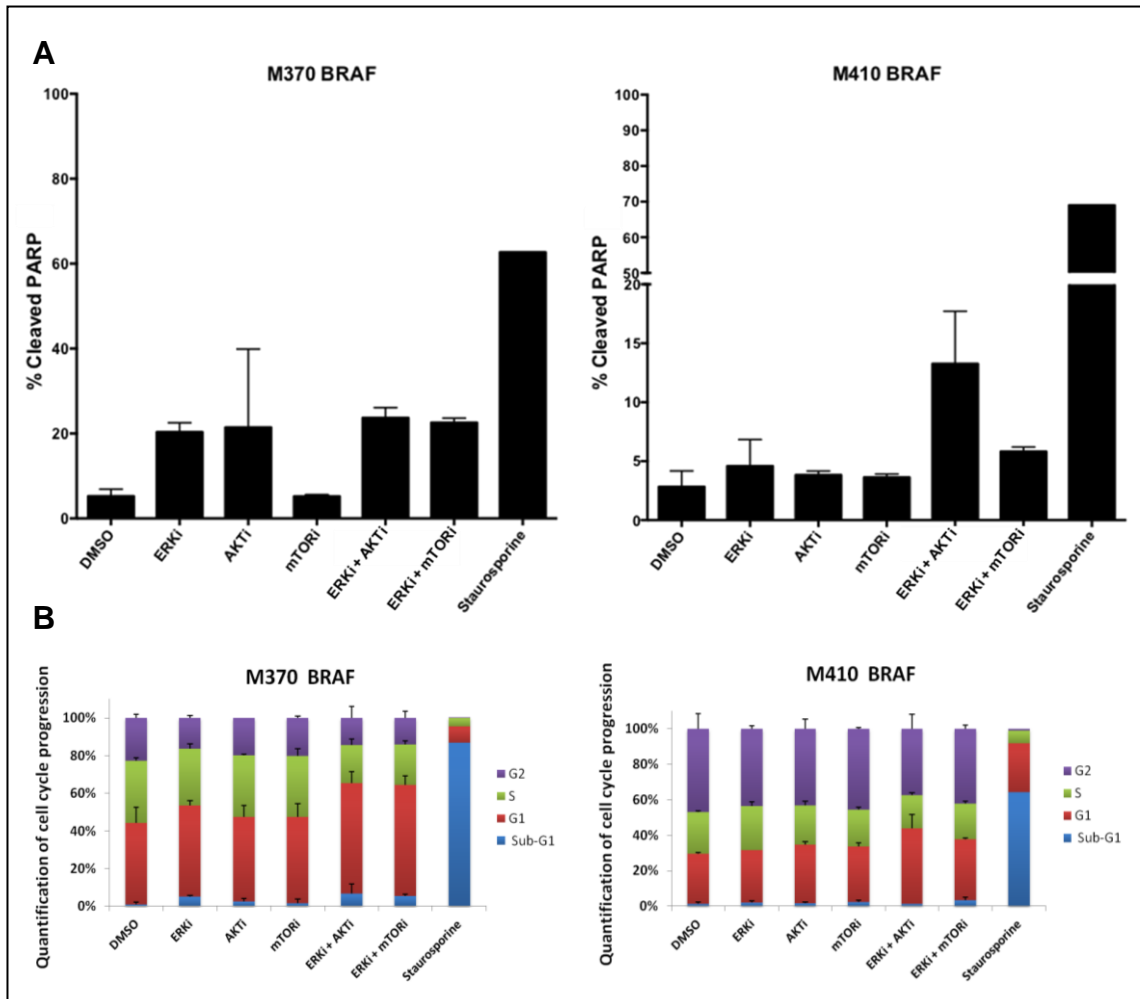


**Figure 12: Apoptosis and cell cycle progression in *BRAF* mutant melanoma cell lines after exposure to DMSO, ERKi, AKTi, mTORi, ERKi combined with AKTi or ERKi combined with mTORi and staurosporine for 48h.** M370 was resistant to ERKi + mTORi and intermediate sensitive to ERKi + AKTi. M410 was sensitive to the combinatorial treatments. Both cell lines were resistant to BRAFi and ERKi alone. **A.** Percentage of apoptotic cells positive for cleaved PARP is shown. Bars represent mean values of two independent experiments ( $n=2$ ). Error bars indicate the standard deviation (*STDV*). **B.** Quantitative analysis of cell cycle progression by DAPI staining using flow cytometry shows the percentage of cells in sub-G1 (equivalent to *G0*; blue), G1 (red), S-phase (green) and G2 (purple). Bars represent mean values of two independent experiments ( $n=2$ ). Error bars indicate the standard deviation (*STDV*).

Cleaved PARP levels which indicate apoptotic cells were slightly elevated in the different treatments of the resistant cell line M370, but between the conditions were no considerable changes to determine. Whereas the combined treatment ERKi with AKTi in M410 had the highest level of cleaved PARP compared to ERKi, AKTi, mTORi in

monotherapy or ERKi combined with mTORi (*Figure 12, Table 4*). Despite the combinatorial treatments had in both cell lines the highest level of cleaved PARP compared to ERKi alone, there was no statistically significant difference to observe (*Table 5*). This probably could be overcome by adding a third independent experiment to these existing data.

Cell cycle data showed in both cell lines that treatment with all inhibitors in monotherapy or in combination resulted in increased levels of sub-G1 (G0), G1 and decrease in S, G2 compared to the vehicle control DMSO. The combinatorial treatments had higher values in sub-G1 and G1 compared to ERKi alone. Overall between the conditions in both cell lines the cell cycle phases had no significant differences.

## **3.2. NRAS mutant melanoma cell lines**

### **3.2.1. Growth inhibitory effects of the inhibitors**

In total 11 *NRAS* mutant melanoma cell line were evaluated for sensitivity to ERKi, ERKi combined with AKTi and ERKi combined with mTORi. Six cell lines were tested with the drugs alone to determine the CI. Every experiment was repeated in duplicates three times ( $n = 6$ ).

Among the 11 *NRAS* mutant melanoma cells, four of them had a *NRAS*<sup>Q61K</sup> mutation (*M244, M245, M408, SKMEL-173*), three were *NRAS*<sup>Q61R</sup> (*M296, M412-A, M412-B*) mutated, another three harbored a *NRAS*<sup>Q61L</sup> mutation (*M311, M318, WM1366*) and the last cell line M243 was *NRAS*<sup>Q61H</sup> mutated<sup>63</sup>.

The figures 13 till 15 present the growth inhibitions curves of *NRAS* mutant melanoma cell lines. Table 6 summarizes the IC<sub>50</sub> values with the CI data. All *NRAS* melanoma cell lines in this study were resistant to vemurafenib, since they don't harbor a *BRAF* mutation. Figure 16 shows the average of the IC<sub>50</sub> values as a bar graph.



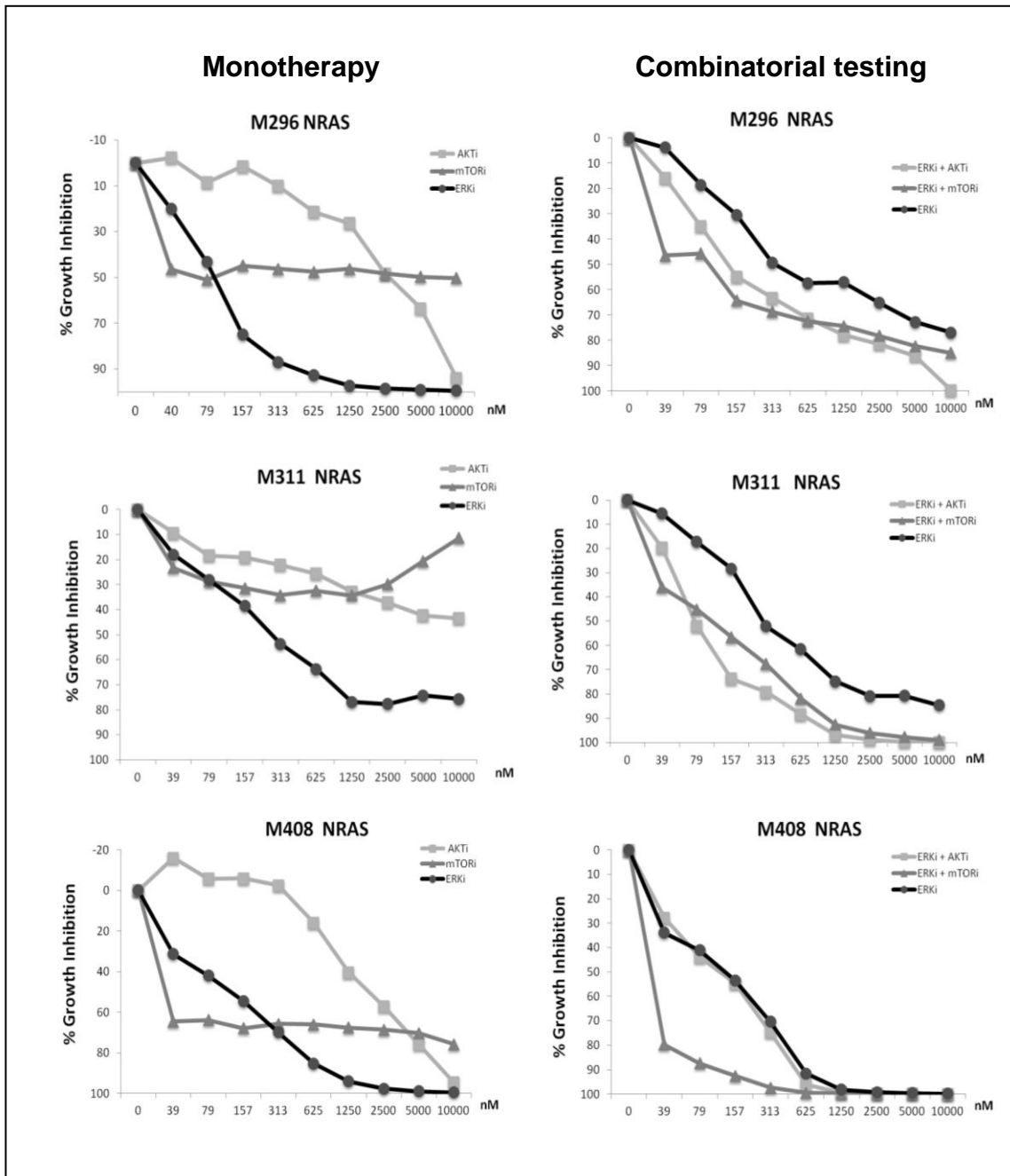


**Figure 13: Growth inhibition curves of treated *NRAS* mutant melanoma cell lines I.** Three *NRAS* mutant melanoma cell lines (*M296*, *M311* and *M408*) are shown in this figure. The left column shows the effect of testing the drugs in monotherapy and the right column shows as a comparison the combinatorial testing of the drugs in the same cell lines. After 120 hours exposing the cells with 0 – 10  $\mu$ M ERKi (circles; left and right column), AKTi (squares; left column), mTORi (triangles; left column), ERKi + AKTi (squares; right column) or ERKi + mTORi (triangles; right column) cell viability was determined by bioluminescence assay. Results are representative data in duplicates from three independent experiments ( $n = 6$ ).

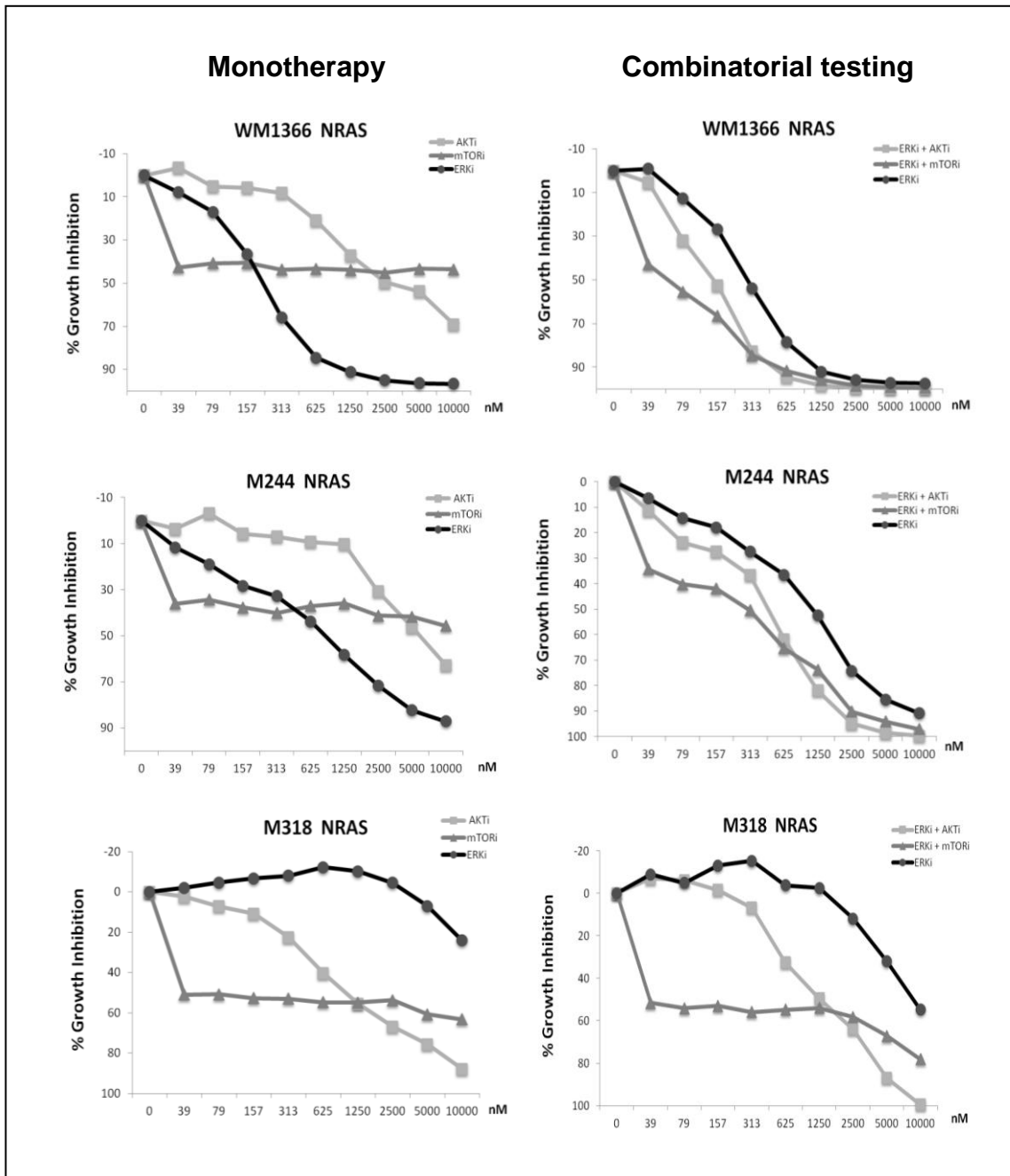


**Figure 14: Growth inhibition curves of treated *NRAS* mutant melanoma cell lines II.** Melanoma cell lines containing *NRAS* mutation (*WM1366*, *M244* and *M318*) are shown in this figure. The left column shows the effect of testing the single drugs and the right column shows the effect of the drugs in combination. After 120 hours treatment with 0 – 10  $\mu$ M ERKi (circles; left and right column), AKTi (squares; left column), mTORi (triangles; left column), ERKi + AKTi (squares; right column) or ERKi + mTORi (triangles; right column) cell viability was determined by bioluminescence assay. Results are representative data in duplicates from three independent experiments ( $n = 6$ ).

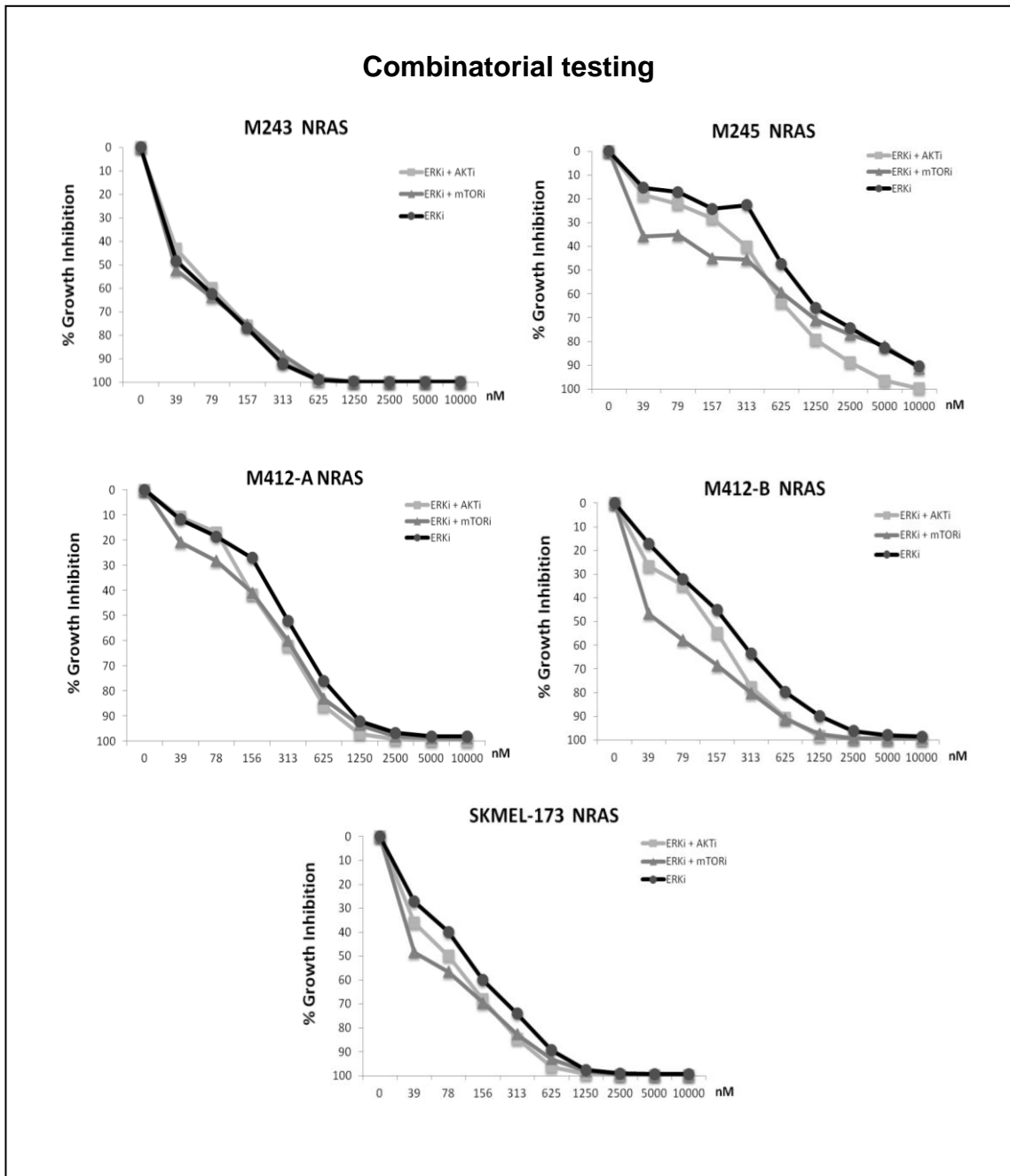


**Figure 15: Growth inhibition curves of treated NRAS mutant melanoma cell lines III.** Five NRAS mutant melanoma cell lines (*M243*, *M245*, *M412-A*, *M412-B* and *SKMEL-173*) are shown in this figure. Both columns show the combinatorial testing of the drugs. After treating the cells for 120 hours with 0 – 10  $\mu$ M ERKi (*circles*), ERKi + AKTi (*squares*) or ERKi + mTORi (*triangles*) cell viability was determined by bioluminescence assay. Results are representative data in duplicates from three independent experiments ( $n = 6$ ).

NRAS		Average of IC <sub>50</sub> (nM)					CI	
BRAFi	Cell lines	ERKi	AKTi	mTORi	ERKi + AKTi	ERKi + mTORi	E + A	E + m
R	M243	9,8	n/a	n/a	11,1	7,9	n/a	n/a
R	M245	445,5	n/a	n/a	286,0	209,5	n/a	n/a
R	M296	480,5	2764,0	25930,2	184,1	66,7	0,4	0,1
R	M311	459,4	21095,7	9,4 x 10 <sup>20</sup>	92,2	136,0	0,2	0,3
R	M408	120,3	2086,2	0,005	66,5	0,1	0,8	23201,0
R	M412-A	399,9	n/a	n/a	243,5	215,6	n/a	n/a
R	M412-B	176,2	n/a	n/a	115,1	26,2	n/a	n/a
R	SKMEL-173	80,0	n/a	n/a	36,7	19,9	n/a	n/a
R	WM1366	342,0	14555,1	567883748,0	168,4	44,3	0,4	0,2
R	M244	705,2	39417,6	5,0 x 10 <sup>13</sup>	393,7	109,5	0,5	0,2
R	M318	37865,2	994,1	124,2	1099,2	51,8	1,7	0,8

■ Resistant (R)    ■ Intermediate (I)    ■ Sensitive (S)

**Table 6: IC<sub>50</sub> and CI values of NRAS mutant melanoma cell lines after exposure to ERKi, AKTi, mTORi, ERKi combined with AKTi or ERKi combined with mTORi.** The cells were treated with 0 – 10 µM of ERKi, AKTi, mTORi or the combination of drugs (*ERKi + AKTi*; *ERKi + mTORi*). After 120 hours incubation of the drugs the cell viability was determined by bioluminescence assay. Results are the mean of the representative data in duplicates from two or three independent experiments. Cells are sensitive (*S*; *green*) if the IC<sub>50</sub> value is less than 1 µM, intermediate sensitive (*I*; *yellow*) if IC<sub>50</sub> is 1 – 2 µM and resistant (*R*; *red*) when IC<sub>50</sub> is more than 2 µM. Combination index values (*CI*) for ERKi combined with AKTi (*E + A*) and ERKi combined with mTORi (*E + m*) are also presented. Values less than 1 indicates synergism, CI = 1 indicates an additive effect and CI > 1 indicates antagonism. All NRAS mutant melanoma cell lines were resistant to vemurafenib since they do not harbor a BRAF mutation. n/a: not applicable.

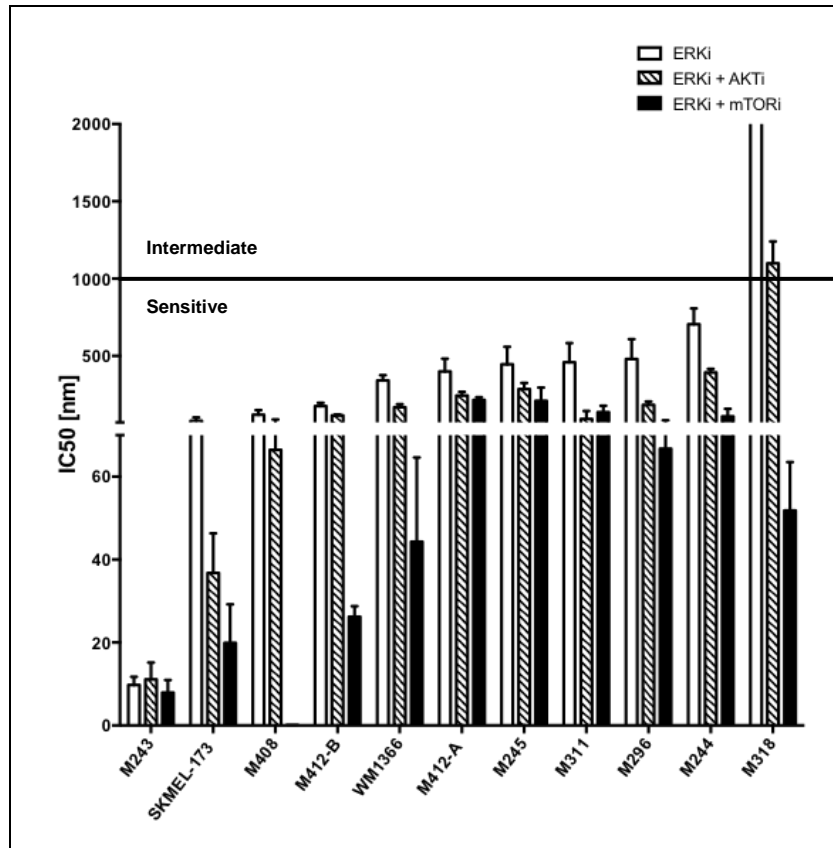


**Figure 16: Bar graph of  $IC_{50}$  values of *NRAS* mutant melanoma cells after exposure to ERKi, ERKi combined with AKTi or ERKi combined with AKTi.** *NRAS* mutant melanoma cell lines were treated with 0 – 10  $\mu$ M ERKi (white bars) or ERKi combined with AKTi (striped bars) or ERKi combined with mTORi (black bars) for 120 hours. Cell viability was determined by ATP-based bioluminescence assay. The average of  $IC_{50}$  values of two or three independent experiments in duplicates are represented by the bars and the error bars indicate the standard deviation (STDV). The horizontal bar at 1  $\mu$ M denotes the threshold between sensitive ( $IC_{50} < 1 \mu$ M) and intermediate sensitivity ( $IC_{50} 1 - 2 \mu$ M).  $IC_{50}$  values higher than 2  $\mu$ M indicate resistant cell lines. The cells are arranged to their  $IC_{50}$  values of ERKi (white bars are increasing).

While all 11 *NRAS* mutant melanoma cell lines were resistant to vemurafenib since they do not harbor a *BRAF* mutation, 10 out of 11 *NRAS* mutant melanoma cell lines were sensitive to ERKi ( $IC_{50} < 1 \mu$ M). Only M318 was resistant to ERKi alone. In general the addition of either AKTi or mTORi to ERKi enhanced the cell growth inhibition compared to ERKi alone, especially in M318, which became intermediate

sensitive to ERKi combined with AKTi and sensitive to ERKi combined with mTORi. In addition the combination ERKi and mTORi showed lower  $IC_{50}$  values in 10 of 11 cell lines compared to ERKi combined with AKTi. The CI values of the combined drugs showed in all cell lines (*beside M408 and M318*) synergistic effects ( $CI < 1$ ). The CI of the combined drugs ERKi and mTORi of M408 had a very high number ( $CI = 23201,0$ ), which indicates antagonism ( $CI > 1$ ), even though the combination of these drugs led to a very good growth inhibition. But this can be explained by the fact that the  $IC_{50}$  value of mTORi alone was already very low ( $IC_{50} = 0,005 \text{ nM}$ ), even lower than the  $IC_{50}$  value of ERKi combined with mTORi ( $IC_{50} = 0,1 \text{ nM}$ ). Therefore the results in very sensitive cell lines should be taken with caution, since the mathematical formula of Chou-Talalay method gave an error number, not being applicable to the sensitivity. The CI of ERKi and AKTi of M318 resulted also in antagonism ( $CI > 1$ ) whereas the CI value in this case was a reasonable value of 1,7 which was calculated by the Chou-Talalay method correctly. The CI of ERKi combined with AKTi indicates in the cell line M318 antagonism because the  $IC_{50}$  of the combination ( $ERKi + AKTi$ ) was higher ( $IC_{50} = 1099,2 \text{ nM}$ ) than the  $IC_{50}$  of AKTi ( $IC_{50} = 994,1 \text{ nM}$ ) alone.

### **3.2.2. Effects of the inhibitors on signaling pathway**

Western blot analyses were performed with M243 and M318 to determine the effects of ERKi combined with AKTi or mTORi on the MAPK- and PI3K/AKT pathway. M243 was sensitive to both combined treatments and ERKi alone. M318 was sensitive to ERKi combined with mTORi, but intermediate sensitive to ERKi combined with AKTi and resistant to ERKi alone. Both cell lines were resistant to BRAFi. M318 showed a greater difference between the  $IC_{50}$  values of ERKi and the combinations of the inhibitors than M243. Therefore was M318 a better responding cell line to the combinatorial treatment than M243. Furthermore M318 demonstrated good synergy for the combination of ERKi and mTORi. After the exposure of DMSO and the inhibitors with or without in combination for 24 hours, western blot analyses were done, which is shown in figure 17, including the quantification of western blots. Figure 18 visualizes the quantification data as a bar graph.

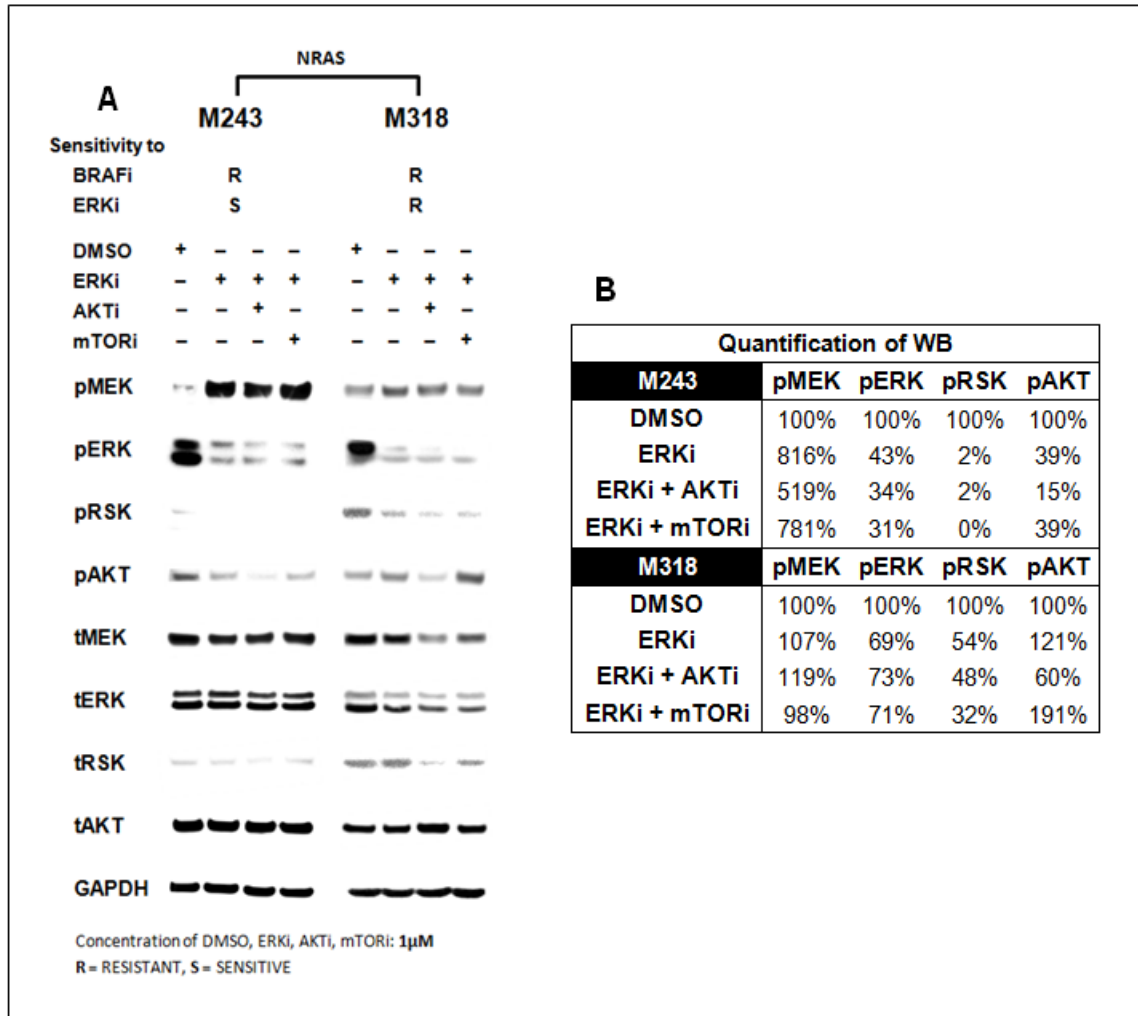


**Figure 17: Western blot analyses of NRAS mutant melanoma cells after exposure to DMSO, ERKi, ERKi combined with AKTi or ERKi combined with mTORi for 24h.** **A.** The cells M243 and M318 were treated with 1  $\mu$ M DMSO (*solvent control*), ERKi, ERKi combined with AKTi or ERKi combined with mTORi for 24h. The effects of the various inhibitors are shown by determining phosphorylated (*p*) or total (*t*) MEK, ERK1/2, RSK and AKT. GAPDH served as loading control between the different conditions. M243 was sensitive to ERKi and the combinatorial treatments. M318 was sensitive to ERKi + mTORi and intermediate sensitive to ERKi + AKTi, but resistant to ERKi alone. Both cell lines were resistant to BRAFi. S: sensitive, R: resistant. **B.** This table presents the quantification of only the phosphorylated proteins.

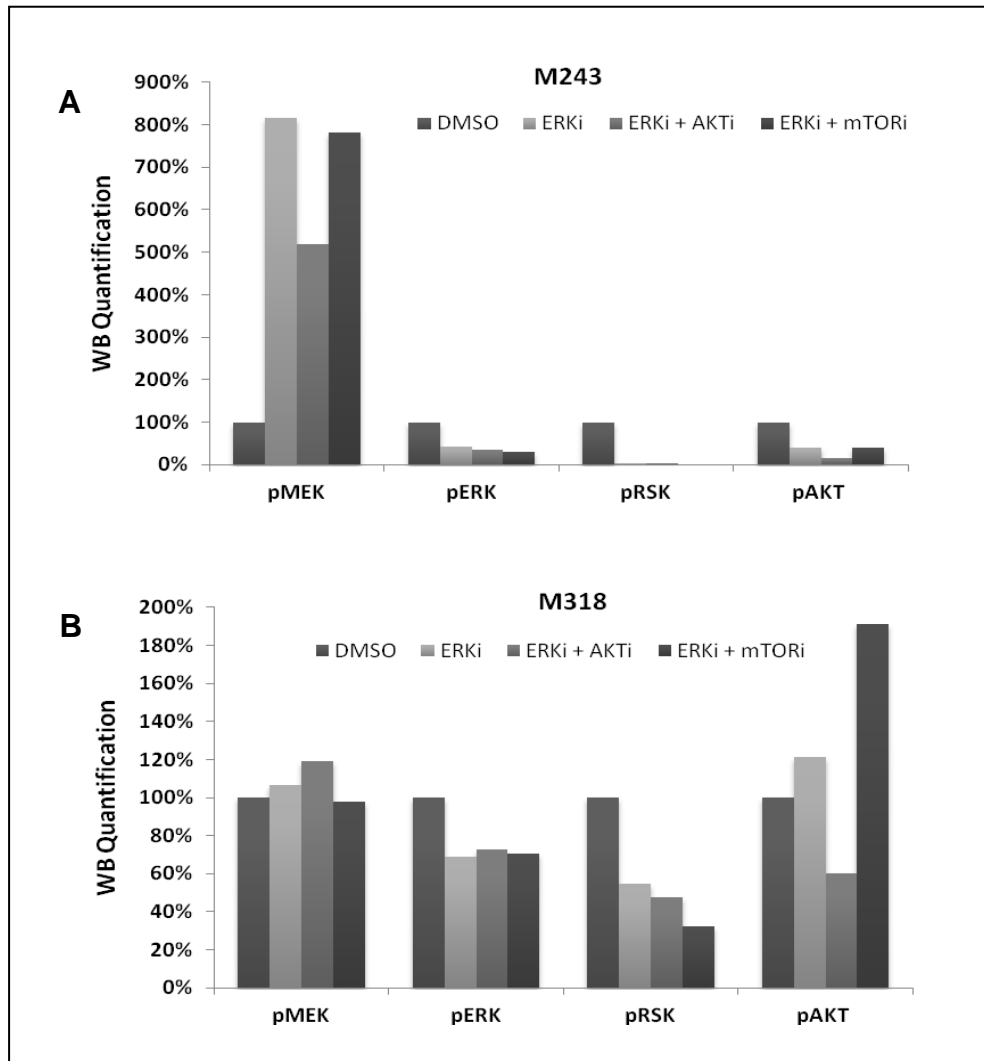


**Figure 18: Quantification of phosphorylated proteins of *NRAS* mutant melanoma cells after exposure to DMSO, ERKi, ERKi combined with AKTi or ERKi combined with mTORi for 24h.** In this figure the phosphorylated (*p*) proteins: MEK, ERK1/2, RSK and AKT are quantified. **A.** M243 was sensitive to all treatments. **B.** M318 was sensitive to ERKi + mTORi and intermediate sensitive to ERKi + AKTi, but resistant to ERKi alone.

As seen in the figures 17 and 18 pMEK levels were increased in M243, when treated with ERKi in monotherapy and as well as with the combinatorial treatments compared to DMSO, the solvent control (*baseline*). Since M243 was very sensitive to all the inhibitors combined or not, it showed after the treatments in pERK, pRSK and pAKT a strong decrease. But the decrease of the protein levels of pRSK did not differ much between the conditions. Protein pERK was more decreased with the combinatorial treatments (*ERKi + AKTi*: 34%; *ERKi + mTORi*: 31%) than with ERKi in monotherapy



(43%). The level of pAKT was inhibited with 15% the most by treating M243 with ERKi combined with AKTi compared to the other two conditions (*ERKi*, *ERKi + mTORi*) with 39%. For M318, treatment with ERKi and ERKi combined with AKTi resulted in an increase in pMEK level, but treating with ERKi combined with mTORi did not show any considerable changes compared to the baseline. The proteins pERK and pRSK were decreased with all the treatments, whereas pRSK was inhibited with ERKi combined with mTORi the strongest (32%) compared to the treatments ERKi alone (54%) and ERKi combined with AKTi (48%). Protein pAKT was increased with ERKi and ERKi combined with mTORi, but inhibited to 60% by ERKi combined with AKTi treatment. GAPDH, as expected, had in both cell lines and in all conditions the same protein levels (*loading control*).

### **3.2.3. Effects of the inhibitors on cell cycle and apoptosis**

Cells were treated with ERKi, AKTi, mTORi, ERKi combined with AKTi or mTORi for 48 hours. The cells were also incubated with 1  $\mu$ M staurosporine, which was the positive control for apoptosis. The effects of ERK and AKT or mTOR inhibition on cell cycle progression and apoptosis were tested. The cells were stained with DAPI and intracellularly for cleaved PARP and analyzed by flow cytometry. The same *NRAS* mutant cell lines (*M243*, *M318*), which were chosen for WB analyses, were also selected for cell cycle and apoptosis studies. M243 was sensitive to ERKi and the combinatorial treatments. M318 was sensitive to ERKi combined with mTORi and intermediate sensitive to ERKi combined with AKTi, but resistant to ERKi alone. Both cell lines were resistant to BRAFi.

The following figures 19 and 20 show the cell cycle progression and apoptosis, whereas figure 20 is presenting these data quantitative as bar graphs. Table 7 shows also the cell cycle progression and apoptosis data quantitative. Table 8 presents the p-values of the t-test. The test compared ERKi in monotherapy with the combinatorial treatments regarding to the apoptotic effects of the inhibitors. The percentages of cleaved PARP in the different conditions were compared for this statistical test. p-values < 0,05 were considered to be statistically significant.

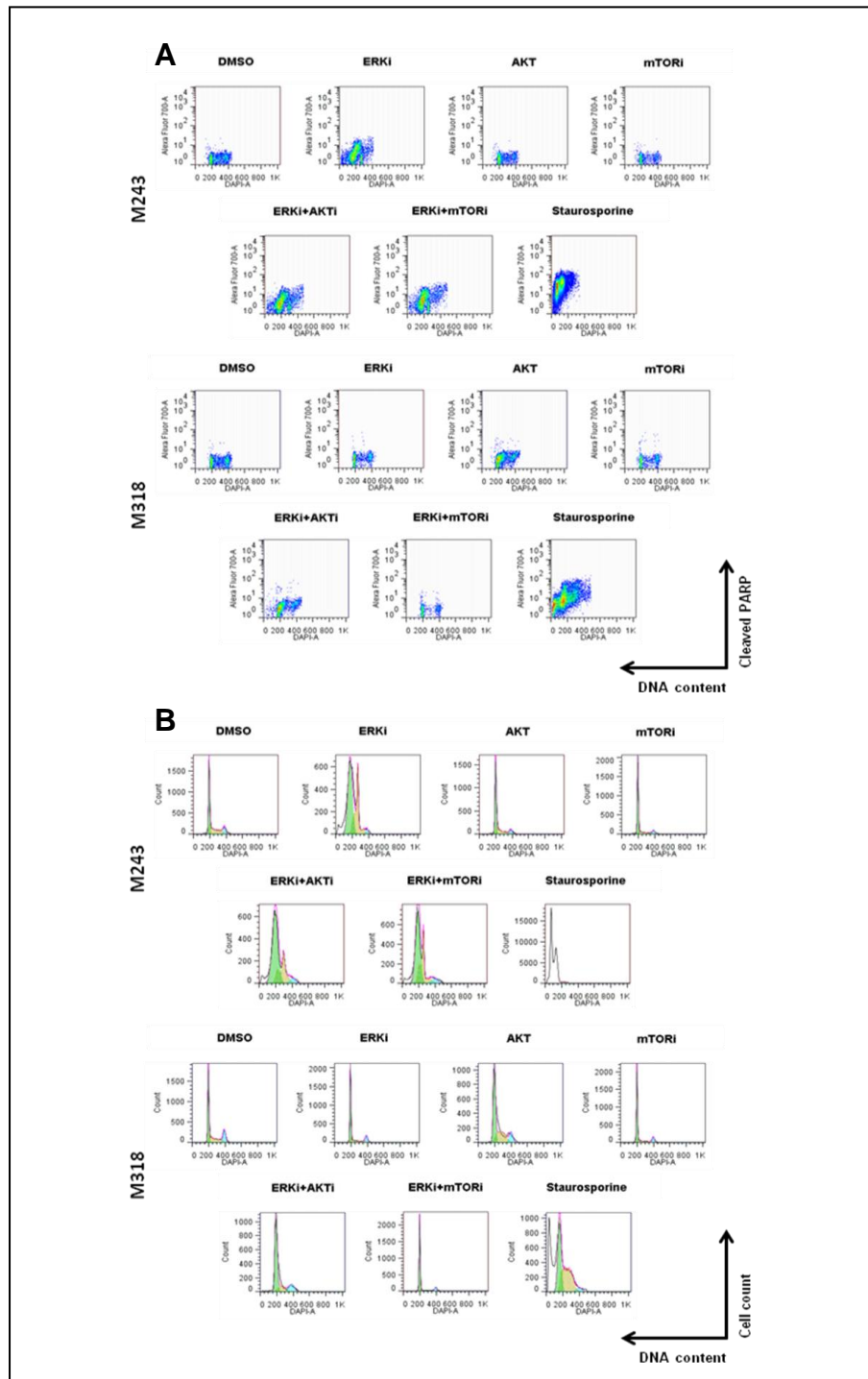


**Figure 19: Cell cycle progression and apoptosis in *NRAS* mutant melanoma cell lines after exposure to DMSO, ERKi, AKTi, mTORi, ERKi combined with AKTi or ERKi combined with mTORi and staurosporine for 48h. M243 and M318 are shown in this figure. Figures are representative of duplicate experiments. **A.** Induced apoptosis was tested by cleaved PARP (*y-axis*). DAPI (*x-axis*). **B.** Cell cycle progression was determined by DAPI staining solution (*x-axis*). Cell count (*y-axis*).**

Quantitative analysis of apoptosis and cell cycle (%)										
M243	Average					STDV				
	PARP	Sub-G1	G1	S	G2	PARP	Sub-G1	G1	S	G2
DMSO	3,164	3,635	47,95	35	15,6	3,261	0,12	5,162	2,828	2,546
ERKi	25,85	7,66	70,8	26,25	7,185	0,919	2,093	0,424	6,435	3,882
AKTi	1,888	2,815	60,55	27,15	10,595	1,657	0,926	1,202	0,212	1,704
mTORi	1,429	3,5	69,2	18,35	11,52	1,076	0,113	0,566	0,636	3,649
ERKi + AKTi	32,7	10,67	63,8	24,8	9,125	5,374	1,174	0,424	2,828	2,369
ERKi + mTORi	38,1	6,965	69,65	31,45	7,055	3,818	0,87	3,323	6,01	0,757
Staurosporine	95,5	95,4	0,86	3,8	0,13	n/a	n/a	n/a	n/a	n/a
M318	Average					STDV				
	PARP	Sub-G1	G1	S	G2	PARP	Sub-G1	G1	S	G2
DMSO	1,525	1,22	49,9	23,5	29,7	0,94	0,099	1,131	6,788	6,364
ERKi	3,62	1,22	62,75	15,2	22,35	1,782	0,042	1,485	4,243	7,425
AKTi	8,505	0,335	49,85	33,55	21,85	4,094	0,474	2,758	7,707	11,243
mTORi	2,09	2,185	65,75	13,45	23,65	0,566	1,138	3,323	3,041	7
ERKi + AKTi	9,86	0,25	65,75	25	14,33	6,703	0,354	11,809	6,223	13,675
ERKi + mTORi	2,1	2,83	69,6	8,25	21,3	0,354	1,131	8,344	1,626	8,344
Staurosporine	69,4	66,1	7,97	24,8	3,02	n/a	n/a	n/a	n/a	n/a

**Table 7: Quantitative analysis of cell cycle progression and apoptosis in *NRAS* mutant melanoma cell lines after exposure to DMSO, ERKi, AKTi, mTORi, ERKi combined with AKTi or ERKi combined with mTORi and staurosporine for 48h.** In this table are M243 and M318 presented. The average was calculated from the data of two independently experiments. Every condition besides the incubation of the cells with staurosporine (*positive control for apoptosis*) was done twice. Percentage of apoptotic cells positive for cleaved PARP is shown in the first column. Quantitative analysis of cell cycle progression by DAPI staining using flow cytometry shows the percentage of cells in sub-G1 (*equivalent to G0*), G1, S-phase and G2. n/a: not applicable. STDV: standard deviation.

p-values of t-test		
Cleaved PARP	M243	M318
ERKi vs. ERKi + AKTi	0,11	0,17
ERKi vs. ERKi + mTORi	0,02*	0,18

**Table 8: Statistical analyzing with t-test of cleaved PARP in *NRAS* mutant melanoma cell lines.** M243 and M318 are shown in this table. ERKi in monotherapy was compared with the combinatorial treatments (*ERKi + AKTi*, *ERKi + mTORi*) for apoptosis. \* p-values < 0,05: statistically significant.

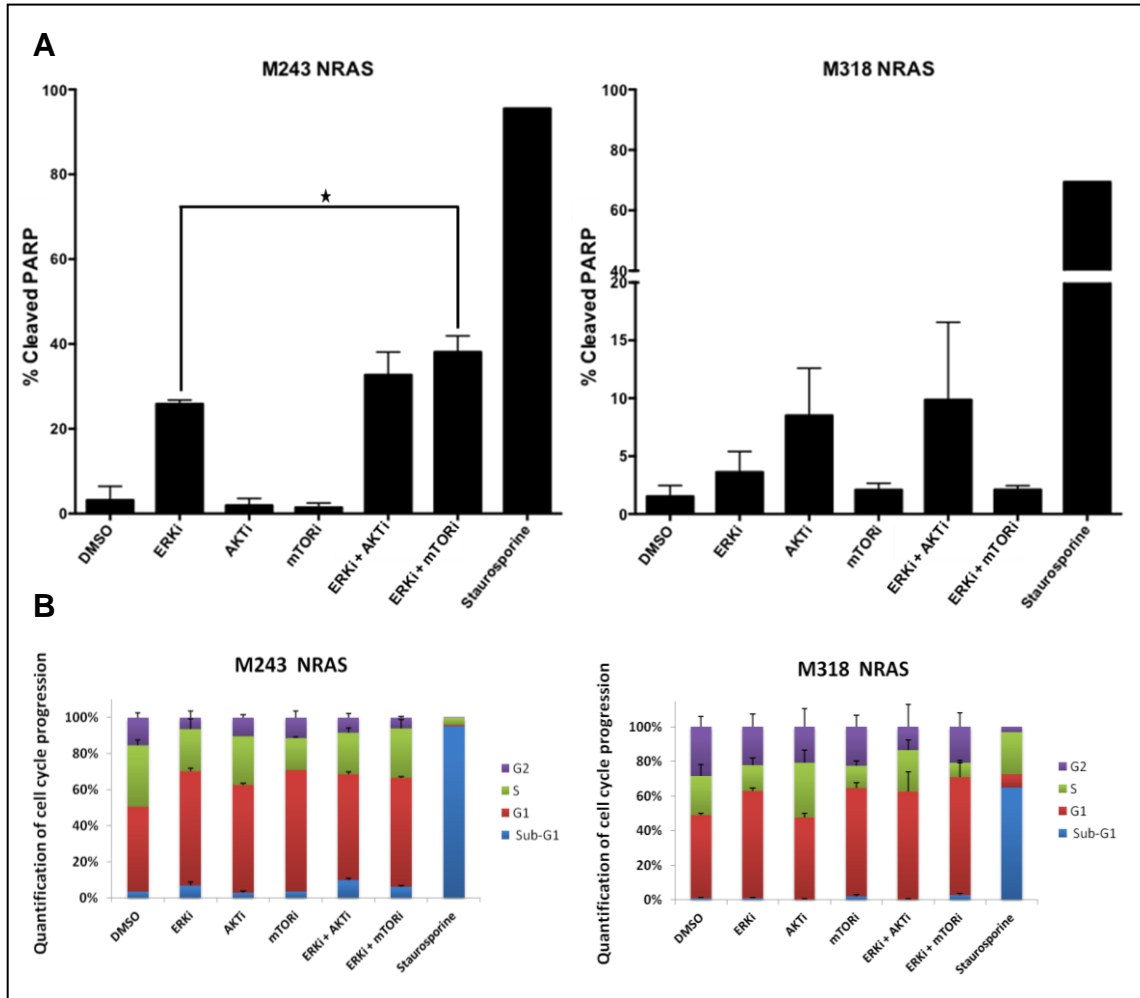


**Figure 20: Apoptosis and cell cycle progression in *NRAS* mutant melanoma cell lines after exposure to DMSO, ERKi, AKTi, mTORi, ERKi combined with AKTi or ERKi combined with mTORi and staurosporine for 48h.** M243 was sensitive to ERKi and the combinatorial treatments. M318 was sensitive to ERKi + mTORi and intermediate sensitive to ERKi + AKTi, but resistant to ERKi alone. Both cell lines were resistant to BRAFi. **A.** Percentage of apoptotic cells positive for cleaved PARP is shown. Bars represent mean values of two independent experiments ( $n=2$ ). Error bars indicate the standard deviation (STDV). \*  $p$ -values < 0,05: statistically significant. **B.** Quantitative analysis of cell cycle progression by DAPI staining using flow cytometry shows the percentage of cells in sub-G1 (equivalent to G0; blue), G1 (red), S-phase (green) and G2 (purple). Bars represent mean values of two independent experiments ( $n=2$ ). Error bars indicate the standard deviation (STDV).

M243 had for the combinatorial treatments higher levels of cleaved PARP, especially for the treatment ERKi combined with mTORi in comparison with ERKi in monotherapy (Figure 20, Table 7). The increase in cleaved PARP of ERKi combined with mTORi was statistically significant (Table 8:  $p$ -value < 0,05) compared to ERKi in monotherapy. Interestingly M318 had the highest level of cleaved PARP in ERKi combined with AKTi, even though M318 was intermediate sensitive for this combinatorial treatment. Compared to the vehicle control DMSO, ERKi alone and ERK combined with mTORi as well as AKTi alone were slightly increased in cleaved PARP (Figure 20, Table 7).

Cell cycle data showed in both cell lines that ERKi in monotherapy, ERKi combined with AKTi and ERKi combined with mTORi resulted in increased levels of sub-G1 (G0), G1 and decrease in S, G2 compared to the vehicle control DMSO. In M318 the combinatorial treatments had higher values in G1 compared to ERKi alone.

### 3.3. Wild-type *BRAF/NRAS* melanoma cell lines

#### 3.3.1. Growth inhibitory effects of the inhibitors

Five *BRAF* and *NRAS* wild-type (WT) melanoma cell line were analyzed for sensitivity to ERKi, ERKi combined with AKTi and ERKi combined with mTORi. Three of these cell lines were tested with the drugs alone to determine the CI. Every cell viability experiment was repeated in duplicates three times ( $n = 6$ ). Across these five *BRAF* and *NRAS* wild-type melanoma cell lines there was one cell line, M418, which is a *KRAS*<sup>G12A</sup> mutant.

The figures 21 and 22 are showing the growth inhibitions curves of WT melanoma cell lines. Table 9 summarizes the IC<sub>50</sub> values with the CI data. Since wild-type melanoma cell lines don't harbor a *BRAF* mutation, they were all resistant to vemurafenib. Figure 23 shows the average of the IC<sub>50</sub> values as a bar graph.

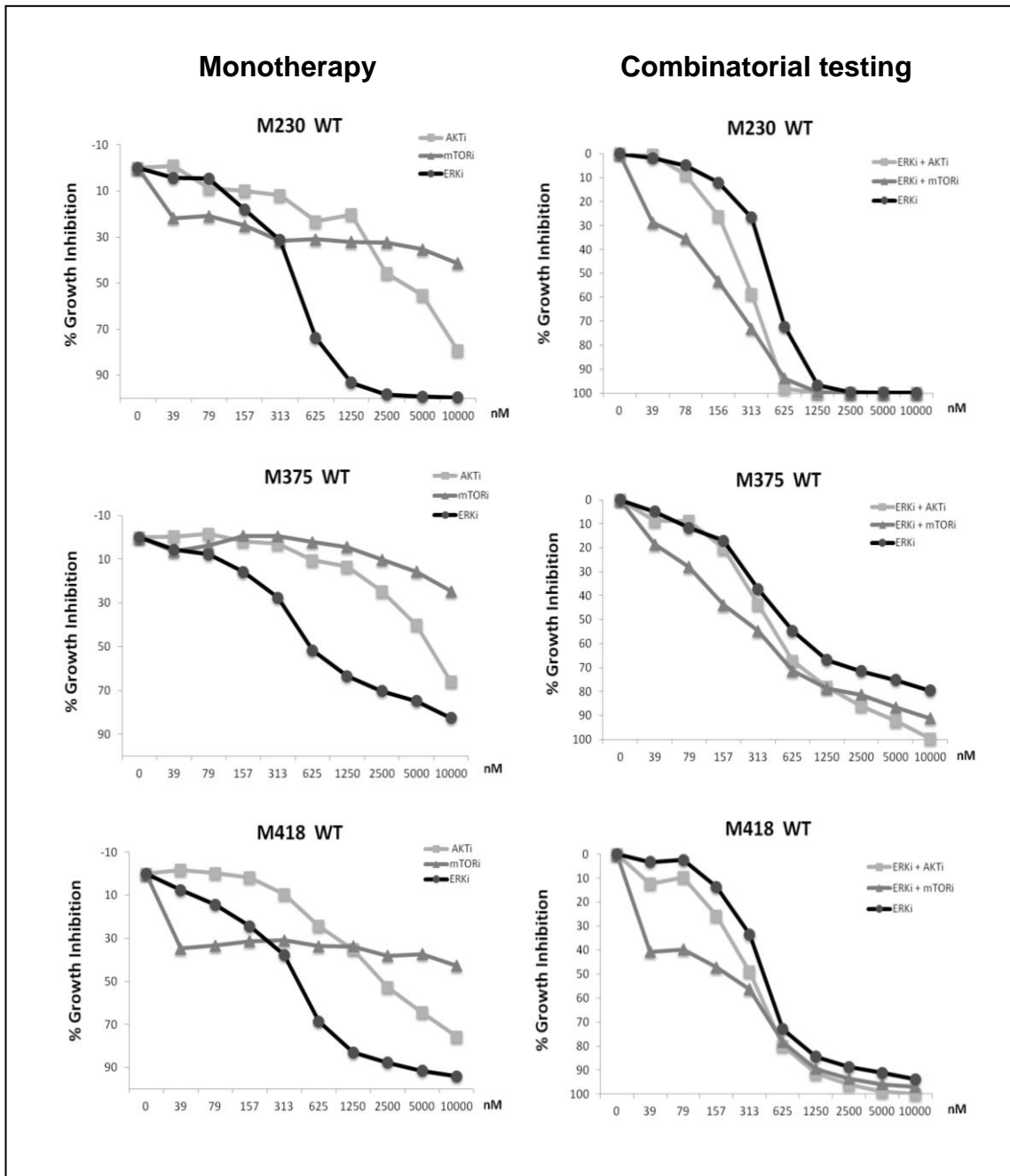


**Figure 21: Growth inhibition curves of treated WT melanoma cell lines I.** Three WT melanoma cell lines (*M230*, *M375* and *M418*) are shown in this figure. The left column shows the effect of testing the drugs in monotherapy and the right column shows as a comparison the combinatorial testing of the drugs in the same cell lines. After 120 hours exposing the cells with 0 – 10  $\mu\text{M}$  ERKi (circles; left and right column), AKTi (squares; left column), mTORi (triangles; left column), ERKi + AKTi (squares; right column) or ERKi + mTORi (triangles; right column) cell viability was determined by bioluminescence assay. Results are representative data in duplicates from three independent experiments ( $n = 6$ ).

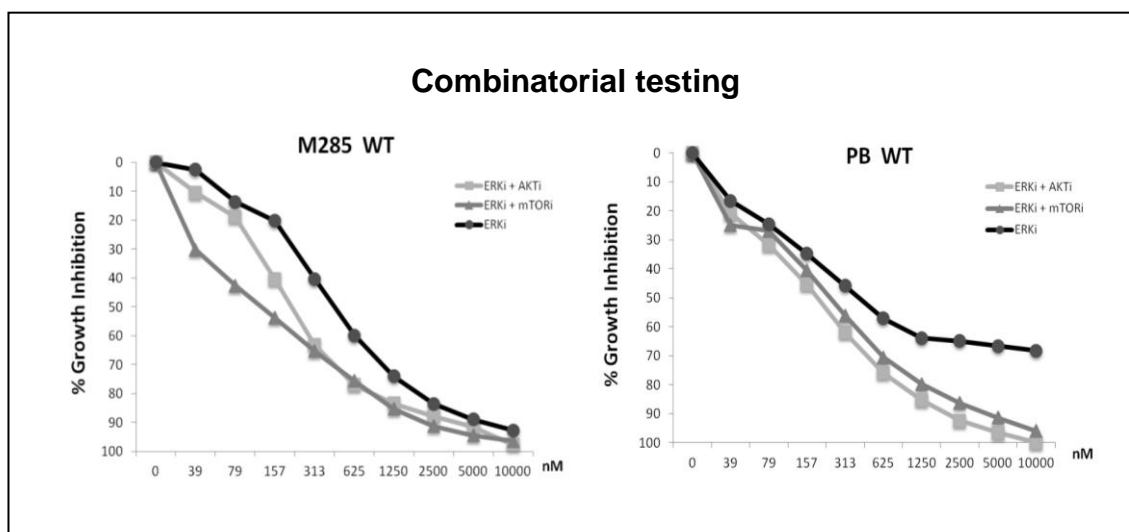


**Figure 22: Growth inhibition curves of treated WT melanoma cell lines II.** The combinatorial testing of the drugs in two WT melanoma cell lines (*M285 and PB*) is shown in this figure. After treating the cells for 120 hours with 0 – 10  $\mu$ M ERKi (*circles*), ERKi + AKTi (*squares*) or ERKi + mTORi (*triangles*) cell viability was determined by bioluminescence assay. Results are representative data in duplicates from three independent experiments ( $n = 6$ ).

WT		Average of IC <sub>50</sub> (nM)					CI	
BRAF <sup>i</sup>	Cell lines	ERKi	AKTi	mTORi	ERKi + AKTi	ERKi + mTORi	E + A	E + m
R	M230	529,4	4072,2	1853043,6	245,4	97,9	0,2	0,1
R	M285	470,0	n/a	n/a	261,4	92,3	n/a	n/a
R	M375	729,4	15513,8	3139966787,4	449,2	362,8	0,5	0,4
R	M418	348,7	1488,8	6511195,1	240,1	86,3	0,7	0,3
R	PB	473,0	n/a	n/a	132,0	191,5	n/a	n/a

■ Resistant (*R*)     
 ■ Intermediate (*I*)     
 ■ Sensitive (*S*)

**Table 9: IC<sub>50</sub> and CI values of WT melanoma cell lines after treating with ERKi, AKTi, mTORi, ERKi combined with AKTi or ERKi combined with mTORi.** The cells were exposed to 0 – 10  $\mu$ M of ERKi, AKTi, mTORi or the combination of drugs (*ERKi + AKTi; ERKi + mTORi*). After 120 hours treatment the cell viability was determined by bioluminescence assay. Results are the mean of the representative data in duplicates from two or three independent experiments. Cells are sensitive (*S; green*) if the IC<sub>50</sub> value is less than 1  $\mu$ M, intermediate sensitive (*I; yellow*) if IC<sub>50</sub> is 1 – 2  $\mu$ M and resistant (*R; red*) when IC<sub>50</sub> is more than 2  $\mu$ M. Combination index values (*CI*) for ERKi combined with AKTi (*E + A*) and ERKi combined with mTORi (*E + m*) are also presented. Values less than 1 indicates synergism, CI = 1 indicates an additive effect and CI > 1 indicates antagonism. WT melanoma cell lines were resistant to vemurafenib since they do not harbor a *BRAF* mutation. n/a: not applicable.

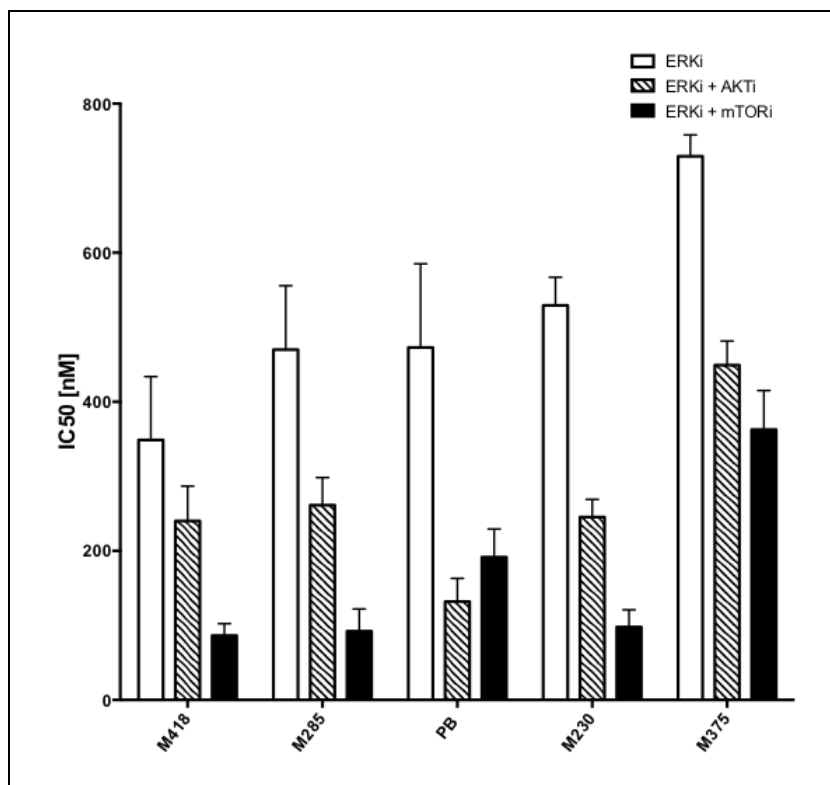


**Figure 23: Bar graph of  $IC_{50}$  values of WT melanoma cells exposed to ERKi, ERKi combined with AKTi or ERKi combined with AKTi.** WT melanoma cell lines were treated with 0 – 10  $\mu$ M ERKi (white bars) or ERKi combined with AKTi (striped bars) or ERKi combined with mTORi (black bars) for 120 hours. Cell viability was determined by ATP-based bioluminescence assay. The average of  $IC_{50}$  values of two or three independent experiments in duplicates are represented by the bars and the error bars indicate the standard deviation (STDV). Cells are sensitive if the  $IC_{50}$  value is less than 1  $\mu$ M, intermediate sensitive if  $IC_{50}$  is 1 – 2  $\mu$ M and  $IC_{50}$  values higher than 2  $\mu$ M indicate resistant cell lines. The cells are arranged to their  $IC_{50}$  values of ERKi (white bars are increasing).



The growth assay studies show that the addition of either AKTi or mTORi to ERKi resulted always in more potent cell growth inhibition compared to ERKi alone. All five WT melanoma cell lines were resistant to vemurafenib since they do not harbor a *BRAF* mutation but showed sensitivity to ERKi with  $IC_{50}$  less than 1  $\mu$ M. These cell lines were also sensitive to the combined treatment with ERKi and AKTi as well as with ERKi and mTORi. The combined treatments always had even lower  $IC_{50}$  values than ERKi alone. Additionally the combination ERKi and mTORi also showed again lower  $IC_{50}$  values in most of the cell lines (*4 out of 5*) compared to ERKi combined with AKTi. The CI values of combining ERKi with AKTi and ERKi with mTORi were calculated in three cell lines and all of them showed a synergistic effect ( $CI < 1$ ).

### **3.3.2. Effects of the inhibitors on signaling pathway**

Western blots were analyzed with M230 and M285 to study the effects of ERKi combined with AKTi or mTORi on the MAPK- and PI3K/AKT pathway. The goal was to select a good responding and a not so good responding cell line to the combinatorial treatments. But all wild-type melanoma cell lines were sensitive to all the treatments, especially to the combinatorial treatments. Therefore M230 and M285 were selected, since they were fast growing cell lines with a good growth rate. After the exposure of DMSO and the inhibitors with or without in combination for 24 hours, western blot analyses were done, which is shown in figure 24, including the quantification of western blots. Figure 25 visualizes the quantification data as a bar graph.

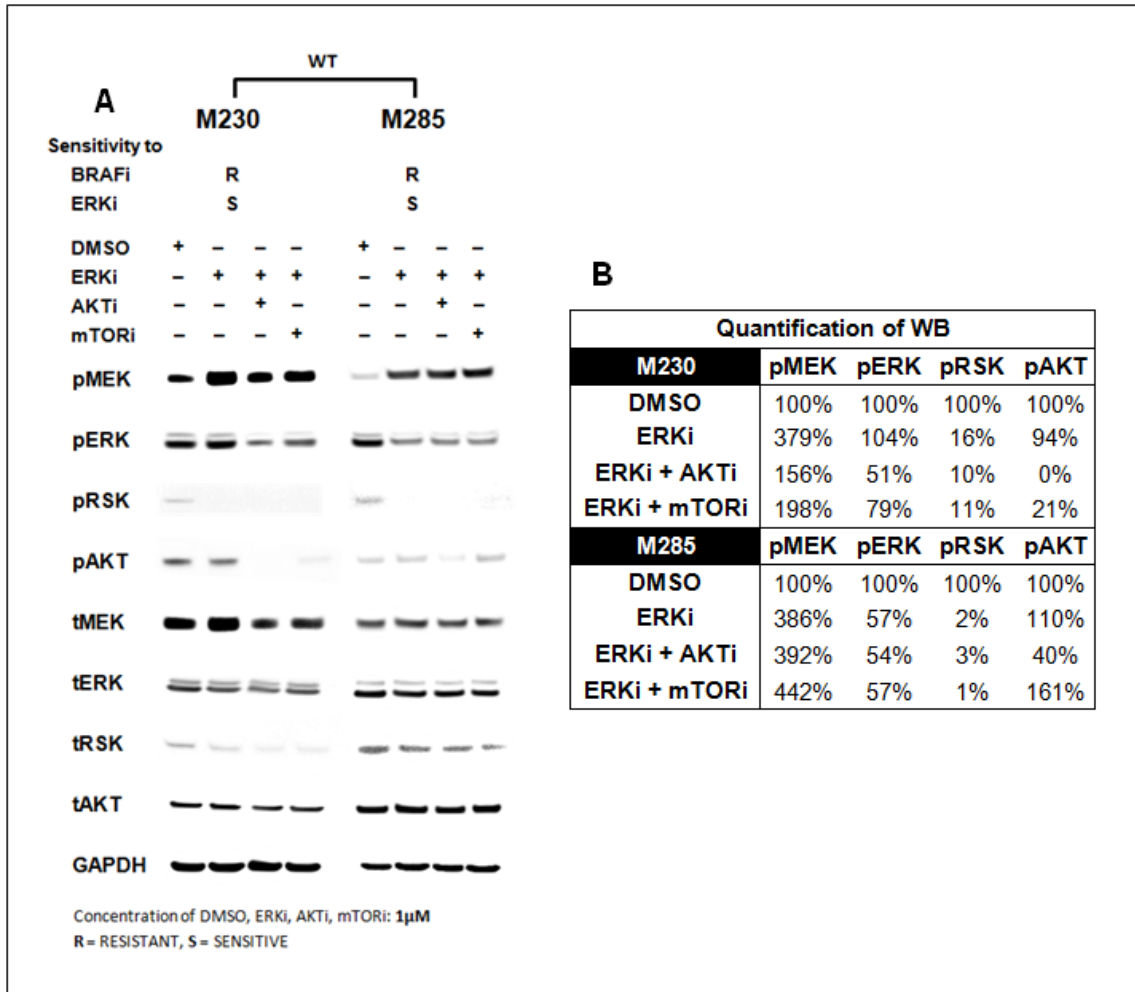


**Figure 24: Western blot analyses of WT melanoma cells after exposure to DMSO, ERK<sup>i</sup>, ERK<sup>i</sup> combined with AKT<sup>i</sup> or ERK<sup>i</sup> combined with mTOR<sup>i</sup> for 24h. A.** The cells M230 and M285 were treated with 1  $\mu$ M DMSO (*solvent control*), ERK<sup>i</sup>, ERK<sup>i</sup> combined with AKT<sup>i</sup> or ERK<sup>i</sup> combined with mTOR<sup>i</sup> for 24h. The effects of the various inhibitors are shown by determining phosphorylated (*p*) or total (*t*) MEK, ERK1/2, RSK and AKT. GAPDH served as loading control between the different conditions. M230 was sensitive to ERK<sup>i</sup> alone and the combinatorial treatments. M285 was sensitive to the inhibitors in or without in combination as well. Both cell lines were resistant to BRAF<sup>i</sup>. S: sensitive, R: resistant. **B.** This table presents the quantification of only the phosphorylated proteins.

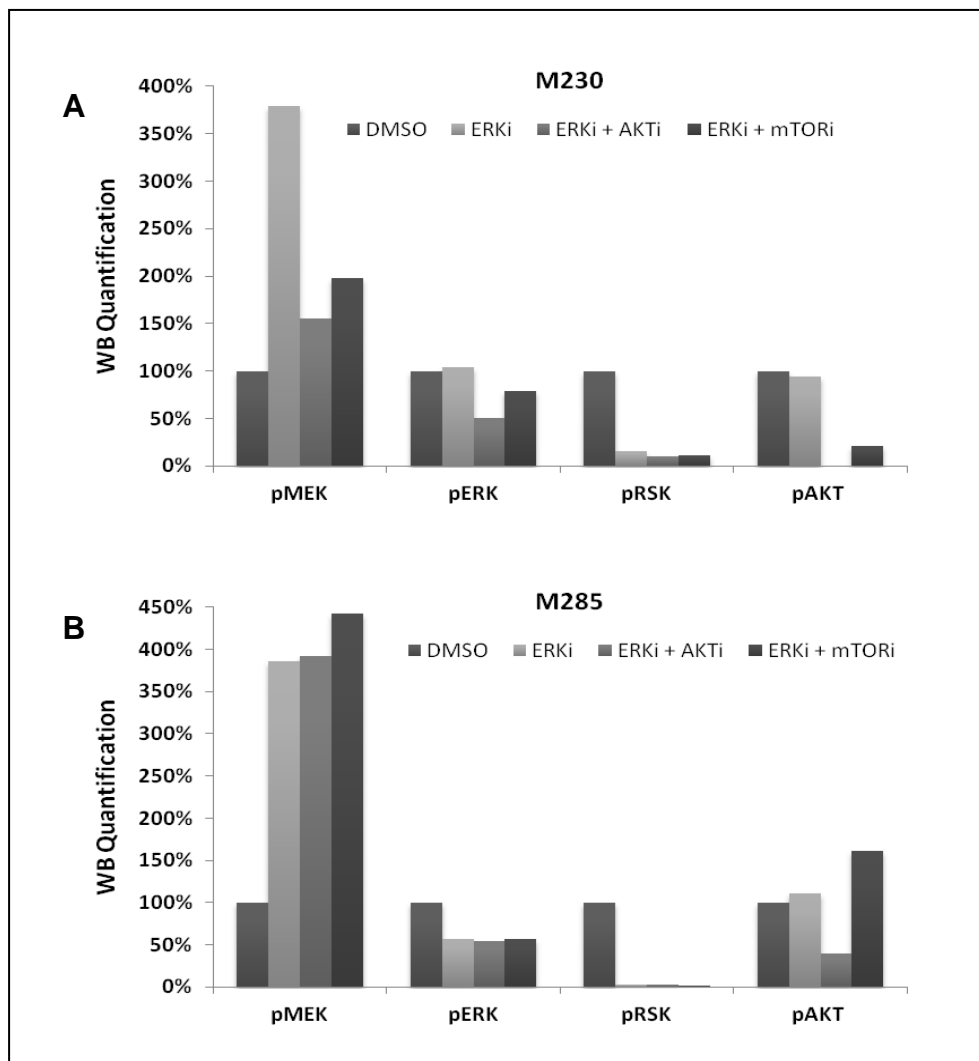


**Figure 25: Quantification of phosphorylated proteins of wild-type melanoma cells after exposure to DMSO, ERKi, ERKi combined with AKTi or ERKi combined with mTORi for 24h.** In this figure the phosphorylated (*p*) proteins: MEK, ERK1/2, RSK and AKT are quantified. **A.** M230 was sensitive to ERKi in monotherapy and to the combinatorial treatments. **B.** M285 was sensitive to the inhibitors in or without in combination as well.

The figures 24 and 25 are showing the WB quantifications of the wild-type cell lines. For M230, treatment with ERKi and the two combinations resulted in an increase in pMEK compared to the baseline (*DMSO as solvent control*). Protein pERK was increased slightly (104%) by treating M230 with ERKi alone, but decreased by the combinatorial treatments, especially by ERKi combined with AKTi (51%). All treatments deeply inhibited pRSK levels and pAKT was completely inhibited (0%) by ERKi combined with AKTi. ERKi in monotherapy slightly decreased pAKT with 94% but ERKi

combined with mTORi inhibited pAKT level to 21%. M285 had an increase in pMEK levels with all the treatments. The proteins pERK and pRSK were decreased by all inhibitors in or without in combination. But the decrease of these protein levels did not differ much between the conditions. Protein pAKT was decreased with ERKi combined with AKTi (40%) but increased in ERKi (110%) and ERKi combined with mTORi (161%). GAPDH, as expected, had in both cell lines and in all conditions the same protein levels (*loading control*).

### **3.3.3. Effects of the inhibitors on cell cycle and apoptosis**

The effects of ERK and AKT or mTOR inhibition on cell cycle progression and apoptosis were tested by flow cytometry. Cells were treated with ERKi, AKTi, mTORi, ERKi combined with AKTi or mTORi for 48 hours. The cells were incubated with 1  $\mu$ M staurosporine as a positive control for apoptosis. The cells were stained with DAPI and cleaved PARP and analyzed by flow cytometry. The WT melanoma cell lines M230 and M285 were chosen for cell cycle and apoptosis studies. Both cell lines were sensitive to ERKi in monotherapy as well as to the combinatorial treatments and resistant to BRAFi alone.

Figure 26 presents the cell cycle progression and apoptosis and figure 27 shows the same data quantitative as bar graphs. Table 10 also presents the cell cycle progression and apoptosis data quantitative. Table 11 shows the statistical analyses. A t-test was performed to compare ERKi in monotherapy with the combinatorial treatments regarding to the apoptotic effects of the inhibitors. The percentages of cleaved PARP in the different conditions were compared for this statistical test. p-values < 0,05 were considered to be statistically significant.

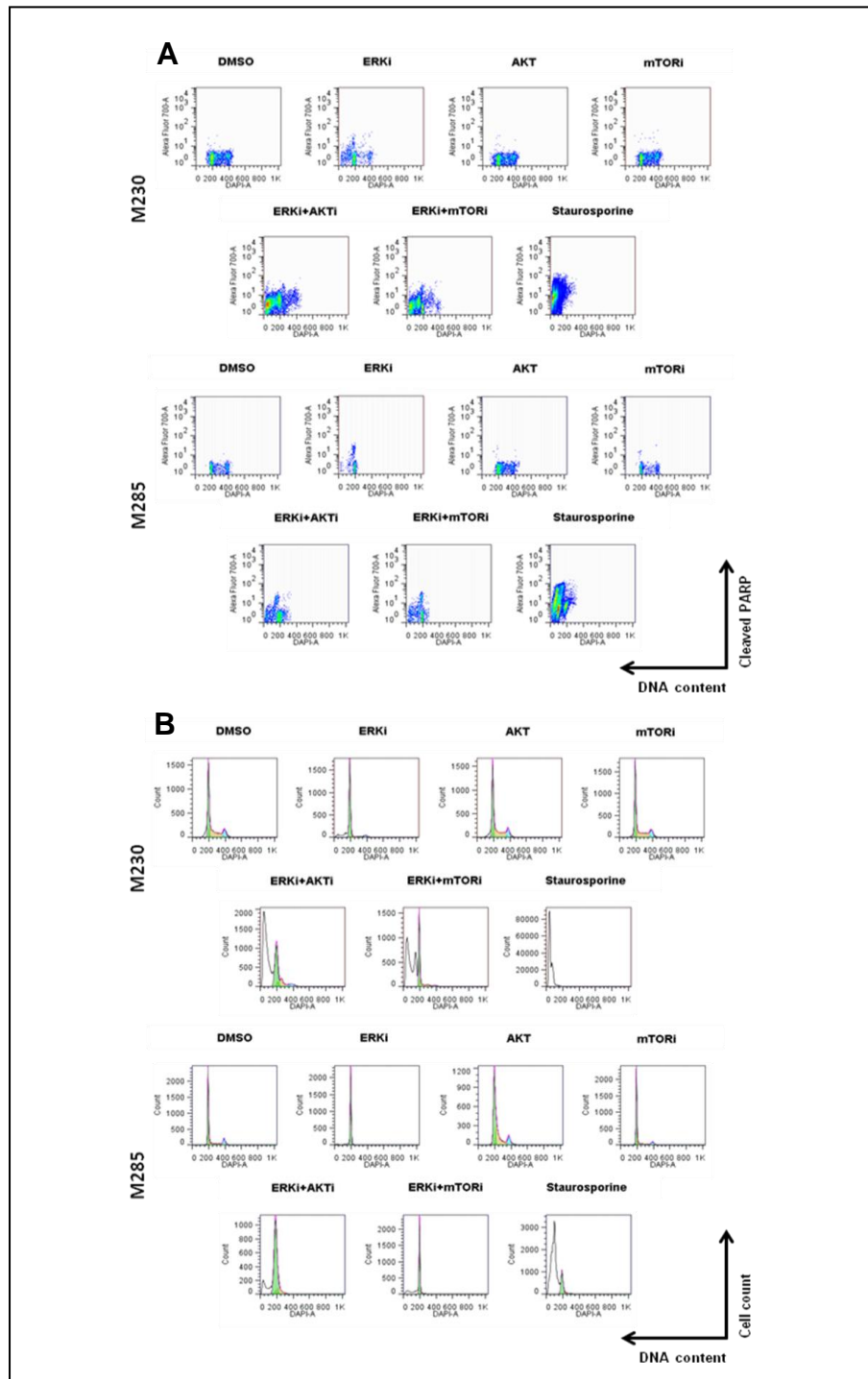


**Figure 26: Cell cycle progression and apoptosis in wild-type melanoma cell lines after exposure to DMSO, ERKi, AKTi, mTORi, ERKi combined with AKTi or ERKi combined with mTORi and staurosporine for 48h.** M230 and M285 are shown in this figure. Figures are representative of duplicate experiments. **A.** Induced apoptosis was tested by cleaved PARP (*y-axis*). DAPI (*x-axis*). **B.** Cell cycle progression was determined by DAPI staining solution (*x-axis*). Cell count (*y-axis*).

Quantitative analysis of apoptosis and cell cycle (%)										
M230	Average					STDV				
	PARP	Sub-G1	G1	S	G2	PARP	Sub-G1	G1	S	G2
DMSO	5,73	7,1	48,95	33,15	14,4	1,527	10,041	2,616	3,465	4,525
ERKi	13,3	10,23	81,2	9,78	4,23	2,263	0,665	1,697	1,725	0,778
AKTi	4,19	5,91	54,3	31,6	15,2	2,249	7,764	7,495	5,515	4,667
mTORi	4,805	1,6	66,7	30,2	14,45	1,181	2,263	15,698	4,525	1,061
ERKi + AKTi	37,35	69,45	20,15	11,9	1,59	8,697	5,02	6,576	2,404	0,255
ERKi + mTORi	30	62	35,4	5,265	1,54	8,768	9,334	10,889	0,728	0,212
Staurosporine	84,1	99,6	0,13	0,25	0	n/a	n/a	n/a	n/a	n/a
M285	Average					STDV				
	PARP	Sub-G1	G1	S	G2	PARP	Sub-G1	G1	S	G2
DMSO	1,87	1,44	63	21,75	11,345	0,891	0,226	3,677	0,071	1,916
ERKi	11,12	12,78	77,75	6,09	2,29	5,063	5,968	6,718	0,113	1,273
AKTi	1,095	0	75,35	23,9	11,7	0,049	0	6,01	1,131	0
mTORi	1,007	1,775	69,85	17,4	9,38	0,018	0,431	0,636	0,424	1,018
ERKi + AKTi	15,335	17,4	74,1	10,135	1,185	9,284	3,677	8,485	0,94	0,346
ERKi + mTORi	19,35	21,65	79,75	5,795	1,7	8,839	6,01	20,86	2,821	0,919
Staurosporine	80,1	84	17,5	0	0,91	n/a	n/a	n/a	n/a	n/a

**Table 10: Quantitative analysis of cell cycle progression and apoptosis in wild-type melanoma cell lines after exposure to DMSO, ERKi, AKTi, mTORi, ERKi combined with AKTi or ERKi combined with mTORi and staurosporine for 48h.** In this table are M230 and M285 presented. The average was calculated from the data of two independently experiments. Every condition besides the incubation of the cells with staurosporine (*positive control for apoptosis*) was done twice. Percentage of apoptotic cells positive for cleaved PARP is shown in the first column. Quantitative analysis of cell cycle progression by DAPI staining using flow cytometry shows the percentage of cells in sub-G1 (*equivalent to G0*), G1, S-phase and G2. n/a: not applicable. STDV: standard deviation.

p-values of t-test		
Cleaved PARP	M230	M285
ERKi vs. ERKi + AKTi	0,03*	0,31
ERKi vs. ERKi + mTORi	0,06	0,19

**Table 11: Statistical analyzing with t-test of cleaved PARP in wild-type melanoma cell lines.** M230 and M285 are shown in this table. ERKi in monotherapy was compared with the combinatorial treatments (*ERKi + AKTi, ERKi + mTORi*) for apoptosis. \* p-values < 0,05: statistically significant.

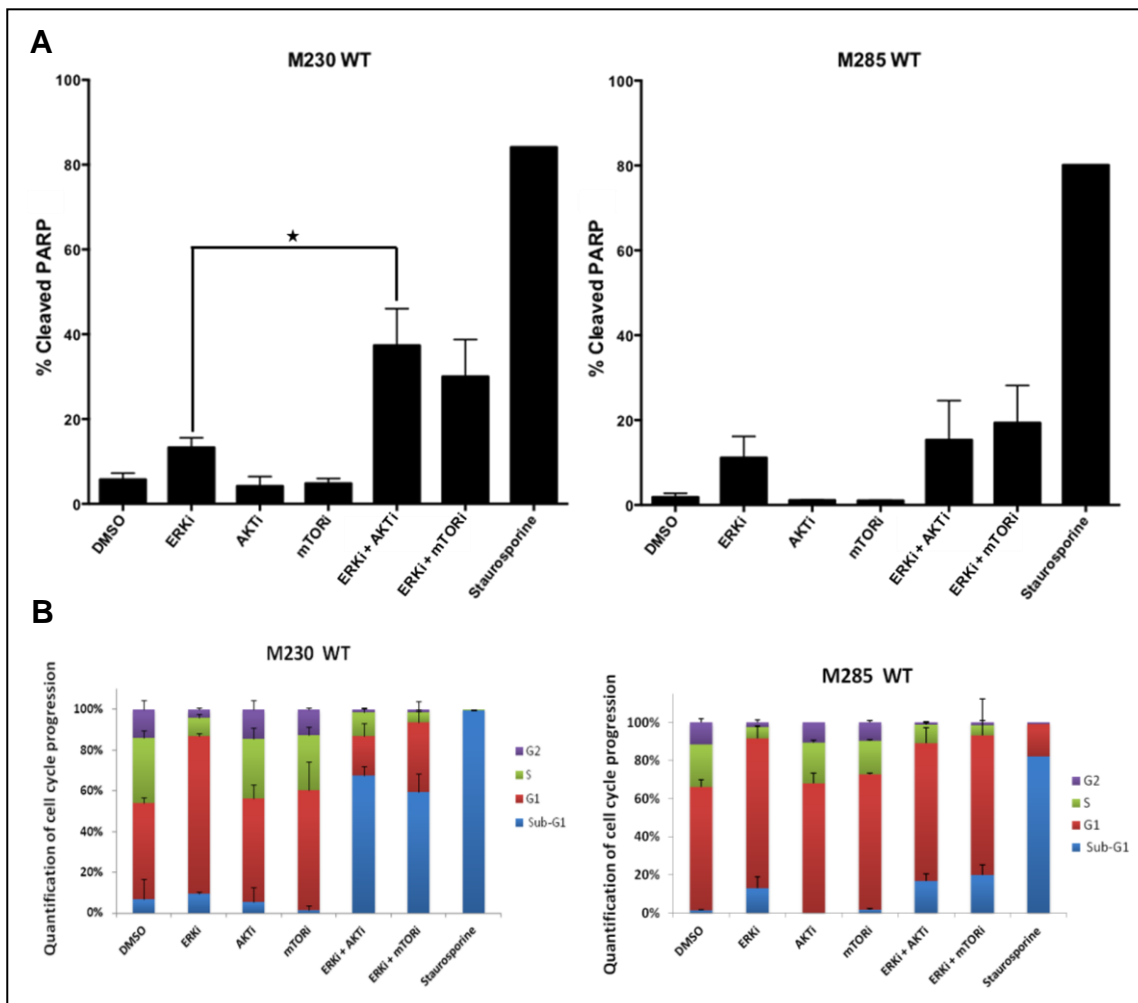


**Figure 27: Apoptosis and cell cycle progression in wild-type melanoma cell lines after exposure to DMSO, ERKi, AKTi, mTORi, ERKi combined with AKTi or ERKi combined with mTORi and staurosporine for 48h.** M230 was sensitive to ERKi alone and the combinatorial treatments. M285 was sensitive to the inhibitors with or without in combination as well. Both cell lines were resistant to BRAFi. **A.** Percentage of apoptotic cells positive for cleaved PARP is shown. Bars represent mean values of two independent experiments ( $n=2$ ). Error bars indicate the standard deviation (*STDV*). \*  $p$ -values  $< 0,05$ : statistically significant. **B.** Quantitative analysis of cell cycle progression by DAPI staining using flow cytometry shows the percentage of cells in sub-G1 (equivalent to G0; blue), G1 (red), S-phase (green) and G2 (purple). Bars represent mean values of two independent experiments ( $n=2$ ). Error bars indicate the standard deviation (*STDV*).

Both wild-type cell lines had after the combinatorial treatment an increase in cleaved PARP levels, which were higher than the cleaved PARP level of ERKi in monotherapy (*Figure 27, Table 10*). The highest level of cleaved PARP in M230 was after the treatment with ERKi combined with AKTi, which was statistically significant (*Table 11:  $p$ -value < 0,05*) compared to the cleaved PARP level after treatment of ERKi alone. M285 had the highest level of cleaved PARP after the combined treatment with ERKi and mTORi compared to the other treatments. Inhibition of AKT or mTOR alone had no increase of cleaved PARP in any of the wild-type melanoma cell lines.

M230 had after the combinatorial treatment a dramatic increase in sub-G1 phase, which was not seen in any other cell lines. Also after the combinatorial treatment in M230 S-phase and G2 were decreased compared to the vehicle control DMSO. In M285 after treatment with ERKi in monotherapy or ERKi in combination with AKTi or mTORi resulted in increased levels of sub-G1 (G0), G1 and decrease in S, G2 compared to the vehicle control DMSO. The combinatorial treatments had higher values in sub-G1 compared to ERKi alone.



## 4. Discussion

Resistance to BRAFi or MEKi has been reported to occur by reactivating of the MAPK pathway<sup>32</sup>, therefore approaches has been developed to target downstream signals in the MAPK pathway for example with ERKi<sup>32, 69, 70</sup>. Indeed, previously published report has shown that ERKi (*SCH-772984*) is very active amongst *BRAF* mutant, *NRAS* mutant, double mutant and wild-type melanoma cell lines<sup>11</sup>. Despite the promising data of ERKi in BRAFi resistant melanoma cell lines, resistance to ERKi also appeared. Increased pAKT levels were observed at baseline levels, which correlated to resistance to ERKi in *BRAF* mutant melanoma cell lines<sup>11</sup>. This indicates a cross-talk between MAPK- and PI3K/AKT pathways<sup>4, 11, 14, 71, 72</sup>, which supports the concept to inhibit both pathways simultaneously<sup>4, 12</sup>. In fact, it was reported that combining AKTi with BRAFi based therapy can effectively inhibit melanoma cells<sup>17</sup>. Moreover it was observed by adding inhibitors of AKT/mTOR pathway to BRAFi or MEKi, resistance to vemurafenib (*BRAF*i) can be reserved<sup>4</sup>. Furthermore the activation of PI3K/AKT pathway has been also suggested to mediate resistance to MAPK inhibitors<sup>4, 21, 30, 73 – 75</sup>. It also has been hypothesized that pAKT levels for *BRAF* mutant melanoma cells may play an important role in resistance<sup>69</sup>. Based on these data, inhibitors of PI3K/AKT/mTOR and MAPK pathway were combined in this study to analyze their effects on a panel of melanoma cell lines with different oncogenic events.

This study reported that combinatorial treatment of ERKi with AKTi or ERKi with mTORi enhanced cell growth inhibition in almost of all the tested cell lines, with only few exceptions. For example the *BRAF* mutant cell line M370 and M409AR1, which were very resistant to BRAFi<sup>11, 58, 63</sup> or ERKi alone did not show any improvement with the combinatorial treatments. The non-V600E *BRAF* mutant melanoma cell line, M381 was resistant to ERKi and BRAFi<sup>11, 58, 63</sup> in monotherapy, but to ERKi combined with AKTi or mTORi it was sensitive. The Dr. Ribas lab tested previously more non-V600E *BRAF* mutant melanoma cell lines (e.g. *M417 BRAF<sup>G466E</sup>*, *M420 BRAF<sup>L597S</sup>*), which were also resistant to ERKi and BRAFi<sup>11</sup>, but perhaps they could also respond like M381, sensitive to the combined treatment (*ERKi + AKTi*, *ERKi + mTORi*). In this case more non-V600E mutant melanomas should be tested out with these combined inhibitors, but these tumors are rare<sup>76</sup> and there is a paucity of available cell lines<sup>63</sup>. Currently, there is no FDA approved and effective targeted therapy for *NRAS* mutant- and wild-type melanomas, which includes about 50% of all melanomas<sup>11</sup>. Therefore new

approaches to treat non-*BRAF* mutant melanomas are needed. While some of the *BRAF* mutant melanoma cell lines were sensitive to BRAFi, vemurafenib<sup>11, 58, 63</sup>, all of the *NRAS* mutant- and WT melanoma cell lines were resistant to vemurafenib since they do not harbor a *BRAF* mutation. But almost all of these cells were sensitive to the combined treatments, especially ERKi with mTORi. Even one of the *NRAS* mutant melanoma cell lines, M318, which was resistant to ERKi alone, became sensitive to ERKi combined with mTORi. The WT melanoma cell lines were sensitive to ERKi and this effect was enhanced by the combination treatment. Therefore WT melanoma cell lines had a very good response to this combinatorial testing. Overall, the majority of the tested cell lines showed that the addition of either AKTi or mTORi to ERKi resulted in more potent cell growth inhibition compared to ERKi alone. Combining ERKi with AKTi or mTORi was particularly synergistic ( $CI < 1 \mu M$ ).

The presence of *AKT1* or *AKT2* amplification in *BRAF* mutant melanoma cell lines did not exclude sensitivity to ERKi alone, since three of five such cell lines were sensitive to ERKi (*M229*, *M249* and *M308*), but two were resistant to ERKi alone (*M233* and *M255*). This resistance was overcome by the combinatorial treatments (see *Table 3*, *Figure 8*). As mentioned before, increased pAKT levels at baseline levels were seen before in treated cells with ERKi<sup>11, 69</sup>, because inhibiting the MAPK pathway up-regulates the PI3K/AKT pathway (*cross-talk*)<sup>4, 11, 14, 71, 72</sup>. In this study the *BRAF* mutant cell lines M370, M410 and as well as M318 (*NRAS mutant*) and M285 (*WT*) that were treated with ERKi alone and ERKi combined with mTORi showed also an increase in pAKT compared to the baseline (*DMSO control*). Treatment with ERKi combined with AKTi decreased pAKT efficiently in these cell lines; in M230 (*WT*) it was also completely inhibited (*Figure 24*). The protein pMEK was in all cell lines, besides M318 treated with ERKi combined with mTORi, accumulated as a consequence of inhibition of ERK in the MAPK pathway. Interestingly, M370 showed increased pERK levels after ERK inhibition with ERKi or the combinatorial treatment, which was not the case in the other cell lines, besides M230 (*Figure 24*). Therefore M370 showed a fast recovery of pERK levels, despite the pRSK levels stayed inhibited. This probably points at a fast up-regulation of the MAPK pathway in this resistant cell line. M230 had a slightly increase in pERK when it was treated with ERKi, but in the combinatorial treatments pERK was decreased. Protein pRSK was in all treated cell lines decreased, especially in the combined treatments for M410 (*BRAF*), M318 (*NRAS*) and M230 (*WT*). Overall

the combinatorial treatment improved the inhibition of the MAPK pathway and adding AKTi to ERKi showed in all tested cell lines a great decrease of pAKT levels.

Inhibition of ERK alone or in combination with AKT or mTOR in all tested cell lines resulted in an increase in the sub-G1 (*G0*) population, the G1 population, as well as an increase in cleaved PARP levels, which indicates apoptotic cells. With the increase in G1-phase, a decreased proportion of cells were observed in S-phase as well as in G2-phase. In general the combinatorial treatments had the highest levels in cleaved PARP compared to ERKi in monotherapy. However most of the cell lines did not translate the arrest in growth from the combination therapy with clear apoptosis, besides in M230 and M243. There was mostly an arrest in G1, a decrease in S and G2 to observe. ERKi combined with AKTi in M230 (*WT*) and ERKi combined with mTORi in M243 (*NRAS*) offered a statistically significant increase in cleaved PARP compared to ERKi alone. Also in terms of effects on the cell cycle, G1 arrest was maximally induced by the combinatorial treatment in the majority of cell lines. In addition the wild-type cell lines had after the combinatorial treatments a significant increase in sub-G1, especially in M230.

It would be interesting to evaluate the effects of these combinatorial treatments in long term studies regarding the mechanisms underlying of possible acquired resistance to these treatments.

## 5. Conclusion

Resistance to BRAF inhibitors and currently no FDA approved targeted therapies for non-*BRAF* mutant melanomas, like *NRAS* mutant and wild-type mutant melanomas, are major problems in the treatment of metastatic melanomas<sup>11, 17</sup>. This study showed that combining an ERK inhibitor with AKT/mTOR inhibitors had a clear benefit in the growth control for a majority of cell lines by causing enhanced growth inhibition, even in *BRAF* mutant cell lines resistant to BRAFi<sup>11, 58, 63</sup> and ERKi alone. This resulted in synergistic effects of most of these cell lines. These combinations of inhibitors were especially effective in wild-type melanoma cell lines, inducing apoptosis in a significant manner. Therefore this combinatorial treatment may be clinically applicable for *NRAS* mutant melanomas, wild-type melanomas or *BRAF* mutant melanomas with innate or acquired resistance.

## 6. References

1. Flaherty, K. T. *et al.* Inhibition of mutated, activated BRAF in metastatic melanoma. *N. Engl. J. Med.* **363**, 809–19 (2010).
2. Ngiow, S. F., Knight, D. A., Ribas, A., McArthur, G. A. & Smyth, M. J. BRAF-targeted therapy and immune responses to melanoma. *Oncoimmunology* **2**, e24462 (2013).
3. Knight, D. A. *et al.* Host immunity contributes to the anti-melanoma activity of BRAF inhibitors. *J. Clin. Invest.* **123**, 1371–81 (2013).
4. Atefi, M. *et al.* Reversing melanoma cross-resistance to BRAF and MEK inhibitors by co-targeting the AKT/mTOR pathway. *PLoS One* **6**, e28973 (2011).
5. Sullivan, R. J. & Flaherty, K. T. BRAF in Melanoma: Pathogenesis, Diagnosis, Inhibition, and Resistance. *J. Skin Cancer* **2011**, 423239 (2011).
6. Jiang, W. *et al.* Clinically relevant genes and regulatory pathways associated with NRASQ61 mutations in melanoma through an integrative genomics approach. *Oncotarget* (2014). [Epub ahead of print] at: <http://www.ncbi.nlm.nih.gov/pubmed/25537510> (download 15.12.2014).
7. Albino, A. P., Le Strange, R., Oliff, A. I., Furth, M. E. & Old, L. J. Transforming ras genes from human melanoma: a manifestation of tumour heterogeneity? *Nature* **308**, 69–72 (1984).
8. Ball, N. J. *et al.* Ras mutations in human melanoma: a marker of malignant progression. *J. Invest. Dermatol.* **102**, 285–90 (1994).
9. Platz, A., Ringborg, U., Brahme, E. M. & Lagerlöf, B. Melanoma metastases from patients with hereditary cutaneous malignant melanoma contain a high frequency of N-ras activating mutations. *Melanoma Res.* **4**, 169–77 (1994).
10. Beeram, M., Patnaik, A. & Rowinsky, E. K. Raf: a strategic target for therapeutic development against cancer. *J. Clin. Oncol.* **23**, 6771–90 (2005).
11. Wong, D. J. L. *et al.* Antitumor activity of the ERK inhibitor SCH722984 against BRAF mutant, NRAS mutant and wild-type melanoma. *Mol. Cancer* **13**, 194 (2014).
12. Lasithiotakis, K. G. *et al.* Combined inhibition of MAPK and mTOR signaling inhibits growth, induces cell death, and abrogates invasive growth of melanoma cells. *J. Invest. Dermatol.* **128**, 2013–23 (2008).
13. Downward, J. Targeting RAS and PI3K in lung cancer. *Nat. Med.* **14**, 1315–6 (2008).
14. Carracedo, A. & Pandolfi, P. P. The PTEN-PI3K pathway: of feedbacks and cross-talks. *Oncogene* **27**, 5527–41 (2008).
15. Downward, J. Targeting RAS signalling pathways in cancer therapy. *Nat. Rev. Cancer* **3**, 11–22 (2003).

16. Meier, F. *et al.* The RAS/RAF/MEK/ERK and PI3K/AKT signaling pathways present molecular targets for the effective treatment of advanced melanoma. *Front. Biosci.* **10**, 2986–3001 (2005).
17. Lassen, A. *et al.* Effects of AKT inhibitor therapy in response and resistance to BRAF inhibition in melanoma. *Mol. Cancer* **13**, 83 (2014).
18. Sosman, J. A. *et al.* Survival in BRAF V600-mutant advanced melanoma treated with vemurafenib. *N. Engl. J. Med.* **366**, 707–14 (2012).
19. Heidorn, S. J. *et al.* Kinase-dead BRAF and oncogenic RAS cooperate to drive tumor progression through CRAF. *Cell* **140**, 209–21 (2010).
20. Poulidakos, P. I., Zhang, C., Bollag, G., Shokat, K. M. & Rosen, N. RAF inhibitors transactivate RAF dimers and ERK signalling in cells with wild-type BRAF. *Nature* **464**, 427–30 (2010).
21. Nazarian, R. *et al.* Melanomas acquire resistance to B-RAF(V600E) inhibition by RTK or N-RAS upregulation. *Nature* **468**, 973–7 (2010).
22. Shi, H. *et al.* Preexisting MEK1 exon 3 mutations in V600E/KBRAF melanomas do not confer resistance to BRAF inhibitors. *Cancer Discov.* **2**, 414–24 (2012).
23. Wagle, N. *et al.* Dissecting therapeutic resistance to RAF inhibition in melanoma by tumor genomic profiling. *J. Clin. Oncol.* **29**, 3085–96 (2011).
24. Johannessen, C. M. *et al.* COT drives resistance to RAF inhibition through MAP kinase pathway reactivation. *Nature* **468**, 968–72 (2010).
25. Shi, H. *et al.* Melanoma whole-exome sequencing identifies (V600E)B-RAF amplification-mediated acquired B-RAF inhibitor resistance. *Nat. Commun.* **3**, 724 (2012).
26. Poulidakos, P. I. *et al.* RAF inhibitor resistance is mediated by dimerization of aberrantly spliced BRAF(V600E). *Nature* **480**, 387–90 (2011).
27. Paraiso, K. H. T. *et al.* PTEN loss confers BRAF inhibitor resistance to melanoma cells through the suppression of BIM expression. *Cancer Res.* **71**, 2750–60 (2011).
28. Shi, H., Kong, X., Ribas, A. & Lo, R. S. Combinatorial treatments that overcome PDGFR $\beta$ -driven resistance of melanoma cells to V600EB-RAF inhibition. *Cancer Res.* **71**, 5067–74 (2011).
29. Girotti, M. R. *et al.* Inhibiting EGF receptor or SRC family kinase signaling overcomes BRAF inhibitor resistance in melanoma. *Cancer Discov.* **3**, 158–67 (2013).
30. Villanueva, J. *et al.* Acquired resistance to BRAF inhibitors mediated by a RAF kinase switch in melanoma can be overcome by cotargeting MEK and IGF-1R/PI3K. *Cancer Cell* **18**, 683–95 (2010).
31. Flaherty, K. T. *et al.* Combined BRAF and MEK inhibition in melanoma with BRAF V600 mutations. *N. Engl. J. Med.* **367**, 1694–703 (2012).

32. Morris, E. J. *et al.* Discovery of a novel ERK inhibitor with activity in models of acquired resistance to BRAF and MEK inhibitors. *Cancer Discov.* **3**, 742–50 (2013).
33. Rehan, M., Beg, M. a, Parveen, S., Damanhour, G. a & Zaher, G. F. Computational insights into the inhibitory mechanism of human AKT1 by an orally active inhibitor, MK-2206. *PLoS One* **9**, e109705 (2014).
34. Cheng, Y. *et al.* MK-2206, a novel allosteric inhibitor of Akt, synergizes with gefitinib against malignant glioma via modulating both autophagy and apoptosis. *Mol. Cancer Ther.* **11**, 154–64 (2012).
35. Hirai, H. *et al.* MK-2206, an allosteric Akt inhibitor, enhances antitumor efficacy by standard chemotherapeutic agents or molecular targeted drugs in vitro and in vivo. *Mol. Cancer Ther.* **9**, 1956–67 (2010).
36. Tan, S., Ng, Y. & James, D. E. Next-generation Akt inhibitors provide greater specificity: effects on glucose metabolism in adipocytes. *Biochem. J.* **435**, 539–44 (2011).
37. NCIthesaurus. Akt Inhibitor MK2206 (Code C90581). Online at: [http://ncit.nci.nih.gov/ncitbrowser/pages/concept\\_details.jsf?dictionary=NCI\\_Thesaurus&version=14.11d&code=C90581&type=all&key=null&b=1&n=0&vse=null](http://ncit.nci.nih.gov/ncitbrowser/pages/concept_details.jsf?dictionary=NCI_Thesaurus&version=14.11d&code=C90581&type=all&key=null&b=1&n=0&vse=null) (download 17.12.2014).
38. ClinicalTrials.gov. Online at: <https://clinicaltrials.gov/ct2/results?term=MK2206> (download 17.12.2014).
39. Mita, M. M. *et al.* Phase I/IIa trial of the mammalian target of rapamycin inhibitor ridaforolimus (AP23573; MK-8669) administered orally in patients with refractory or advanced malignancies and sarcoma. *Ann. Oncol.* **24**, 1104–11 (2013).
40. NCIthesaurus. Ridaforolimus (Code C49061). Online at: [http://ncit.nci.nih.gov/ncitbrowser/pages/concept\\_details.jsf?dictionary=NCI\\_Thesaurus&version=14.11d&code=C49061&type=all&key=null&b=1&n=0&vse=null](http://ncit.nci.nih.gov/ncitbrowser/pages/concept_details.jsf?dictionary=NCI_Thesaurus&version=14.11d&code=C49061&type=all&key=null&b=1&n=0&vse=null) (download 17.12.2014).
41. ClinicalTrials.gov. Online at: <https://clinicaltrials.gov/ct2/results?term=MK-8669+&Search=Search> (download 17.12.2014).
42. Chapman, P. B. *et al.* Improved survival with vemurafenib in melanoma with BRAF V600E mutation. *N. Engl. J. Med.* **364**, 2507–16 (2011).
43. Hauschild, A. *et al.* Dabrafenib in BRAF-mutated metastatic melanoma: a multicentre, open-label, phase 3 randomised controlled trial. *Lancet* **380**, 358–65 (2012).
44. Zhang, J., Yang, P. L. & Gray, N. S. Targeting cancer with small molecule kinase inhibitors. *Nat. Rev. Cancer* **9**, 28–39 (2009).
45. Sullivan, R. J. & Flaherty, K. MAP kinase signaling and inhibition in melanoma. *Oncogene* **32**, 2373–9 (2013).
46. Von Eeuw, E. *et al.* Antitumor effects of the investigational selective MEK inhibitor TAK733 against cutaneous and uveal melanoma cell lines. *Mol. Cancer* **11**, 22 (2012).

47. Wang, H. *et al.* Identification of the MEK1(F129L) activating mutation as a potential mechanism of acquired resistance to MEK inhibition in human cancers carrying the B-RafV600E mutation. *Cancer Res.* **71**, 5535–45 (2011).
48. Emery, C. M. *et al.* MEK1 mutations confer resistance to MEK and B-RAF inhibition. *Proc. Natl. Acad. Sci. U. S. A.* **106**, 20411–6 (2009).
49. Dai, B. *et al.* STAT3 mediates resistance to MEK inhibitor through microRNA miR-17. *Cancer Res.* **71**, 3658–68 (2011).
50. Hodi, F. S. *et al.* Improved survival with ipilimumab in patients with metastatic melanoma. *N. Engl. J. Med.* **363**, 711–23 (2010).
51. Beck, K. E. *et al.* Enterocolitis in patients with cancer after antibody blockade of cytotoxic T-lymphocyte-associated antigen 4. *J. Clin. Oncol.* **24**, 2283–9 (2006).
52. Homet, B. & Ribas, A. New drug targets in metastatic melanoma. *J. Pathol.* **232**, 134–41 (2014).
53. Iwai, Y. *et al.* Involvement of PD-L1 on tumor cells in the escape from host immune system and tumor immunotherapy by PD-L1 blockade. *Proc. Natl. Acad. Sci. U. S. A.* **99**, 12293–7 (2002).
54. Blank, C. *et al.* PD-L1/B7H-1 inhibits the effector phase of tumor rejection by T cell receptor (TCR) transgenic CD8+ T cells. *Cancer Res.* **64**, 1140–5 (2004).
55. Okazaki, T. & Honjo, T. PD-1 and PD-1 ligands: from discovery to clinical application. *Int. Immunol.* **19**, 813–24 (2007).
56. Mahoney, K. M. & Atkins, M. B. Prognostic and predictive markers for the new immunotherapies. *Oncology (Williston Park)*. **28**, (2014).
57. Poole, R. M. Pembrolizumab: first global approval. *Drugs* **74**, 1973–81 (2014).
58. Søndergaard, J. N. *et al.* Differential sensitivity of melanoma cell lines with BRAFV600E mutation to the specific Raf inhibitor PLX4032. *J. Transl. Med.* **8**, 39 (2010).
59. Cooper, G. M. *The Eukaryotic Cell Cycle*. (Sinauer Associates, 2000). Online at: <http://www.ncbi.nlm.nih.gov/books/NBK9876/> (download 19.12.2014).
60. Boulares, A. H. *et al.* Role of Poly(ADP-ribose) Polymerase (PARP) Cleavage in Apoptosis: CASPASE 3-RESISTANT PARP MUTANT INCREASES RATES OF APOPTOSIS IN TRANSFECTED CELLS. *J. Biol. Chem.* **274**, 22932–22940 (1999).
61. Technical Data Sheet. Alexa Fluor® 700 Mouse Anti-Cleaved PARP (Asp 214). Online at: <http://www.bdbiosciences.com/ds/pm/tds/560640.pdf> (download 09.12.2014).
62. Niehr, F. *et al.* Combination therapy with vemurafenib (PLX4032/RG7204) and metformin in melanoma cell lines with distinct driver mutations. *J. Transl. Med.* **9**, 76 (2011).
63. Ribas, A. (information provided from Ribas lab).



64. CellTiter-Glo® Luminescent Cell Viability Assay Technical Bulletin. Online at: [https://www.promega.com/~media/files/resources/protocols/technical\\_bulletins/0/celltiter\\_glo\\_luminescent\\_cell\\_viability\\_assay\\_protocol.pdf](https://www.promega.com/~media/files/resources/protocols/technical_bulletins/0/celltiter_glo_luminescent_cell_viability_assay_protocol.pdf) (download 06.12.2014).
65. Crouch, S. P., Kozlowski, R., Slater, K. J. & Fletcher, J. The use of ATP bioluminescence as a measure of cell proliferation and cytotoxicity. *J. Immunol. Methods* **160**, 81–8 (1993).
66. Kabir, J., Lobo, M. & Zachary, I. Staurosporine induces endothelial cell apoptosis via focal adhesion kinase dephosphorylation and focal adhesion disassembly independent of focal adhesion kinase proteolysis. *Biochem. J.* **367**, 145–55 (2002).
67. Chou, T.-C. Drug combination studies and their synergy quantification using the Chou-Talalay method. *Cancer Res.* **70**, 440–6 (2010).
68. Chou, T. C. & Talalay, P. Quantitative analysis of dose-effect relationships: the combined effects of multiple drugs or enzyme inhibitors. *Adv. Enzyme Regul.* **22**, 27–55 (1984).
69. Carlino, M. S. *et al.* Differential activity of MEK and ERK inhibitors in BRAF inhibitor resistant melanoma. *Mol. Oncol.* **8**, 544–54 (2014).
70. Hatzivassiliou, G. *et al.* ERK inhibition overcomes acquired resistance to MEK inhibitors. *Mol. Cancer Ther.* **11**, 1143–54 (2012).
71. Mendoza, M. C., Er, E. E. & Blenis, J. The Ras-ERK and PI3K-mTOR pathways: cross-talk and compensation. *Trends Biochem. Sci.* **36**, 320–8 (2011).
72. Aksamitiene, E., Kiyatkin, A. & Kholodenko, B. N. Cross-talk between mitogenic Ras/MAPK and survival PI3K/Akt pathways: a fine balance. *Biochem. Soc. Trans.* **40**, 139–46 (2012).
73. Su, F. *et al.* Resistance to selective BRAF inhibition can be mediated by modest upstream pathway activation. *Cancer Res.* **72**, 969–78 (2012).
74. Chen, B. *et al.* BRAFV600E negatively regulates the AKT pathway in melanoma cell lines. *PLoS One* **7**, e42598 (2012).
75. Gopal, Y. N. V. *et al.* Basal and treatment-induced activation of AKT mediates resistance to cell death by AZD6244 (ARRY-142886) in Braf-mutant human cutaneous melanoma cells. *Cancer Res.* **70**, 8736–47 (2010).
76. Long, G. V. *et al.* Prognostic and clinicopathologic associations of oncogenic BRAF in metastatic melanoma. *J. Clin. Oncol.* **29**, 1239–46 (2011).

## Acknowledgments

To accomplish this master thesis was sometimes challenging, especially to get started with the internship at UCLA, but with the great support of great people it was possible for me. So with these few words, I want to thank the following people.

To Toni Ribas; thank you very much for this great opportunity to come to your research lab at UCLA and work on this great and interesting research project. I have learned so much with your guidance and my internship at UCLA. Thanks for everything.

To Austrian Marshall Plan Foundation; I am really thankful to this foundation because without the financial support of this great organisation I couldn't have done this rewarding research project. So thank you very much.

To my parents and brother; thank you for your trust in me to go so far away from home to accomplish my dream. Also I want to thank my parents for their financial support, which helped me a lot.

To all the Ribas lab members, especially to Lidia Robert and Blanca Homet, you all were great colleagues and became soon my friends. I really enjoyed spending time with you all. Thanks Lidia and Blanca for your support and teaching me everything for this study.

To my university in Austria (*Fachhochschule Campus Wien*); thanks for the opportunity, that students can experience to study overseas. I want to thank here particularly Gabriele Neuditschko, for her help and patience with all the paperwork for this internship. Thanks a lot.

Last but not least, thanks to all my wonderful friends that I met during my stay in Los Angeles. A special thanks to Kerry and David for helping me to settle in and to my kind roommates Christina, Esther and Taylor. I had great times with you all and thanks for your emotional support, I miss you all very much.

## Statutory Declaration

Erklärung:

Ich erkläre, dass die vorliegende Masterarbeit von mir selbst verfasst wurde und ich keine anderen als die angeführten Behelfe verwendet bzw. mich auch sonst keiner unerlaubten Hilfe bedient habe.

Ich versichere, dass ich diese Masterarbeit bisher weder im In- noch im Ausland (einer Beurteilerin/einem Beurteiler zur Begutachtung) in irgendeiner Form als Prüfungsarbeit vorgelegt habe.

Weiters versichere ich, dass die von mir eingereichten Exemplare (ausgedruckt und elektronisch) identisch sind.

Datum: .....

Unterschrift: .....

# Appendix

## List of figures

<b>Figure 1:</b> MAPK- and PI3K/AKT/mTOR signaling pathway ( <i>modified according to</i> <sup>26</sup> ). .....	11
<b>Figure 2:</b> Microscopic imaging of melanoma cell lines before any treatment.....	15
<b>Figure 3:</b> Gating strategy of cell cycle and apoptosis analyses. ....	24
<b>Figure 4:</b> Growth inhibition curves of treated <i>BRAF</i> mutant melanoma cell lines I. ....	27
<b>Figure 5:</b> Growth inhibition curves of treated <i>BRAF</i> mutant melanoma cell lines II. ....	28
<b>Figure 6:</b> Growth inhibition curves of treated <i>BRAF</i> mutant melanoma cell lines III. ....	29
<b>Figure 7:</b> Growth inhibition curves of treated <i>BRAF</i> mutant melanoma cell lines IV. ....	30
<b>Figure 8:</b> Bar graph of IC <sub>50</sub> values of <i>BRAF</i> mutant melanoma cells treated with ERKi, ERKi combined with AKTi or ERKi combined with AKTi.....	32
<b>Figure 9:</b> Western blot analyses of <i>BRAF</i> mutant melanoma cells after exposure to DMSO, ERKi, ERKi combined with AKTi or ERKi combined with mTORi for 24h. ....	34
<b>Figure 10:</b> Quantification of phosphorylated proteins of <i>BRAF</i> mutant melanoma cells after exposure to DMSO, ERKi, ERKi combined with AKTi or ERKi combined with mTORi for 24h. ....	35
<b>Figure 11:</b> Cell cycle progression and apoptosis in <i>BRAF</i> mutant melanoma cell lines after exposure to DMSO, ERKi, AKTi, mTORi, ERKi combined with AKTi or ERKi combined with mTORi and staurosporine for 48h. ....	37
<b>Figure 12:</b> Apoptosis and cell cycle progression in <i>BRAF</i> mutant melanoma cell lines after exposure to DMSO, ERKi, AKTi, mTORi, ERKi combined with AKTi or ERKi combined with mTORi and staurosporine for 48h. ....	39
<b>Figure 13:</b> Growth inhibition curves of treated <i>NRAS</i> mutant melanoma cell lines I. ....	41
<b>Figure 14:</b> Growth inhibition curves of treated <i>NRAS</i> mutant melanoma cell lines II. ....	42
<b>Figure 15:</b> Growth inhibition curves of treated <i>NRAS</i> mutant melanoma cell lines III. ....	43
<b>Figure 16:</b> Bar graph of IC <sub>50</sub> values of <i>NRAS</i> mutant melanoma cells after exposure to ERKi, ERKi combined with AKTi or ERKi combined with AKTi.....	45
<b>Figure 17:</b> Western blot analyses of <i>NRAS</i> mutant melanoma cells after exposure to DMSO, ERKi, ERKi combined with AKTi or ERKi combined with mTORi for 24h.....	47

<b>Figure 18:</b> Quantification of phosphorylated proteins of <i>NRAS</i> mutant melanoma cells after exposure to DMSO, ERKi, ERKi combined with AKTi or ERKi combined with mTORi for 24h. ....	48
<b>Figure 19:</b> Cell cycle progression and apoptosis in <i>NRAS</i> mutant melanoma cell lines after exposure to DMSO, ERKi, AKTi, mTORi, ERKi combined with AKTi or ERKi combined with mTORi and staurosporine for 48h. ....	50
<b>Figure 20:</b> Apoptosis and cell cycle progression in <i>NRAS</i> mutant melanoma cell lines after exposure to DMSO, ERKi, AKTi, mTORi, ERKi combined with AKTi or ERKi combined with mTORi and staurosporine for 48h. ....	52
<b>Figure 21:</b> Growth inhibition curves of treated WT melanoma cell lines I. ....	54
<b>Figure 22:</b> Growth inhibition curves of treated WT melanoma cell lines II. ....	55
<b>Figure 23:</b> Bar graph of IC <sub>50</sub> values of WT melanoma cells exposed to ERKi, ERKi combined with AKTi or ERKi combined with AKTi. ....	56
<b>Figure 24:</b> Western blot analyses of WT melanoma cells after exposure to DMSO, ERKi, ERKi combined with AKTi or ERKi combined with mTORi for 24h. ....	58
<b>Figure 25:</b> Quantification of phosphorylated proteins of wild-type melanoma cells after exposure to DMSO, ERKi, ERKi combined with AKTi or ERKi combined with mTORi for 24h. ....	59
<b>Figure 26:</b> Cell cycle progression and apoptosis in wild-type melanoma cell lines after exposure to DMSO, ERKi, AKTi, mTORi, ERKi combined with AKTi or ERKi combined with mTORi and staurosporine for 48h. ....	61
<b>Figure 27:</b> Apoptosis and cell cycle progression in wild-type melanoma cell lines after exposure to DMSO, ERKi, AKTi, mTORi, ERKi combined with AKTi or ERKi combined with mTORi and staurosporine for 48h. ....	63

## List of tables

<b>Table 1:</b> 31 melanoma cell lines with their mutational status and sensitivity to vemurafenib ( <i>BRAF</i> <sub>i</sub> , <i>PLX4032</i> ).....	18
<b>Table 2:</b> Primary and secondary antibodies of western blot analyses. ....	22
<b>Table 3:</b> IC <sub>50</sub> and CI values of <i>BRAF</i> mutant melanoma cell lines after treating with ERKi, AKTi, mTORi, ERKi combined with AKTi or ERKi combined with mTORi...31	31
<b>Table 4:</b> Quantitative analysis of cell cycle progression and apoptosis in <i>BRAF</i> mutant melanoma cell lines after exposure to DMSO, ERKi, AKTi, mTORi, ERKi combined with AKTi or ERKi combined with mTORi and staurosporine for 48h...38	38
<b>Table 5:</b> Statistical analyzing with t-test of cleaved PARP in <i>BRAF</i> mutant melanoma cell lines.....	38
<b>Table 6:</b> IC <sub>50</sub> and CI values of <i>NRAS</i> mutant melanoma cell lines after exposure to ERKi, AKTi, mTORi, ERKi combined with AKTi or ERKi combined with mTORi...44	44
<b>Table 7:</b> Quantitative analysis of cell cycle progression and apoptosis in <i>NRAS</i> mutant melanoma cell lines after exposure to DMSO, ERKi, AKTi, mTORi, ERKi combined with AKTi or ERKi combined with mTORi and staurosporine for 48h...51	51
<b>Table 8:</b> Statistical analyzing with t-test of cleaved PARP in <i>NRAS</i> mutant melanoma cell lines.....	51
<b>Table 9:</b> IC <sub>50</sub> and CI values of WT melanoma cell lines after treating with ERKi, AKTi, mTORi, ERKi combined with AKTi or ERKi combined with mTORi . ....	55
<b>Table 10:</b> Quantitative analysis of cell cycle progression and apoptosis in wild-type melanoma cell lines after exposure to DMSO, ERKi, AKTi, mTORi, ERKi combined with AKTi or ERKi combined with mTORi and staurosporine for 48h...62	62
<b>Table 11:</b> Statistical analyzing with t-test of cleaved PARP in wild-type melanoma cell lines.....	62